

**PROBABILITY-BASED SIMULATION OF 2-D VELOCITY DISTRIBUTION AND  
DISCHARGE ESTIMATION IN OPEN CHANNEL FLOW**

by

Shih-Meng Hsu

BS, National Sun Yat-Sen University, 1996

MS, National Sun Yat-Sen University, 1998

Submitted to the Graduate Faculty of  
the School of Engineering in partial fulfillment  
of the requirements for the degree of

Doctor of Philosophy

University of Pittsburgh

2004

UNIVERSITY OF PITTSBURGH

SCHOOL OF ENGINEERING

This dissertation was presented

by

Shih-Meng Hsu

It was defended on

April 7, 2004

and approved by

Rafael G. Quimpo, Professor, Civil and Environmental Engineering

Tin-Kan Hung, Professor, Civil and Environmental Engineering

Jeen-Shang Lin, Associate Professor, Civil and Environmental Engineering

Mainak Mazumdar, Professor, Industrial Engineering

Dissertation Director: Chao-Lin Chiu, Professor, Civil and Environmental Engineering

# PROBABILITY-BASED SIMULATION OF 2-D VELOCITY DISTRIBUTION AND DISCHARGE ESTIMATION IN OPEN CHANNEL FLOW

Shih-Meng Hsu, PhD

University of Pittsburgh, 2004

A probability-based method is presented that can be used to simulate 2-D velocity distribution in rectangular open channels and to estimate the flow discharge. The method is based on Chiu's velocity distribution equation. A technique for estimating a parameter of 2-D velocity equation has been developed, by which the 2-D velocity distribution in rectangular open channels can be simulated by using one or several velocity samples, or even without using any velocity data.

The present study also developed an efficient method of discharge estimation in rivers, which is applicable regardless of whether flow is steady or unsteady. It only requires a quick velocity sampling. The relation between the surface velocity and the vertical mean velocity has been studied. It can be used for developing a non-contact method of discharge measurement.

Under the same framework of analysis, a new slope-area method has been developed to determine the flow discharge. It can reduce errors due to the uncertainties in Manning's  $n$  and the energy coefficient  $\alpha$  that exist in the widely-used slope-area method.

## TABLE OF CONTENTS

<b>ACKNOWLEDGMENTS .....</b>	<b>xii</b>
<b>1.0 INTRODUCTION.....</b>	<b>1</b>
1.1 BACKGROUND OF STUDY .....	1
1.2 OBJECTIVES AND SCOPES OF STUDY .....	4
1.3 LITERATURE REVIEW .....	5
<b>2.0 CHIU’S VELOCITY DISTRIBUTION EQUATION.....</b>	<b>12</b>
2.1 VELOCITY DISTRIBUTION EQUATION BASED ON PROBABILITY CONCEPT	12
2.2 DEFININITION AND EXPRESSIONS OF $\xi$ .....	15
2.3 PARAMETER M AND RATIO OF MEAN AND MAXIMUM VELOCITIES .....	19
2.4 ENERGY AND MOMENTUM COEFFICIENTS.....	21
2.5 LOCATION OF MAXIMUM VELOCITY AND ITS RELATION TO M.....	22
2.6 FUCTIONAL RELATIONS OF $\bar{u}/u_D$ , $\bar{u}/\bar{u}_v$ , $\bar{y}/D$ AND $\bar{y}_v/D$ TO $M$ .....	24
2.6.1 Relation between $\bar{u}$ and $u_D$ .....	24
2.6.2 Relation between $\bar{u}$ and $\bar{u}_v$ .....	24
2.6.3 Relation between $\bar{y}/D$ and $M$ .....	25
2.6.4 Relation between $\bar{y}_v/D$ and $M$ .....	26

<b>3.0</b>	<b>2-D VELOCITY DISTRIBUTION IN RECTANGULAR CHANNELS .....</b>	<b>27</b>
3.1	THE FUNCTION OF $N_i$ IN 2-D ISOVELS .....	27
3.2	ESTIMATION OF $N$ .....	30
3.2.1	Relation between $N$ and $M$ .....	30
3.2.2	Relation between $N$ and $B/D$ , $n$ and $S$ .....	32
3.2.3	Verification of Relation between $N$ and $M$ .....	36
3.3	MODEL VERIFICATION .....	39
3.4	APPLICATION .....	47
3.4.1	Simulation of 2-D Velocity.....	47
3.4.2	Estimation of $M$ by simulation of 2-D velocity distribution.....	53
<b>4.0</b>	<b>EFFICIENT METHODS OF DISCHARGE ESTIMATION .....</b>	<b>60</b>
4.1	SPECIAL FEATURES OF Y-AXIS .....	60
4.1.1	Stability of Y Axis .....	61
4.1.2	Concept of Maximum Correlation in Selection of Y Axis as Sampling Site .....	64
4.2	DEVELOPMENT OF EFFICIENT METHODS OF DISCHARGE MEASUREMENT	70
4.2.1	Regularities in Open Channel Flows and Their Applications in Discharge Measurements .....	70
4.2.2	Estimations of $M$ .....	72
4.2.3	Estimations of $u_{\max}$ and $\overline{u}_v$ .....	73
4.3	MODEL VERIFICATION .....	76
4.3.1	$\overline{y}/D - M$ and $\overline{y}_v/D - M$ Relations.....	76
4.3.2	Comparison of $u_{\max}$ Obtained from Velocity Sampling .....	82

4.3.3	Verification of Efficient Methods of Discharge Estimation .....	88
<b>5.0</b>	<b>RELATION BETWEEN SURFACE AND VERTICAL MEAN VELOCITIES .....</b>	<b>95</b>
5.1	BACKGROUND .....	95
5.2	COMPUTATION AND STABILITY OF $\bar{u}_v/u_D$ IN A CHANNEL SECTION.....	96
5.3	RELATION BETWEEN $\bar{u}_v/u_D$ AND DISCHARGE AND B/D.....	100
5.4	RELATION BETWEEN $\bar{u}_v/u_D$ AND M .....	104
<b>6.0</b>	<b>A MODIFIED SLOPE-AREA METHOD FOR DISCHARGE ESTIMATION ....</b>	<b>107</b>
6.1	BACKGROUND and OVERVIEW .....	107
6.2	NEW SLOPE-AREA METHOD.....	108
6.2.1	Manning's n Based on Probability Concept .....	108
6.2.2	New Slope-Area Method with Two Selected Channel Sections .....	110
6.2.3	New Slope-Area Method with Multiple Channel Sections.....	112
6.3	MODEL VERIFICATION .....	115
<b>7.0</b>	<b>CONCLUSION AND FUTURE WORK .....</b>	<b>120</b>
7.1	CONCLUSION.....	120
7.2	FUTURE WORK.....	124
	<b>BIBLIOGRAPHY .....</b>	<b>125</b>

## LIST OF TABLES

Table 3-1 Summary of $N$ and $M$ .....	31
Table 3-2 Relation between $N$ and $B/D$ ( $n = 0.03$ , $S = 0.0001$ ).....	33
Table 3-3 Relation between $N$ and Manning's $n$ ( $B/D = 2$ , $S = 0.0001$ ) .....	34
Table 3-4 Relation between $N$ and $S$ ( $B/D = 2$ , $n = 0.03$ ).....	35
Table 3-5 Comparison of Variance for the Selected Values of $M$ .....	54
Table 4-1 Comparison of the Correlation Between Vertical and Cross-sectional Mean Velocities, Unsteady Flow in Flume with Unvegetated Plain (Tu et al. 1995) .....	66
Table 4-2 Comparison of the Correlation Between Vertical and Cross-sectional Mean Velocity, River South Esk at bridge 2 (Bridge and Jarvis 1985).....	68
Table 4-3 Comparison of Discharge Obtained by Different Methods, Ohio River at Sewickley (USGS data, 1942-1944).....	86
Table 4-4 Comparison of Discharge Obtained by Different Methods, South Esk River at Bridge 4 (Bridge and Jarvis 1985).....	87
Table 6-1 Comparison of Discharges Obtained by Different Methods by Slope-Area Method with Two Sections (Guo 1990).....	117
Table 6-2 Accuracy of New Slope-Area Method with Two Channel Sections at Different Temperatures (Guo 1990).....	118
Table 6-3 Comparison of Discharges Obtained by Different Methods with Seven Channel Sections (Guo 1990) .....	119

## LIST OF FIGURES

Figure 2.1 Probability Distribution $f(u/u_{\max})$ .....	14
Figure 2.2 Patterns of Velocity Distribution and Curvilinear Coordinate System: (a) Pattern I: $u_{\max}$ occurs on the water surface; (b) Pattern II: $u_{\max}$ occurs below the water surface.....	17
Figure 2.3 The Relation Between $\bar{u}$ and $u_{\max}$ in Skagit River at Mt. Vernon, Washington .....	20
Figure 2.4 Variations of Velocity Distribution and Locations of $\bar{u}$ , $\bar{u}_v$ and $u_{\max}$ with $M$ .....	23
Figure 3.1 Simulated 2-D Velocity Distribution.....	28
Figure 3.2 Comparison of 2-D Velocity Distributions with Different $N$ (a) $N = 0.6$ ; (b) $N = 1.6$ .....	29
Figure 3.3 Relationship between $N$ and $M$ (Simulation).....	32
Figure 3.4 Relation between $N$ and $M$ .....	38
Figure 3.5 Simulated Two-dimensional Velocity Distribution Based in the Rectangular Channel .....	41
Figure 3.6 Velocity Distribution on $y$ axis (Guo 1990).....	42
Figure 3.7 Measured and simulated 2D velocities (4-foot wide Flume, Run 41, Bortz 1989).....	43
Figure 3.8 Measured and Simulated 2-D Velocities (8-foot Wide Flume with 0.19mm Sand, Run 14, Guy, et al. 1956-61).....	44
Figure 3.9 Measured and Simulated 2-D Velocities (8-foot Wide Flume with 0.28mm Sand, Run 28, Guy, et al. 1956-61).....	45
Figure 3.10 Measured and Simulated 2-D Velocities (2-foot Wide Flume with 0.32 mm Sand, Run 7, Guy, et al. 1956-61).....	46

Figure 3.11 Simulations of Two-dimensional Velocity Distribution at Channel Sections where $n = 0.03$ , $S = 0.0001$ , $B = 2$ m , $D = 1$ m $Q = 0.42$ m <sup>3</sup> /s , $\bar{u} = 0.21$ m/s . (a) $M = 5.6$ , $h = 0$ , $u_{\max} = 0.255$ m/s, $N_i = 1.16$ ; (b) $M = 4$ , $h = 0.242$ m, $u_{\max} = 0.273$ m/s, $N_i = 1.45$ ; (c) $M = 3$ , $h = 0.377$ m, $u_{\max} = 0.292$ m/s, $N_i = 1.62$ ; (d) $M = 2$ , $h = 0.479$ m, $u_{\max} = 0.320$ m/s, $N_i = 1.73$ .....	50
Figure 3.12 Simulations of Two-dimensional Velocity Distribution at Channel Sections where $M = 3$ , $h/D = 0.376$ and $N = 1.62$ . (a) $D = 0.2$ m, $h = 0.075$ m, $u_{\max} = 0.140$ m/s, $\bar{u} = 0.10$ m/s , $Q = 0.04$ m <sup>3</sup> /s; (b) $D = 1$ m, $h = 0.377$ m, $u_{\max} = 0.292$ m/s, $\bar{u} = 0.21$ m/s, $Q = 0.42$ m <sup>3</sup> /s; (c) $D = 1.86$ m, $h = 0.700$ m, $u_{\max} = 0.348$ m/s, $\bar{u} = 0.25$ m/s , $Q = 0.93$ m <sup>3</sup> /s .....	52
Figure 3.13 Determining Parameter M based on Velocity Samples from Three Verticals (a) $M = 2.5$ ; (b) $M = 2.9$ ; (c) $M = 3$ ; (d) $M = 3.1$ ; (e) $M = 3.5$ ; (f) $M = 5$ .....	57
Figure 3.14 Estimation of M from Velocity Samples on Y Axis(a) Velocity distribution on y axis; (b) Simulated two-dimensional velocity distribution .....	59
Figure 4.1 Determining the Location of Y Axis: (a) Velocity distribution on water surface; (b) Velocity distribution below water surface .....	62
Figure 4.2 Analysis of Location of Y Axis, Skagit River at Mt. Vernon .....	63
Figure 4.3 A sketch of Flume Section (Tu et al. 1995).....	65
Figure 4.4 Correlations Between Vertical and Cross-sectional Mean Velocity, Unsteady Flow in Flume with Unvegetated Plain (Tu et al. 1995).....	67
Figure 4.5 Sketch of Channel Cross Section in River South Esk at Bridge 2 .....	68
Figure 4.6 Correlation Between Vertical and Cross-sectional Mean Velocity, River South Esk at Bridge 2 (Bridge and Jarvis 1985).....	69
Figure 4.7 Network of Regularities in Open Channel Flows.....	71
Figure 4.8 Determining the Locations of $\bar{u}$ and $\bar{u}_v$ , and Velocity Distribution on Y Axis in Laboratory Flume .....	78
Figure 4.9 Determining the Locations of $\bar{u}$ and $\bar{u}_v$ , and Velocity Distribution on Y Axis in Trapezoidal Flume at Section $3\Pi/8$ .....	79
Figure 4.10 Determining the Locations of $\bar{u}$ and $\bar{u}_v$ , and Velocity Distribution on Y Axis in Ohio River at Sewickely .....	80

Figure 4.11 Accuracy of $\bar{y}/D-M$ and $\bar{y}_v/D-M$ Relations.....	81
Figure 4.12 Velocity Distribution Profile ( $u_{\max}$ from all velocity samples) .....	84
Figure 4.13 Velocity Distribution Profile ( $u_{\max}$ from velocity samples within 95% confidence Interval of $h/D$ ) .....	85
Figure 4.14 Comparison of Efficient Methods 1 and 2 of Discharge Estimation at Section S0 .....	90
Figure 4.15 Comparison of Efficient Methods 1 and 2 of Discharge Estimation at Section CPI0 .....	91
Figure 4.16 Comparison of Efficient Methods 1 and 2 of Discharge Estimation at Section $\Pi/4$ .....	92
Figure 4.17 Comparison of Efficient Methods 1 and 2 of Discharge Estimation at Section $\Pi/2$ .....	93
Figure 4.18 Comparison of Different Methods of Estimating Discharge: (a) Ratios of estimated discharges to the known; (b) Locations of the four sections .....	94
Figure 5.1 Values of $\bar{u}_v/u_D$ in Channel Section and Estimation of Overall Average in Ohio River at Sewickley .....	97
Figure 5.2 Values of $\bar{u}_v/u_D$ in Channel Section and Estimation of Overall Average in Rio Grande Conveyance Channel at Section 250.....	98
Figure 5.3 Values of $\bar{u}_v/u_D$ in Channel Section and Estimation of Overall average in River South Esk at Bridge 2 .....	99
Figure 5.4 Values of $\bar{u}_v/u_D$ in Channel Section and Estimation of Overall Average in River South Esk at Bridge 4.....	100
Figure 5.5 Relations between $\bar{u}_v/u_D$ and Q and B/D in River South Esk at Bridge 2 .....	101
Figure 5.6 Relations between $\bar{u}_v/u_D$ and Q and B/D in River South Esk at Bridge 4 .....	102
Figure 5.7 Relations between $\bar{u}_v/u_D$ and Q and B/D in Rio Grande Conveyance Channel at Section 250.....	103
Figure 5.8 Relations between $\bar{u}_v/u_D$ and Q and B/D in Ohio River at Sewickley .....	104

Figure 5.9 Relation between $\bar{u}_v / u_D$ and M.....	106
Figure 6.1 Definition sketch for new slope-area formula.....	114

## ACKNOWLEDGMENTS

I wish to express my sincere gratitude and thanks to my advisor, Dr. Chao-Lin Chiu, for all the advice, encouragement and guidance that he provided during the course of this research.

I would like to thank the committee members, Dr. Tin-Kan Hung, Dr. Rafael G. Quimpo, Dr. Jeen-Shang Lin, and Mainak Mazumdar, for reviewing this work and their helpful suggestion and comments.

I am deeply indebted to Dr. Bang-Fuh Chen, my master's advisor, for encouraging me to the graduate study.

Finally, I wish to dedicate this work to my parents, my sister, and Vivien. Their patient love and understanding enabled me to never give up during the hardest time.

## **1.0 INTRODUCTION**

### **1.1 BACKGROUND OF STUDY**

The velocity distribution in a channel cross section is affected by channel geometry, roughness of the channel and the presence of bends<sup>(1)\*</sup> and must be studied and determined prior to solving various hydraulic problems in natural rivers. For instance, the discharge measurement is one of problems and one of the most important tasks in water resources management. The second example is the estimation of the energy and momentum coefficients in open channel flows. These two coefficients depend on the velocity distribution. These coefficients are greater than one, but assumed to be unity because of the absence of a simple method to estimate them. If the velocity distribution can be determined, the energy and momentum coefficients can be evaluated at a channel section. Another example related to the velocity distribution is the distribution of sediment concentration in open channel flow, which is essential to the control and management of reservoir sedimentation, river channels, and pollutant transport. Since the shear stress distribution is a main factor affecting the distribution of sediment concentration in open channel flow, it needs to be considered in the derivation of sediment concentration. However, the shear stress distribution, in turn, depends on the velocity distribution. Therefore, modeling of the distribution of sediment concentration depends on how the velocity distribution is modeled.

---

\* Parenthetical references placed superior to the line of text refer to the bibliography.

The most popular velocity distribution formulas are the Prantal-von Karman logarithmic law and the power law. Nevertheless, these two equations are invalid at or near the channel bed and inaccurate near the water surface, typically when the maximum velocity occurs below the water surface. Therefore, these two equations can not be used in solving the problems concerned with river flows.

Chiu (1987,1989)<sup>(2, 3)</sup> derived a velocity distribution equation using the probability concept and entropy-maximization principle. Chiu's velocity distribution equation is capable of describing the variation of velocity in both vertical and transverse directions with the maximum velocity occurring on or below the water surface. The velocity distribution equation does not have the limitations and weakness of other current velocity distribution equations. The new velocity distribution equation in physical space corresponds to an exponential probability distribution that has a single parameter M called "Entropy Parameter". The M value is useful as an index for characterizing and comparing various patterns of velocity distribution in open-channel flow systems. The entropy parameter of a channel section can be determined through the relation between the mean and maximum velocities. On the other hand, the ratio of the mean and maximum velocities at a channel section is a function of M, and tends to stay constant, although it may vary from section to section along a channel<sup>(4)</sup>. The ratio being constant at a channel section can be viewed as a natural law<sup>(5)</sup>. In order to maintain the constant ratio, nature tends to adjust factors that influence flow characteristic at the cross section, such as the velocity distribution, discharge, sediment concentration, roughness, slope, and geometrical shape of the channel<sup>(4, 5)</sup>. Therefore, the ratio represents the overall characteristics of the flow system and controls the flow variables interacting with the channel. Many similar results<sup>(6, 7, 8)</sup> obtained from

various channels in a wide range of flow also show that the ratio is a constant at a given channel section.

In deterministic hydraulics, the importance of the maximum velocity is not mentioned. Under the framework of the probability and entropy-based approach, the maximum velocity can be clearly linked to the mean velocity and other hydraulic variables<sup>(9, 10)</sup>. Due to the importance of the maximum velocity, Chiu and Tung (2002)<sup>(8)</sup> investigated the location and magnitude of maximum velocity in open channel flow. They found that the location of the maximum velocity was also a function of the entropy parameter  $M$ .

Chiu's velocity distribution equation is also capable of describing the velocity distributions not only on a vertical axis as depicted above, but also in an entire channel section. The velocity distribution in an entire section is two-dimensional. Actually, the flow in open channels is a three-dimensional motion. The flow component in the longitudinal direction is called the primary flow. Other flow components in the transverse direction are the secondary flow that forms a circular motion around an axis parallel to the primary flow. The secondary flow has significant effects in open channel flow and has been studied for more than a century. The measurements of the primary flow at a channel section can help understand flow properties and explain the location and magnitude of maximum velocity as well as the presence of the secondary flow. The simulations of the primary flow enable generating velocity data in an entire section to supplement the available data.

In order to simulate the 2-D velocity distribution in a channel section by using Chiu's velocity equation, there are parameters that need to be determined<sup>(2, 10, 15)</sup>.

## **1.2 OBJECTIVES AND SCOPES OF STUDY**

Based on the Chiu's velocity distribution equation, the present study has four objectives: The first objective is to develop methods that can be used to simulate a two-dimensional velocity distribution in open channel flows. The second objective is to develop efficient methods of discharge estimation. The third objective is to verify the relation between the surface velocity and the vertical mean velocity as the basis of a non-contact method for discharge measurement. The fourth objective is to develop a new slope-area method that is based on the probability concept that can be used as an efficient method of discharge estimation.

### 1.3 LITERATURE REVIEW

The prediction of velocity field for an open channel flow has been investigated for many years. The problem is treated by solving the Navier-Stokes hydrodynamic equations combined with turbulent models. These models depend on the deterministic law of physics that treats fluid flow as boundary-value problems and makes predictions with certainty. However, to develop a velocity distribution model, Chiu (1987)<sup>(2)</sup> proposed a new approach to the problem based on a probability concept.

In the late 1970s and the early 1980s<sup>(12, 13, 14)</sup>, Chiu and some researchers derived three-dimensional mathematical models of open channel flow and used them to determine various hydraulic variables and processes, such as the distribution of primary flow velocity, secondary flow, shear stress distribution, channel cross section, discharge rate, flow resistance, and sediment transport. These contributions made a better understanding of the three-dimensional structure of open channel flow. The developed mathematical model used a curvilinear coordinate system formed by the isovels of primary flow (lines on which the velocity is everywhere equal). Compared to the Cartesian coordinate system, the curvilinear coordinate system is capable of describing flows in irregular open channels.

In 1983 Chiu and Lin<sup>(9)</sup> used the same framework of a curvilinear coordinate system in hydraulic analysis used in earlier papers, however, with a better expression of the coordinate in Chiu's velocity distribution model. His velocity distribution equation became capable of simulating various patterns of primary flow velocity distribution that might have the maximum velocity on or below water surface. They used actual velocity data in estimating model parameters to deal with a nonuniform and nonsymmetrical three-dimensional flow. However, in many applications, such data are unavailable. Therefore, in 1986 Chiu and Chiou<sup>(10)</sup> proposed a

parameter estimation method for a system of three-dimensional mathematical model of flow in open channels, which does not require velocity data. The method was applied to a study of the two-dimensional velocity distribution in rectangular open channels. The interaction among the primary and secondary flow and the shear stress distribution was also investigated under various values of width-to-depth ratio, Manning's  $n$ , and slope of channels.

By applying the probability concept, in 1987 Chiu<sup>(2)</sup> proceeded to model the distributions of the velocity, shear stress, and sediment concentration in open channel flow. The new velocity distribution equation derived is superior to the well-known Prandtl-von Karman universal velocity distribution equation in many aspects.

Chiu (1987, 1988)<sup>(2, 15)</sup> derived a two-dimensional velocity distribution equation by entropy maximization in a channel cross section, which is valid regardless of the location of maximum velocity. A dimensionless parameter named  $M$  in the derived equation has been found useful as an index for characterizing and comparing various patterns of velocity distribution. Subsequently, the state of the art velocity distribution equation became a benchmark for various applications in open-channel flow and pipe-flow studies, and he has been using it until now.

### **Developments of the methods of discharge measurement**

Discharge measurement is always an important task in hydraulic engineering. The flow data are needed for multiple purposes, such as flood forecasting, water resources management, hydrologic analysis, and water-quality monitoring. The United States Geological Survey is responsible for measuring flow in rivers and streams. The procedure they use and technology for estimating discharge are widely accepted as the standard. They formalized the procedure for

gaging streams, which is still being used today and currently referenced in many textbooks in hydrology and open channel hydraulics.

The U.S. Geological Survey operates a network of about 7,000 streamflow-gaging stations that monitor discharges at selected locations throughout the United States<sup>(16)</sup>. The traditional method of discharge measurement at these gaging stations has not changed for over 100 years. A current meter with a heavy lead weight is placed into the river to take velocity samples. Multiple depth and velocity measurements are conducted across the channel, and computations of discharge over sub-areas are summed up to give the total discharge. The discharge requires periodic direct measurements of river width, depth and velocity at a selected station. These discharge values are used to establish a relation between the stage and discharge, referred to as a stage-discharge rating curve.

For accuracy of a rating curve, data need to be collected over the entire range of flow conditions. However, during high flows, direct measurements of flows with a current meter or any instrument that must be placed in the water could not only pose safety hazards to personnel, but also lead to high measurement errors. To improve shortcomings of the conventional method, in 1996 the USGS established a committee, Hydro 21, to identify and evaluate techniques that might be more cost-effective and safely monitor flow discharge<sup>(17)</sup>. After much thought and discussion, they decided to explore a “non-contact method”.

On April 21, 1999, the USGS and the Applied Physics Laboratory of the University of Washington collaborated to carry out the first field experiment on the Skagit River, Mt. Vernon, Washington using radar technology that was designed to measure river discharge without any instrument having to touch the water<sup>(18)</sup>. Three sets of surface-velocity data at 25 verticals across the river section were collected. By assuming the velocity distribution was logarithmic, the mean

velocity on a vertical was estimated to be 85% of surface velocity<sup>(19)</sup>. Independent estimations of river discharge were also made by using a conventional current meter, a moving boat method with an ADCP, and using a stage-discharge rating curve for the site. Comparison of different methods indicates that the discharge determined by using non-contact methods falls within the accuracy standards of conventional procedures, and thus demonstrate the feasibility of the new technology in replacement of conventional methods.

Between March 15 and May 17, 2002, the USGS conducted an extensive flow measurement experiment on the San Joaquin River at Vernalis, California for the purpose of evaluating radar technologies for continuous non-contact river discharge measurement (Mason, 2002)<sup>(20)</sup>.

Recently, Hydro 21 Committee suggested the use of remotely measured surface velocity for determining discharge<sup>(21)</sup>. The validity of this approach depends on a stable relation between the vertical mean velocity and the surface mean velocity. However, the ratio of the mean velocity to the surface velocity in logarithmic law is 0.85. Cheng (2002)<sup>(21)</sup> analyzed the detailed velocity profiles and surface velocity data, which were obtained from Mason's measurements on the San Joaquin River, and proposed the ratio to be in the range of 0.80 and 0.93 with a mean value of 0.88. Since the conclusion was only based on a small sample, he also suggested examining a large number of case studies.

Chiu and Said (1995)<sup>(4)</sup> developed a technique for determining discharge from the entropy parameter  $M$  of a channel section and a velocity profile on a single vertical where the maximum velocity occurs in a channel cross section. The  $M$  value of a channel section can be determined from the relation between the maximum and mean velocities. It tends to remain

constant as the velocity distribution fluctuates. The value of  $M$  being constant for a channel section can simplify the discharge determination.

In 1997 Xia<sup>(6)</sup> explored the relation between the maximum velocity and the cross-sectional mean velocity by analyzing velocity data on five different straight reaches in the Mississippi River. The result confirmed the early finding of Chiu and Said (1995).

Later in 2002, Chiu and Tung<sup>(8)</sup> found a relation between  $M$  and the location of maximum velocity when the maximum velocity occurs below water surface. This finding gave more efficient procedure for estimating the discharge than the earlier method of Chiu and Said (1995).

During high flows, the conventional device of velocity measurement is not applicable. The indirect method of discharge measurement is therefore designed to estimate the missing peak discharge after flood flows. Dalrymple and Beson (1967)<sup>(32)</sup> developed a technique used to determine peak discharges from measurements of high-water marks. This technique is called the slope-area method in which peak discharge can be estimated by utilizing the well-known Manning's equation.

Because this method is based on one-dimensional, gradually varied, steady flow equation, errors associated with the method, may be large due to the complexity of natural rivers. Jarrett (1987)<sup>(33)</sup> reviewed the results of 70 slope-area measurements from different rivers throughout the U.S. and found that the accuracy of the indirect measurement may be affected by Manning's  $n$ , energy loss due to expansion or contraction, the condition of unsteady flow, scour near channel bed, degree of stream slope, and the number of cross sections.

In applying the slope-area method, Manning's  $n$  is assumed to be constant. A suitable  $n$  value at a given section can be selected by the guidelines from many textbooks or reports

published by the U.S. Geological Survey. Rantz (1982)<sup>(19)</sup> stated: “Selection of a friction coefficient  $n$  remains essentially an “art” that is developed through experience”. However, many researchers had investigated variations of  $n$  in natural rivers and proposed that the value of  $n$  varies with the water stage<sup>(1)</sup>.

The estimation of the energy coefficient  $\alpha$  is another difficult problem in applying the slope-area method. In the absence of site-specific information on velocity distribution, the U.S. Geological Survey assumed that  $\alpha = 1$  for unsubdivided unit cross sections<sup>(32)</sup>. For compound sections, an approximate velocity distribution is obtained by applying Manning’s formula independently to each subarea, with the result:  $\alpha = \sum (K_i^3 / A_i^2) / (K^3 / A^2)$ , in which  $K_i$  and  $A_i$  are the conveyance and area of the  $i$ th subarea;  $K$  and  $A$  are the conveyance and area for the cross section<sup>(32)</sup>.

Chow (1959)<sup>(1)</sup> stated that  $\alpha$  varies in prismatic open channels having straight alignments between 1.03 and 1.36. King and Brater (1963)<sup>(34)</sup> experimentally investigated the coefficient  $\alpha$  in open channels of various cross sections. Fox and McDonald (1985)<sup>(35)</sup> stated that  $\alpha$  varies with Reynolds number, in which the result is based on the power law. Chen (1992)<sup>(36)</sup> derived a theoretical energy coefficient that implemented the power law for turbulent shear flow in circular pipes and wide channels.

The values of  $\alpha$  in these earlier studies were obtained from the certain type of flow system and the traditional velocity formulas. Therefore, these  $\alpha$  values had limited applications. Chiu (1991)<sup>(37)</sup> applied his velocity distribution equation in deriving a theoretical equation that gives  $\alpha$  in terms of the entropy parameter  $M$ .

Because there is no reliable method that based on fluid-dynamics principle that is applicable for determining  $\alpha$  and  $n$ , the slope-area method is still being used by the U.S. Geological Survey today.

## 2.0 CHIU'S VELOCITY DISTRIBUTION EQUATION

### 2.1 VELOCITY DISTRIBUTION EQUATION BASED ON PROBABILITY CONCEPT

Well-known velocity distribution models include the Prandtl-von Karman logarithmic law and the simple power law. Nevertheless, they cannot describe velocity distribution patterns, in which the maximum velocity occurs below the water surface. Velocity distribution should be capable of depicting all possible patterns of distribution. By applying the probability concept and the principle of maximum information entropy (Shannon 1948, Chiu 1989)<sup>(3, 22)</sup>, Chiu (1989)<sup>(3)</sup> derived a new velocity distribution equation for fluid flows, the general form of which is:

$$u = \frac{u_{\max}}{M} \ln \left[ 1 + (e^M - 1) \frac{\xi - \xi_0}{\xi_{\max} - \xi_0} \right] \quad (2-1)$$

in which  $u$  = velocity that monotonically increases with  $\xi$ ;  $u_{\max}$  = maximum velocity in a channel cross section. A value of  $\xi$  is assigned to each isovel along which the velocity is constant value;  $\xi_{\max}$  = the maximum value of  $\xi$  at which  $u = u_{\max}$ ;  $\xi_0$  = the minimum value of  $\xi$  that occurs along the channel bed, and also an isovel along which  $u = 0$ ;  $M$  is an entropy parameter. Eq. (2-1) is equivalent to

$$\frac{\xi - \xi_0}{\xi_{\max} - \xi_0} = \int_0^u f(u) du \quad (2-2)$$

$f(u)$  in Eq. (2-2) is a probability density function. The simplest form of  $f(u)$  that can be derived by entropy-maximization<sup>(3)</sup> is

$$f(u) = \exp(a_1 + a_2 u) \quad (2-3)$$

in which the parameters  $a_1$  and  $a_2$  are related to  $M$  and  $u_{\max}$  in Eq. (2-1) by

$$e^{a_1} = \frac{M}{u_{\max}(e^M - 1)} \quad (2-4)$$

$$a_2 = \frac{M}{u_{\max}} \quad (2-5)$$

$f(u)$  in Eq. (2-3) satisfies the following constraints:

$$\int_0^{u_{\max}} f(u) du = 1 \quad (2-6)$$

$$\int_0^{u_{\max}} u f(u) du = \bar{u} = \frac{Q}{A} \quad (2-7)$$

Eq. (2-6) is the constraint on  $f(u)$  to satisfy the definition of probability density function. Eq.

(2-7) is the constraint on  $f(u)$  to make the mean velocity  $\bar{u}$  in the flow cross section to be  $Q/A$

where  $Q$  is the discharge, and  $A$  is the cross-sectional area of the flow.

Substitution of Eq. (2-4) and (2-5) into Eq. (2-3) gives

$$f(u) = \frac{M}{u_{\max}(e^M - 1)} \exp\left(M \frac{u}{u_{\max}}\right) \quad (2-8)$$

Since  $f(u/u_{\max}) = u_{\max} f(u)$ , Eq. (2-8) is equivalent to

$$f\left(\frac{u}{u_{\max}}\right) = \frac{M}{(e^M - 1)} \exp\left(M \frac{u}{u_{\max}}\right) \quad (2-9)$$

Eq. (2-9) shows that  $f(u/u_{\max})$  is an exponential distribution characterized by the single parameter  $M$  as shown in Figure (2.1). It indicates that, as  $M$  decreases,  $f(u/u_{\max})$  becomes more uniform.

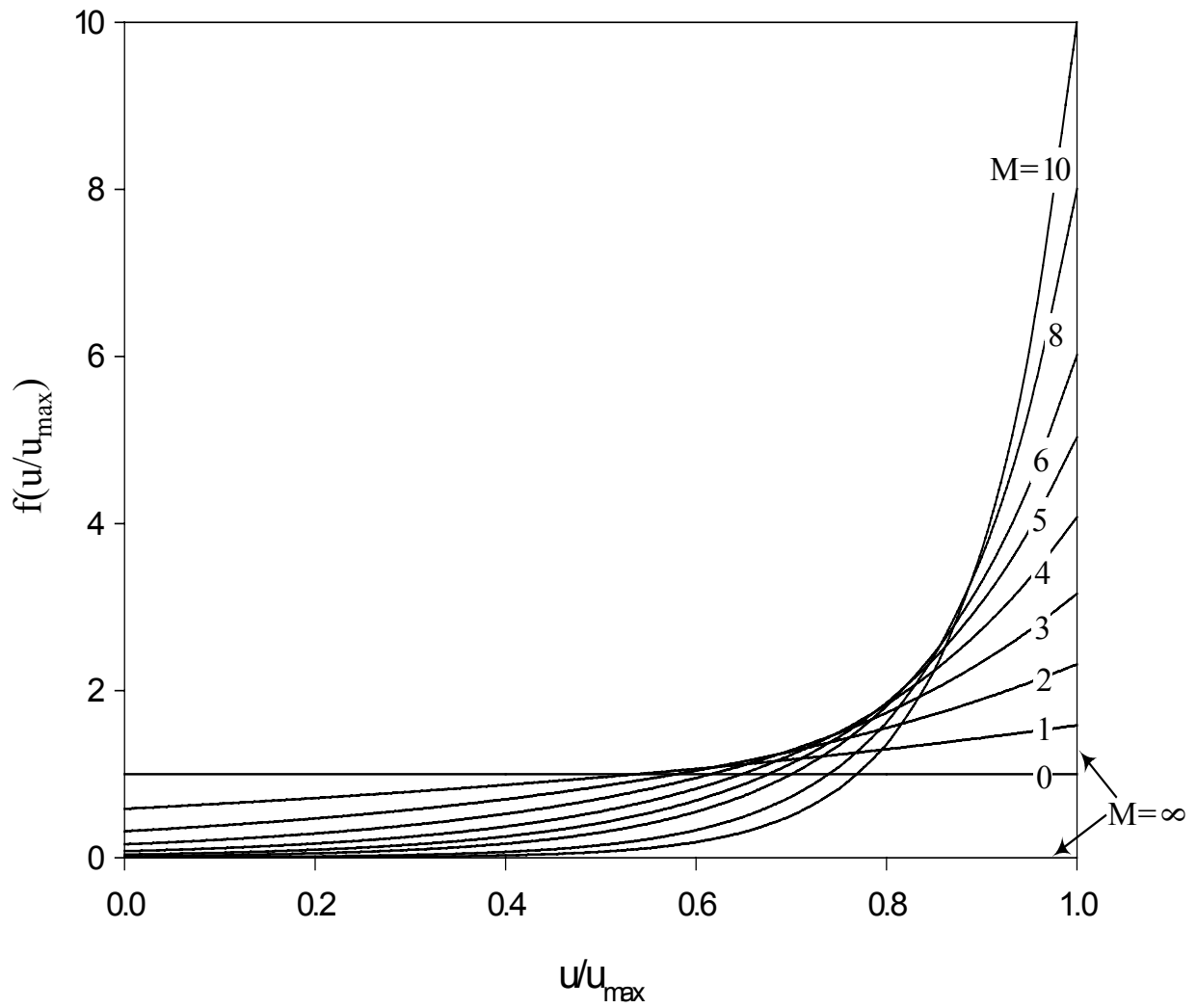


Figure 2.1 Probability Distribution  $f(u/u_{\max})$

## 2.2 DEFININITION AND EXPRESSIONS OF $\xi$

By defining  $\xi$  in terms of coordinates in the physical plane, Eqs. (2-1) and (2-2) can describe one- or two-dimensional velocity distributions. Eq. (2-2) indicates that  $(\xi - \xi_0)/(\xi_{\max} - \xi_0)$  is equal to the cumulative distribution function, or the probability of velocity being less than or equal to  $u$ . If a large number of  $\xi$  values are randomly generated within the range  $(\xi_0, \xi_{\max})$  and substituted into Eq. (2-1) to obtain a set of velocity samples, the probability of velocity being between  $u$  and  $u + du$  is  $f(u)du$ .  $(\xi - \xi_0)/(\xi_{\max} - \xi_0)$  is equivalent to the ratio of the area in which the velocity is less than or equal to  $u$  to the total cross-sectional area. For a wide rectangular channel,  $(\xi - \xi_0)/(\xi_{\max} - \xi_0)$  can be expressed as  $y/D (= By/BD)$  because isovels can be approximated as horizontal lines, in which  $y$  = the vertical distance from the channel bed;  $D$  = the water depth; and  $B$  is the channel width. Similarly, for a pipe flow, the isovels are concentric circles,  $(\xi - \xi_0)/(\xi_{\max} - \xi_0) = (\pi R^2 - \pi r^2)/\pi R^2 = 1 - (r/R)^2$  where  $r$  = radial distance from the pipe center at which the velocity is  $u$ ; and  $R$  = pipe radius. For open channel flow, in which  $u_{\max}$  may occur on or below the water, a suitable equation for  $\xi$  has been derived by Chiu and Chiou (1986)<sup>(10)</sup>:

$$\xi = Y(1 - Z)^{N_i} \exp(N_i Z - Y + 1) \quad (2-10)$$

in which

$$Y = \frac{y + \delta_y}{D + \delta_y - h} \quad (2-11)$$

$$Z = \frac{|z|}{B_i + \delta_i} \quad (2-12)$$

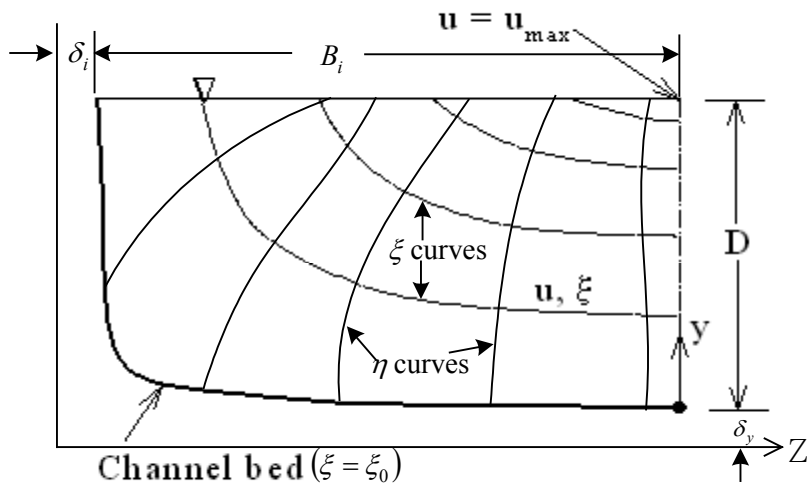
Figures 2.2 (a) and (b) show the chosen coordinate and other variables and parameters that appear in Eqs. (2-10)-(2-12), in which  $D$  = water depth at  $y$ -axis;  $B_i$  ( $i=1$  or  $2$ )= transverse distance on the water surface between the  $y$ -axis and either the left or right side of a channel cross section;  $z$  = coordinate in the transverse direction;  $y$  = coordinate in the vertical direction; and  $\delta_y$ ,  $\delta_i$ ,  $N_i$ , and  $h$  are parameters.  $\delta_y$  and  $\delta_i$  vary with the geometrical shape of the channel cross section (or the shape of the zero-velocity isovel). Both  $\delta_y$  and  $\delta_i$  approach zero if the channel cross section tends towards a rectangular shape. Both values increase as the cross-sectional shape deviates from the rectangular. The parameter  $h$  controls the shape and slope of isovels, in particular, near the water surface and in the vicinity of the point of maximum velocity. If  $h > 0$ ,  $u_{\max}$  occurs below the water surface and  $h$  is the depth of  $u_{\max}$  below the water surface; the velocity increases with  $y$  only up to  $y = D - h$ , and decreases with  $y$  in the region  $(D - h, D)$ . If  $h \leq 0$ ,  $u_{\max}$  occurs on the water surface.

The  $\eta$  curves shown in Figure (2.2) are orthogonal trajectories of  $\xi$  curves, which can be derived from Eq. (2-10) as

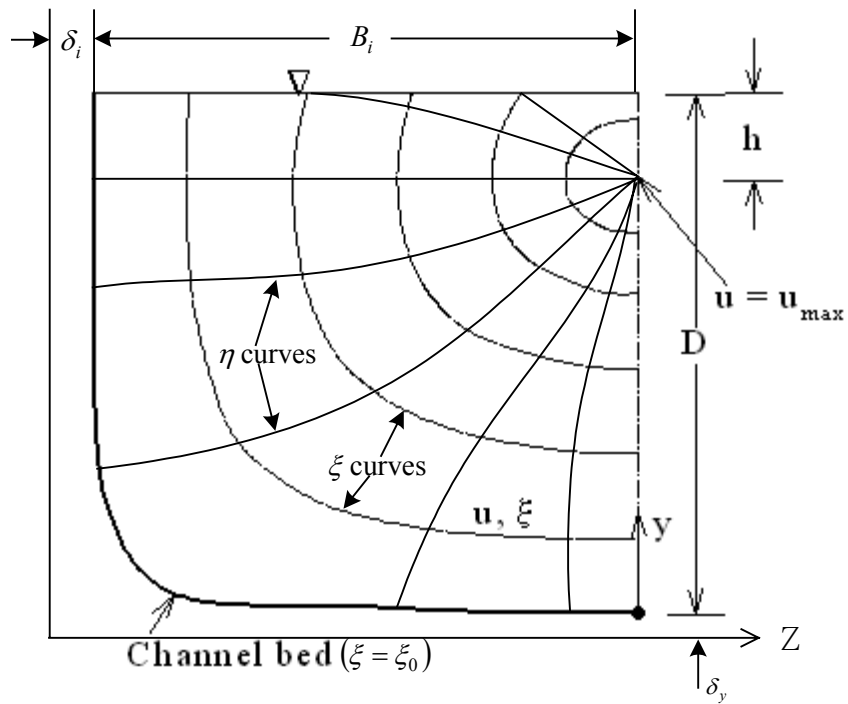
$$\eta = \pm \frac{1}{Z} \left( |1 - Z| \right)^{N_i \left[ \frac{(D + \delta_y - h)}{(B_i + \delta_i)} \right]^2} \exp \left[ Z + N_i \left( \frac{D + \delta_y - h}{B_i + \delta_i} \right)^2 Y \right] \quad (2-13)$$

in which  $\eta$  takes the negative sign only when  $y > D - h$  and  $h > 0$ . In other cases,  $\eta$  takes the positive sign. The network of  $\xi - \eta$  curves can be used as a coordinate system in modeling two-dimensional velocity and shear-stress distributions and related hydraulic transport processes.

Substitution of Eq. (2-10) into (2-1), two-dimensional velocity distributions in open channel flow can be expressed as shown in Figure (2.2).



(a)



(b)

Figure 2.2 Patterns of Velocity Distribution and Curvilinear Coordinate System: (a) Pattern I:  $u_{\max}$  occurs on the water surface; (b) Pattern II:  $u_{\max}$  occurs below the water surface

For a one-dimensional velocity distribution on “y axis” defined hereafter as the vertical axis on which  $u_{\max}$  occurs,  $\xi$  can be expressed as

$$\xi = \frac{y}{D-h} \exp\left(1 - \frac{y}{D-h}\right) \quad (2-14)$$

as  $z = 0$  and  $\delta_y = 0$  in Eq. (2-10). The reason of  $\delta_y = 0$  is that  $\delta_y$  on the y axis is not sensitive to the present velocity distribution equation and usually too small<sup>(2,7)</sup>.

By applying Eq. (2-1) with  $\xi$  defined by Eq. (2-14) to describe a one-dimensional velocity distribution, there are three cases:

- (I) The maximum velocity  $u_{\max}$  occurs at a distance  $h$  ( $h > 0$ ) below the water surface, or  $y = D - h$  above the channel bed. In the case,  $\xi_{\max} = 1$  in Eq. (2-14) so that Eq. (2-1) with  $\xi_0 = 0$  gives

$$u = \frac{u_{\max}}{M} \ln \left[ 1 + (e^M - 1) \frac{y}{D-h} \exp\left(1 - \frac{y}{D-h}\right) \right] \quad (2-15)$$

- (II)  $u_{\max}$  occurs on the water surface and  $h = 0$  so that  $\xi_{\max} = 1$ . Eq. (2-15) becomes

$$u = \frac{u_{\max}}{M} \ln \left[ 1 + (e^M - 1) \frac{y}{D} \exp\left(1 - \frac{y}{D}\right) \right] \quad (2-16)$$

Eq. (2-16) gives  $du/dy = 0$  at the water surface and hence can describe a velocity curve is perpendicular to the water surface.

- (III)  $u_{\max}$  occurs on the water surface and  $h < 0$  ( $du/dy > 0$ ). In this case,  $h$  no longer has the same physical meaning as that in cases (I) and (II). It is only a coefficient that can

fine-tune the curvature of the velocity distribution. The maximum value of  $\xi$  is

$$\xi_{\max} = \frac{D}{D-h} \exp\left(1 - \frac{D}{D-h}\right), \text{ therefore Eq. (2-16) becomes}$$

$$u = \frac{u_{\max}}{M} \ln\left[1 + (e^M - 1) \frac{y}{D} \exp\left(\frac{D-y}{D-h}\right)\right] \quad (2-17)$$

As  $h$  approaches to negative infinity, Eq. (2-17) becomes

$$u = \frac{u_{\max}}{M} \ln\left[1 + (e^M - 1) \frac{y}{D}\right] \quad (2-18)$$

Eq. (2-18) describes the velocity distribution in wide open channels.

From Eqs. (2-15)-(2-18), it is clear that  $(\xi - \xi_0)/(\xi_{\max} - \xi_0)$  in Eq. (2-1) can be adjusted to describe various patterns of velocity distribution.

### 2.3 PARAMETER M AND RATIO OF MEAN AND MAXIMUM VELOCITIES

Substitution of Eq. (2-6) and (2-7) into Eq. (2-3) gives

$$\frac{\bar{u}}{u_{\max}} = \phi = \frac{e^M}{e^M - 1} - \frac{1}{M} \quad (2-19)$$

Figure 2-3 illustrates the  $\bar{u} - u_{\max}$  relation based on the U. S. Geological Survey data collected from the Skagit River at Mt. Vernon during a fifteen-year period. Most data were collected by the current meter during 1986-2000, but some data, which were obtained during an unsteady flow period on April 21, 1999, also included measurements by an Acoustic Doppler Current Profiler (ADCP). In this Figure,  $\bar{u}$  was determined as  $Q/A$ , and  $u_{\max}$  was obtained by regression using the velocity samples on the y axis. The linear relation in the figure shows that the  $\phi$  value is 0.64, and the corresponding  $M$  obtained by Eq. (2-19) is 1.80. The high value of  $R^2$  indicates the  $M$  value is very stable during various flow over the long time period. This figure

and many similar results<sup>(4, 6, 7)</sup> obtained from both laboratory and field data also illustrate the stable relation between  $\bar{u}$  and  $u_{\max}$ , whether the flow is steady or not. Since these results indicate the stability and invariance of  $\phi$  or  $M$  at a given channel section, it, in turn, confirms the resilience of the probability law  $f(u/u_{\max})$  shown in Eq. (2-9), which means that the flow at a channel section maintain the same distribution  $f(u/u_{\max})$  at any discharges. Thus, Eq. (2-1) is applicable under various flow patterns observed at a channel station.

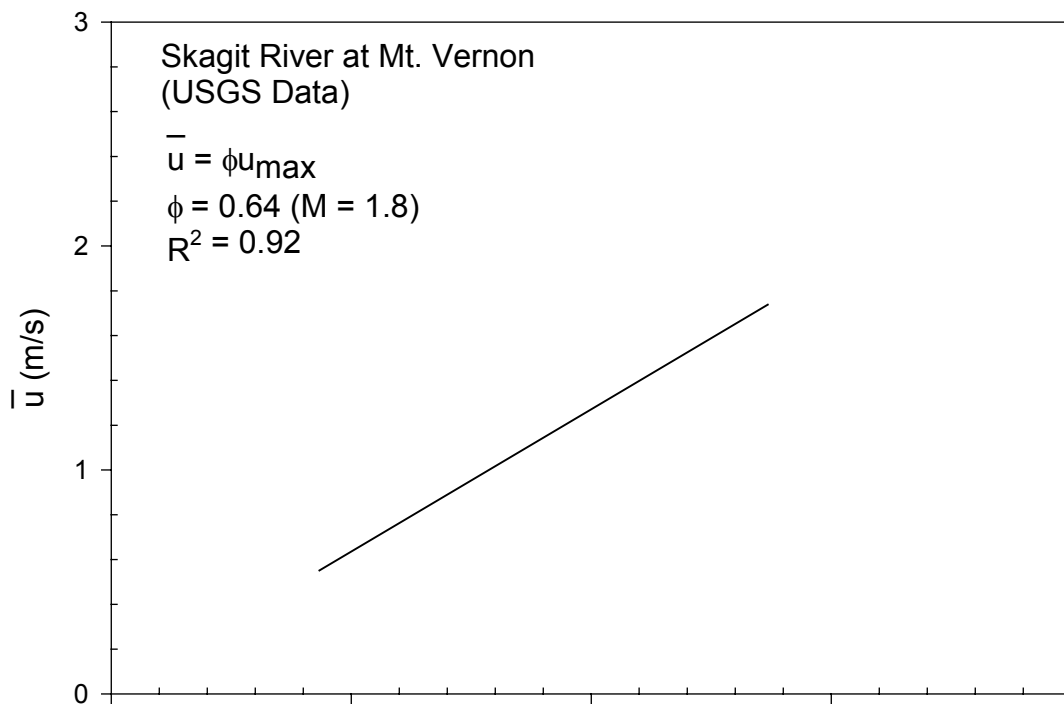


Figure 2.3 The Relation Between  $\bar{u}$  and  $u_{\max}$  in Skagit River at Mt. Vernon, Washington

## 2.4 ENERGY AND MOMENTUM COEFFICIENTS

The energy and momentum coefficients are the important measures of the rates of energy and momentum transport through a channel section. These coefficients are defined as  $\overline{u^3}/\overline{u^3}$  and  $\overline{u^2}/\overline{u^2}$ , respectively, in which  $\overline{u^3}$  and  $\overline{u^2}$  are the mean values of  $u^3$  and  $u^2$ , respectively.

The estimation of these two mean values is difficult when integrating them over the cross-sectional area in the physical plane, especially in natural channels. By using the probability density function in Eq. (2-3), these mean values can be expressed and obtained by

$$\int_0^{u_{\max}} u^3 f(u) du = \overline{u^3} = \alpha \overline{u^3} \quad (2-20)$$

$$\int_0^{u_{\max}} u^2 f(u) du = \overline{u^2} = \beta \overline{u^2} \quad (2-21)$$

Substitution of Eq. (2-3) into Eq. (2-20) gives the energy coefficient as a function of  $M$  <sup>(15)</sup>:

$$\alpha = \frac{(e^M - 1)^2 [e^M (M^3 - 3M^2 + 6M - 6) + 6]}{[e^M (M - 1) + 1]^3} \quad (2-22)$$

Substitution of Eq. (2-3) into Eq. (2-21) gives the momentum coefficient as a function of  $M$  :

$$\beta = \frac{(e^M - 1)[e^M (M^2 - 2M + 2) - 2]}{[e^M (M - 1) + 1]^2} \quad (2-23)$$

Therefore,  $\alpha$  and  $\beta$  can be determined by a single value of  $M$ . Since  $M$  is constant at a channel section,  $\alpha$  and  $\beta$  should be constant as well.

## 2.5 LOCATION OF MAXIMUM VELOCITY AND ITS RELATION TO M

When the maximum velocity  $u_{\max}$  occurs below the water surface, let  $h$  denote the location of maximum velocity below the water surface. According to the theory and analysis of many sets of both laboratory and field data, Chiu and Tung (2002)<sup>(8)</sup> found a relation between  $h$  and  $M$  as:

$$\frac{h}{D}(M) = -0.2 \ln \frac{G(M)}{58.3} \quad (2-24)$$

in which

$$G(M) = \frac{e^M - 1}{M\phi} \quad (2-25)$$

Eq. (2-24) is only valid in the range of  $M$  between 1.0 and 5.6 and represents the average relation between  $h/D$  and  $M$ . If  $M$  is greater than 5.6,  $u_{\max}$  occurs on the water surface and

$(\xi - \xi_0)/(\xi_{\max} - \xi_0)$  can be approximated as  $\frac{y}{D}$ . Figure (2.4) illustrates the velocity distributions

using Eq. (2.15) with the relation of Eq. (2-24) for  $M$  from 1 to 5.6. The locations of  $u_{\max}$ ,  $\bar{u}$  and  $\bar{u}_v$  on each of these velocity profiles are also shown in the Figure, in which  $\bar{u}_v$  is the mean velocity on the  $y$  axis. Figure (2-4) shows that when  $M$  is less than 5.6,  $u_{\max}$  occurs below the water surface and the location of  $u_{\max}$  dips deeper into water as  $M$  decreases. When  $M = 5.6$ ,  $u_{\max}$  occurs on the water surface, and isovels in a channel section are orthogonal to the water surface. From this figure, it is also easy to visualize the variations of velocity distribution at various channel cross sections.

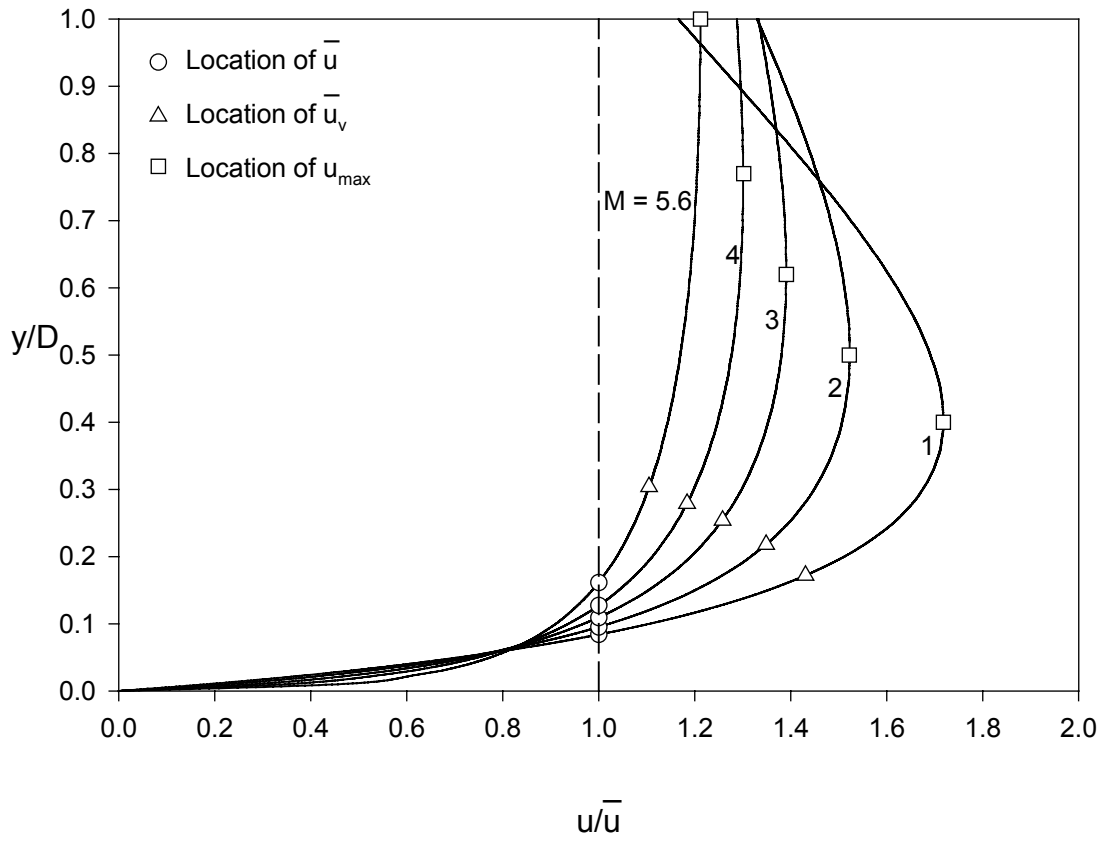


Figure 2.4 Variations of Velocity Distribution and Locations of  $\bar{u}$ ,  $\bar{u}_v$  and  $u_{\max}$  with  $M$

## 2.6 FUCTIONAL RELATIONS OF $\bar{u}/u_D$ , $\bar{u}/\bar{u}_v$ , $\bar{y}/D$ AND $\bar{y}_v/D$ TO $M$

### 2.6.1 Relation between $\bar{u}$ and $u_D$

By substituting Eq. (2-19) into Eq. (2-15), the velocity distribution on y axis can be expressed as

$$u = \frac{\bar{u}}{M\phi} \ln \left[ 1 + (e^M - 1) \frac{y}{D-h} \exp \left( 1 - \frac{y}{D-h} \right) \right] \quad (2-26)$$

Eq. (2-26) gives a different expression of the velocity distribution in comparison with Eq. (2-15). Substituting  $y = D$  into Eq. (2-26), the velocity on the water surface can be determined.

Therefore, the ratio of the cross-sectional mean velocity  $\bar{u}$  to the water surface velocity  $u_D$  on the y axis as a function of  $M$  can be expressed as follows:

$$\frac{\bar{u}}{u_D} = \frac{M\phi}{K(M)} = a(M) \quad 1 \leq M \leq 5.6 \quad (2-27)$$

where

$$k(M) = \ln \left[ 1 + (e^M - 1) \frac{1}{1 - \frac{h}{D}(M)} \exp \left( 1 - \frac{1}{1 - \frac{h}{D}(M)} \right) \right] \quad (2-28)$$

### 2.6.2 Relation between $\bar{u}$ and $\bar{u}_v$

The mean velocity along the y axis can be expressed as

$$\bar{u}_v = \frac{1}{D} \int_0^D u dy \quad (2-29)$$

in which velocity  $u$  can be expressed by either Eq. (2-26) or (2-15). By combining Eq. (2-26)

and (2-29), the ratio of the cross-sectional mean velocity  $\bar{u}$  to the vertical mean velocity  $\bar{u}_v$  on

the y-axis as a function of  $M$  can be expressed as:

$$\frac{\bar{u}}{\bar{u}_v} = \frac{M\phi}{I(M)} = b(M) \quad 1 \leq M \leq 5.6 \quad (2-30)$$

where

$$I(M) = \int_0^1 \ln \left[ 1 + (e^M - 1) \frac{\frac{y}{D}}{1 - \frac{h}{D}(M)} \exp \left( 1 - \frac{\frac{y}{D}}{1 - \frac{h}{D}(M)} \right) \right] d \left( \frac{y}{D} \right) \quad (2-31)$$

### 2.6.3 Relation between $\bar{y}/D$ and $M$

Eq. (2-1) can be written for the mean velocity in the channel cross section with  $\xi_0 = 0$  :

$$\frac{\bar{u}}{u_{\max}} = \phi = \frac{1}{M} \ln \left[ 1 + (e^M - 1) \frac{\bar{\xi}}{\xi_{\max}} \right] \quad (2-32)$$

in which  $\bar{\xi}$  is  $\xi$  at which  $u = \bar{u}$ . When  $u_{\max}$  occurs at  $y = D - h$ ,  $\xi_{\max} = 1$  and hence  $\bar{\xi}/\xi_{\max}$  can be expressed on the  $y$  axis as:

$$\frac{\bar{\xi}}{\xi_{\max}} = \frac{\frac{\bar{y}}{D}}{1 - \frac{h}{D}} \exp \left( 1 - \frac{\frac{\bar{y}}{D}}{1 - \frac{h}{D}} \right) \quad (2-33)$$

$\bar{y}/D$  in Eq. (2-33) is the location of the point on  $y$  axis at which the velocity is equal to  $\bar{u}$ .

Substitution of Eq. (2-33) into Eq. (2-32) gives the relation among  $M$ ,  $h/D$  and  $\bar{y}/D$  when  $u_{\max}$  occurs below the water surface. Furthermore, Eqs. (2-32) and (2-33) combined with Eq. (2-24) yield that  $\bar{y}/D$  can be expressed in terms of  $M$ . In other words, when  $u_{\max}$  occurs below the water surface,  $\bar{y}/D$  and  $h/D$  are constant at a given channel section and hence  $M$  is known.

To maintain the two constants at a channel section over various discharges, the point at which  $u_{\max}$  occurs dips deeper below the water surface when the discharge or the water depth  $D$  increases.

#### 2.6.4 Relation between $\bar{y}_v/D$ and $M$

Eq. (2-26) is equivalent to:

$$\frac{\bar{u}_v}{\bar{u}} = \frac{1}{M\phi} \ln \left[ 1 + (e^M - 1) \frac{\bar{\xi}_v}{\bar{\xi}_{\max}} \right] \quad (2-34)$$

in which  $\bar{\xi}_v$  is  $\xi$  at which  $u = \bar{u}_v$ . When  $u_{\max}$  occurs at  $y = D - h$ ,  $\bar{\xi}_{\max} = 1$  and hence  $\bar{\xi}_v / \bar{\xi}_{\max}$  can be expressed on the  $y$  axis as:

$$\frac{\bar{\xi}_v}{\bar{\xi}_{\max}} = \frac{\frac{\bar{y}_v}{D}}{1 - \frac{h}{D}} \exp \left( 1 - \frac{\frac{\bar{y}_v}{D}}{1 - \frac{h}{D}} \right) \quad (2-35)$$

$\bar{y}_v/D$  in Eq. (2-35) is the location of  $\bar{u}_v$  on  $y$  axis.

Substitution of Eq. (2-35) into Eq. (2-34) gives

$$\frac{\bar{u}_v}{\bar{u}} = \frac{1}{M\phi} \ln \left[ 1 + (e^M - 1) \frac{\frac{\bar{y}_v}{D}}{1 - \frac{h}{D}} \exp \left( 1 - \frac{\frac{\bar{y}_v}{D}}{1 - \frac{h}{D}} \right) \right] \quad (2-36)$$

Eq. (2-36) shows the relation among  $M$ ,  $h/D$  and  $\bar{y}_v/D$  when  $u_{\max}$  occurs below the water surface. With the relationship between  $h$  and  $M$  given by Eq. (2-24),  $\bar{u}_v/\bar{u}$  in Eq. (2-36) is equal to  $1/b(M)$  and hence a function of  $M$ . Therefore,  $\bar{y}_v/D$  in Eq. (2-36) also is a function of  $M$ .

### 3.0 2-D VELOCITY DISTRIBUTION IN RECTANGULAR CHANNELS

#### 3.1 THE FUNCTION OF $N_i$ IN 2-D ISOVELS

According to Eq. (2-10), if the channel is rectangular, both  $\delta_x$  and  $\delta_y$  are equal to zero. As y axis is located at the middle of the channel section, it is symmetric at both sides. Therefore, the value of  $N_i$  at each side of y axis is equal to  $N$  ( $N_1 = N_2 = N$ ). At a given cross section,  $M$  is known and  $h$  can be obtained  $M$  from by Eq. (2-24), Thus, Eq. (2-1) only has  $N$  as the unknown parameter. Therefore, once  $N$  is determined, a two-dimensional velocity distribution can be simulated by Eq. (2-10) and Eq. (2-1). Figure 3.1 shows a simulated two-dimensional velocity distribution in a rectangular channel with the channel width = 2 m, the water depth = 1 m,  $u_{\max} = 1$  m/s,  $M = 3$ ,  $h = 0.377$ , and  $N = 1$ . Since  $N = 1$  is assumed, this isovel pattern may not be the exact image when it comes to the practical cases. By using the same condition as Figure 3.1 except different values of  $N$ , Figures 3.2 (a-b) indicate the variations of velocity distribution. Comparing Figure 3.1 with Figure 3.2 (e.g. look at a certain isovel among the three figures, says an isovel line of  $u = 0.2$  m/s), it is apparent that in the case of  $N = 0.6$ , the location of the isovel is closer to the bank of a channel cross section than the one when  $N = 1.6$ . The smaller values of  $N$ , the greater will be velocities near the left or right bank of a channel cross section. Thus, it is possible to use a smaller  $N_i$  to describe a velocity distribution with greater velocities occurring near the boundary.

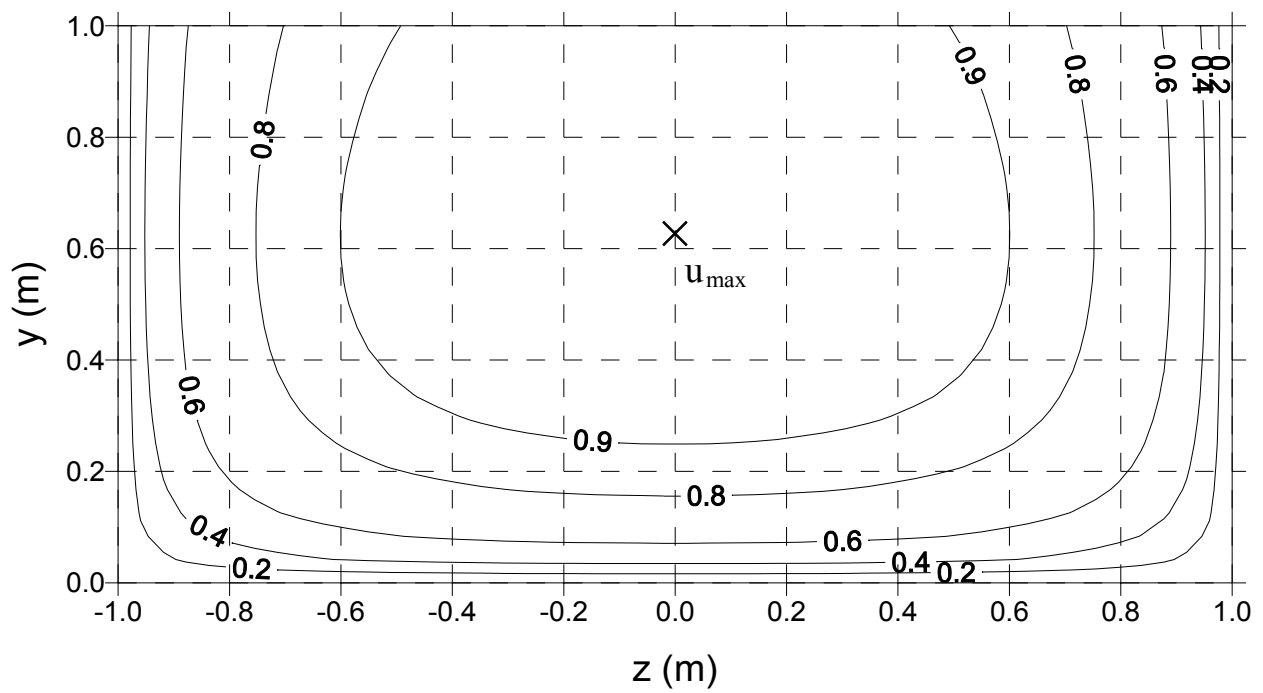
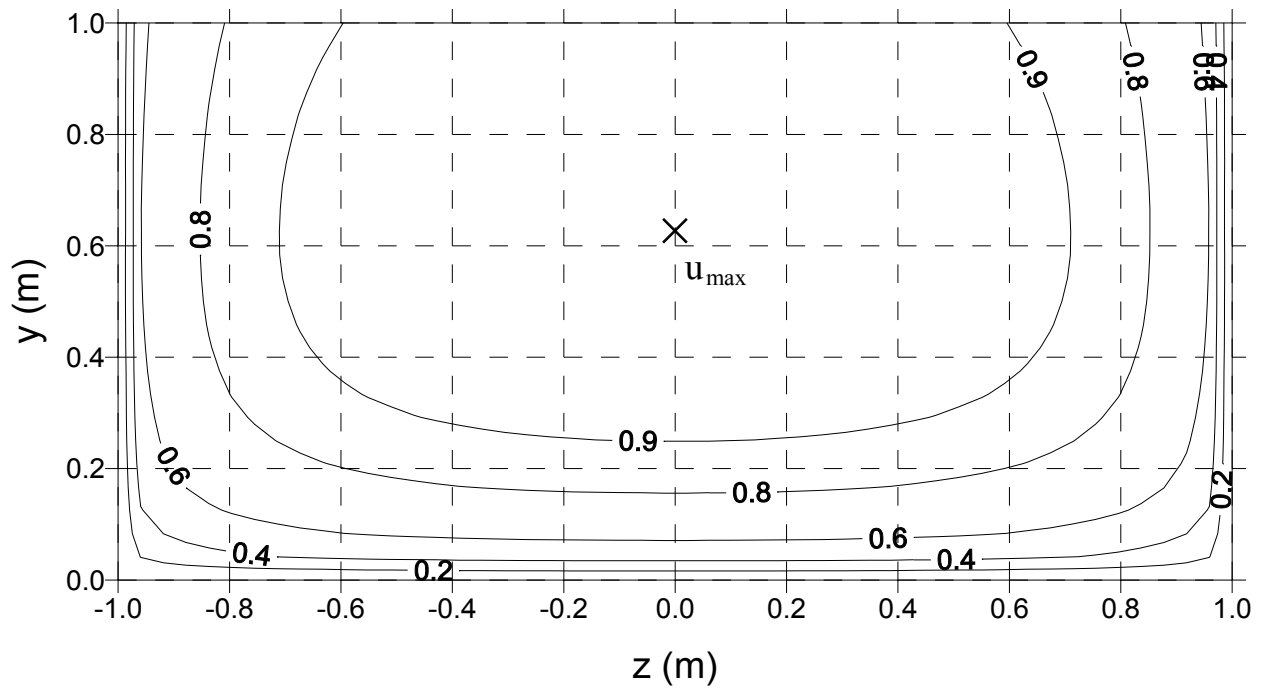
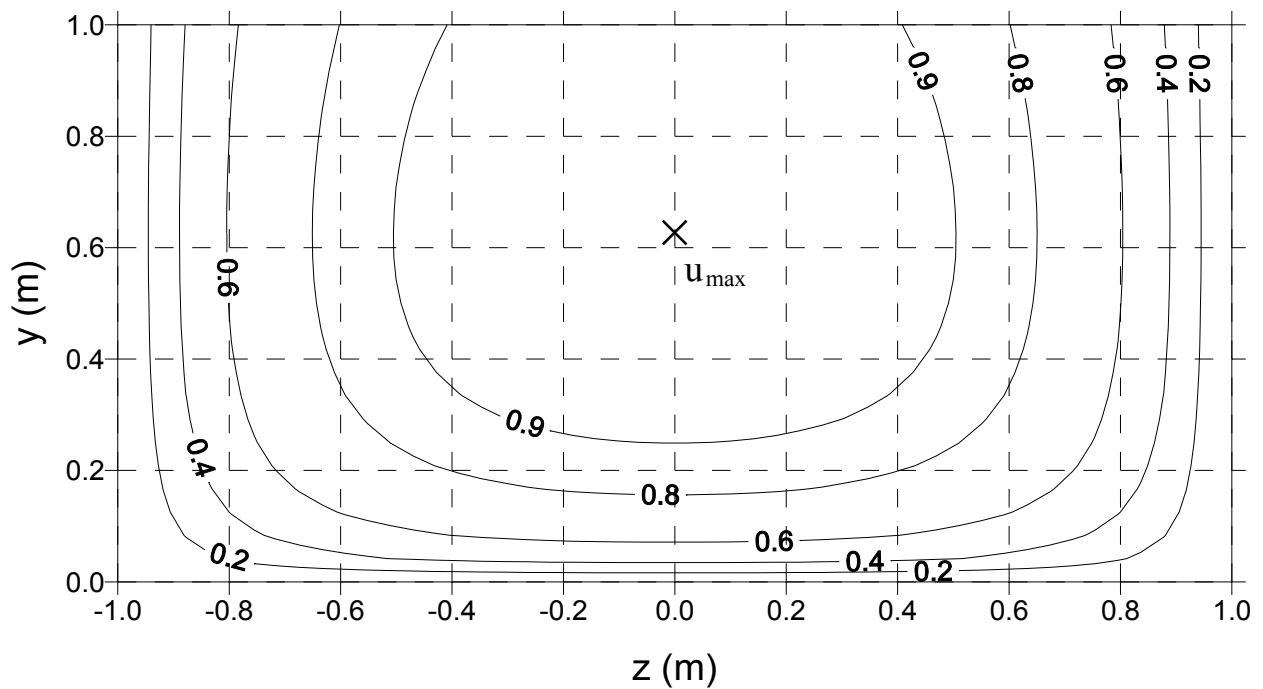


Figure 3.1 Simulated 2-D Velocity Distribution



(a)



(b)

Figure 3.2 Comparison of 2-D Velocity Distributions with Different  $N$  (a)  $N = 0.6$ ; (b)  $N = 1.6$

## 3.2 ESTIMATION OF $N$

### 3.2.1 Relation between $N$ and $M$

In accordance with analysis in section 3.1,  $N$  is the only parameter left in simulating the two-dimensional velocity distribution when  $M$  is known. Hence as long as a relationship between  $N$  and  $M$  can be learned, simulation of the two-dimensional velocity distribution will be greatly simplified. The following analysis represents such an attempt.

The procedure of estimating  $N$  at a given cross section is listed below:

1. Compute the mean velocity  $\bar{u}$  and the discharge  $Q_{obs}$  at a given cross section by the Manning formula with given values of the channel width  $B$ , the water depth  $D$ , the channel slope  $S$ , and the roughness coefficient  $n$ .
2. Use Eq. (2-19) with a known  $M$  and the computed  $\bar{u}$  from step 1, to determine  $u_{max}$ .
3. Determine the location of  $u_{max}$  from the value of  $h$  as a function of  $M$ .
4. Determine  $N$  from the known values of  $M$ ,  $u_{max}$ ,  $h$  and  $D$  by means of Eq. (2-1) to generate the velocity data as many as possible in the entire section.
5. Compute the discharge  $Q_{est}$  with the computed velocities from step 4, using the conventional two-point method (Chow 1959), in which velocities are taken at 0.2 and 0.8 of the water depth at each vertical.
6. Compare  $Q_{est}$  with  $Q_{obs}$ .
7. If  $|Q_{est} - Q_{obs}| > 0.001$ , repeat step 4 to 6 until a reasonable  $N$  may be found.

Based on the above procedure, different  $M$  (ranging from 1 to 5.6) and the corresponding  $N$  are computed and listed in Table 3-1. The simulated  $N - M$  relation is plotted

in Figure 3.3. Thus, the parameter  $N$  can be estimated through the N-M relation. In engineering practice, either Table 3-1 or Figure 3.3 may be used to estimate  $N$ .

Table 3-1 Summary of  $N$  and  $M$

M	N	M	N	M	N	M	N
1	1.630	2.2	1.715	3.4	1.556	4.6	1.342
1.1	1.657	2.3	1.709	3.5	1.538	4.7	1.324
1.2	1.677	2.4	1.700	3.6	1.522	4.8	1.306
1.3	1.693	2.5	1.689	3.7	1.504	4.9	1.288
1.4	1.706	2.6	1.677	3.8	1.486	5.0	1.270
1.5	1.717	2.7	1.665	3.9	1.468	5.1	1.254
1.6	1.724	2.8	1.651	4.0	1.450	5.2	1.236
1.7	1.729	2.9	1.637	4.1	1.432	5.3	1.218
1.8	1.730	3.0	1.622	4.2	1.414	5.4	1.200
1.9	1.730	3.1	1.606	4.3	1.396	5.5	1.182
2.0	1.728	3.2	1.590	4.4	1.378	5.6	1.164
2.1	1.722	3.3	1.572	4.5	1.360		

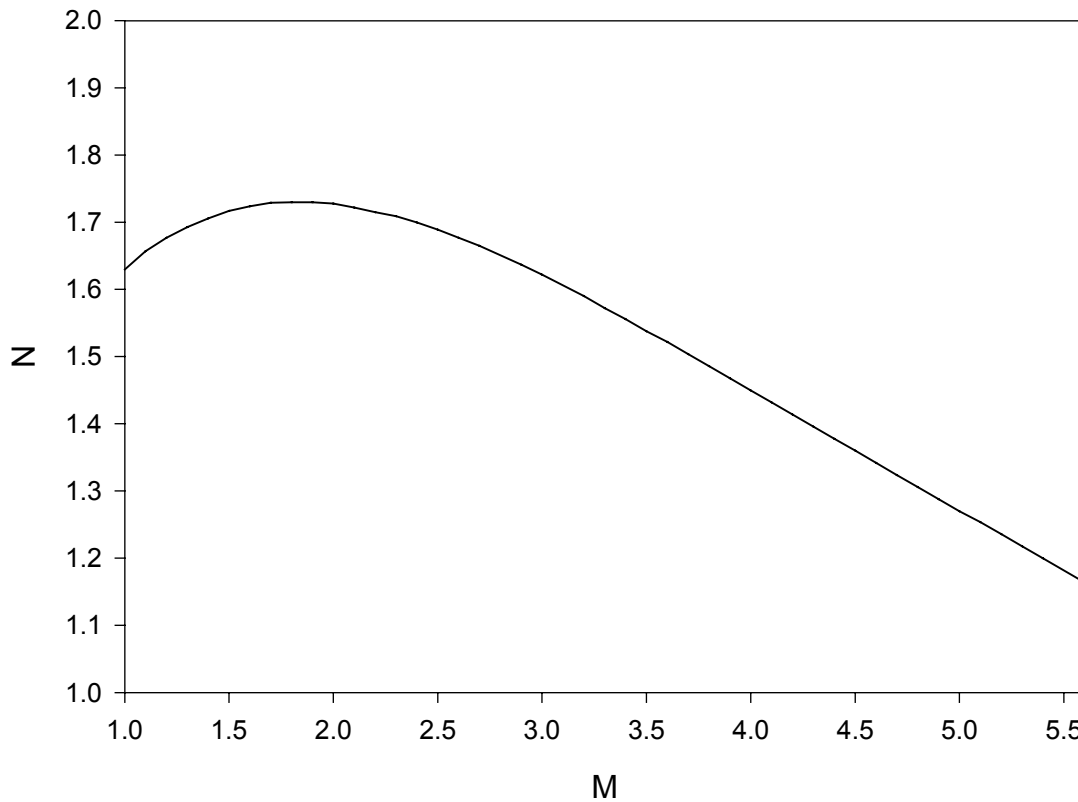


Figure 3.3 Relationship between  $N$  and  $M$  (Simulation)

### 3.2.2 Relation between $N$ and $B/D$ , $n$ and $S$

A set of values of  $B/D$ , Manning's  $n$ , and channel slope  $S$  must be given prior to estimating  $N$  at a given cross section. Varying one of these three variables while keeping the other two constant, its correlation with  $N$  can be compared. Table 3-2 shows  $N$  does not vary with the width-to-depth ratio. Similarly, effects of  $n$  and  $S$  were also analyzed. Table 3-3 indicates  $N$  remains constant as Manning's  $n$  varies from 0.015 to 0.045. Table 3-4 shows that  $N$  does not vary with the channel slope. Therefore, there are no apparent relationships between  $N$  and  $B/D$ ,  $n$  and  $S$ .

Moreover, the three tables also show that  $N$  does not vary with discharge at a channel section. Accordingly,  $N$  is constant at a given channel section.

Table 3-2 Relation between  $N$  and  $B/D$  ( $n = 0.03$ ,  $S = 0.0001$ )

B/D = 2, D = 1 m			
$\bar{u} = 0.21$ m/s, $Q = 0.42$ m <sup>3</sup> /s			
$M$	$u_{\max}$	$h/D$	$N$
2	0.3198	0.4967	1.728
3	0.292	0.3771	1.622
4	0.2732	0.2415	1.450
5	0.2603	0.0934	1.270
B/D = 5, D = 1 m			
$\bar{u} = 0.27$ m/s, $Q = 1.33$ m <sup>3</sup> /s			
$M$	$u_{\max}$	$h/D$	$N$
2	0.4057	0.4967	1.728
3	0.3704	0.3771	1.622
4	0.3465	0.2415	1.450
5	0.3301	0.0934	1.270
B/D = 10, D = 1 m			
$\bar{u} = 0.30$ m/s, $Q = 2.95$ m <sup>3</sup> /s			
$M$	$u_{\max}$	$h/D$	$N$
2	0.4496	0.4967	1.728
3	0.4105	0.3771	1.622
4	0.384	0.2415	1.450
5	0.3659	0.0934	1.270

Table 3-3 Relation between  $N$  and Manning's  $n$  ( $B/D = 2, S = 0.0001$ )

n = 0.015			
$\bar{u} = 0.42 \text{ m/s}, Q = 0.84 \text{ m}^3/\text{s}$			
$M$	$u_{\max}$	$h/D$	$N$
2	0.6397	0.4967	1.728
3	0.5841	0.3771	1.622
4	0.5464	0.2415	1.450
5	0.5206	0.0934	1.270
n = 0.030			
$\bar{u} = 0.21 \text{ m/s}, Q = 0.42 \text{ m}^3/\text{s}$			
$M$	$u_{\max}$	$h/D$	$N$
2	0.3198	0.4967	1.728
3	0.292	0.3771	1.622
4	0.2732	0.2415	1.450
5	0.2603	0.0934	1.270
n = 0.045			
$\bar{u} = 0.14 \text{ m/s}, Q = 0.28 \text{ m}^3/\text{s}$			
$M$	$u_{\max}$	$h/D$	$N$
2	0.2132	0.4967	1.728
3	0.1947	0.3771	1.622
4	0.1821	0.2415	1.450
5	0.1735	0.0934	1.270

Table 3-4 Relation between  $N$  and  $S$  ( $B/D = 2, n = 0.03$ )

S = 0.0001			
$\bar{u} = 0.21 \text{ m/s}, Q = 0.42 \text{ m}^3/\text{s}$			
$M$	$u_{\max}$	$h/D$	$N$
2	0.3198	0.4967	1.728
3	0.292	0.3771	1.622
4	0.2732	0.2415	1.450
5	0.2603	0.0934	1.270
S = 0.001			
$\bar{u} = 0.66 \text{ m/s}, Q = 1.33 \text{ m}^3/\text{s}$			
$M$	$u_{\max}$	$h/D$	$N$
2	1.0115	0.4967	1.728
3	0.9235	0.3771	1.622
4	0.8639	0.2415	1.450
5	0.8231	0.0934	1.270
S = 0.01			
$\bar{u} = 2.10 \text{ m/s}, Q = 4.20 \text{ m}^3/\text{s}$			
$M$	$u_{\max}$	$h/D$	$N$
2	3.1985	0.4967	1.728
3	2.9203	0.3771	1.622
4	2.7319	0.2415	1.450
5	2.6028	0.0934	1.270

### 3.2.3 Verification of Relation between $N$ and $M$

In order to simulate two-dimensional velocity distributions in rectangular channels, some parameters such as  $N$ ,  $M$ ,  $h$ , and  $u_{\max}$  should be obtained in advance when using equation (2.1). Once  $M$  is given,  $h$  can be obtained from Eq. (2-24).  $u_{\max}$  is determined from  $M$ , and  $\bar{u}$  computed by using Manning's formula.  $N$  is obtained by a try-and-error method with the criterion that the discharge computed with a value of  $N$  must be equal to observed one. However, values of  $B/D$ , Manning's  $n$ , and  $S$  must be known prior to estimating  $N$ . Manning's  $n$  and  $S$  are difficult to obtain in natural rivers. The velocity data are easier to obtain. Thus, it is easier to estimate  $M$ ,  $h$  and  $u_{\max}$  at a channel section from velocity data.

#### **Description of data**

Data for this study were collected from rectangular channels. Velocity data may be collected along one or more verticals in a channel section. Four sets of data obtained by Guo (1990)<sup>(23)</sup>, Coleman (1990)<sup>(24)</sup>, Bortz (1989)<sup>(25)</sup> and Guy, et al. (1956-1961)<sup>(26)</sup> were used.

- a. Zhen-Ren Guo<sup>(23)</sup> of the South China Institute conducted an experiment in supercritical flows. The channel, 10 cm wide and 180 cm long, had a constant slope of 0.00156. The flow was nonuniform, starting from a head tank and ending at a free fall. All data were collected in a steady flow of 669 cm<sup>3</sup>/s at eleven different sections along the flume. The velocity samplers were taken at the middle of each cross section using a laser-Doppler velocimeter.

- b. The second set of data used in the study were provided by Coleman<sup>(24)</sup>. The experiment was performed in a flume, 1000 mm wide, and was run under different sediment conditions at the channel bed.
- c. The third set of data was obtained by Bortz<sup>(25)</sup> from 43 runs with three different channel slopes. The flume was 65 feet long, with 4 feet wide, and 2 feet deep. The flow rate, water depth, and channel bed slope were all easily adjustable.
- d. The last set of data was obtained by Guy, et al.<sup>(26)</sup> in a recirculating flume, 2 and 8 feet wide, 2 feet deep, and 150 feet long. The flow could be adjusted from 0 to 22 cfs by using two pumps and a valve control on the discharge line. The channel slope could be adjusted from 0 to 1.5 percent.

#### **N value determined from actual data**

When using actual data to determine  $N$ ,  $\bar{u}$  is given, but  $M$ ,  $h$  and  $u_{\max}$  may not be available. A method to estimate these parameters from measured data is to estimate  $u_{\max}$  first by regression using Eq. (2-15) with velocity data on y axis. Once  $u_{\max}$  is obtained,  $M$  can be computed by Eq. (2-19) with the given value of  $\bar{u}$ . After that,  $h$  can be given by Eq. (2-24). When three parameters are all determined,  $N$  can be estimated by following the same steps 4 to 7 of the procedure as given in Section 3.2.1. Results can be verified by using laboratory data as shown in Figure 3.4.

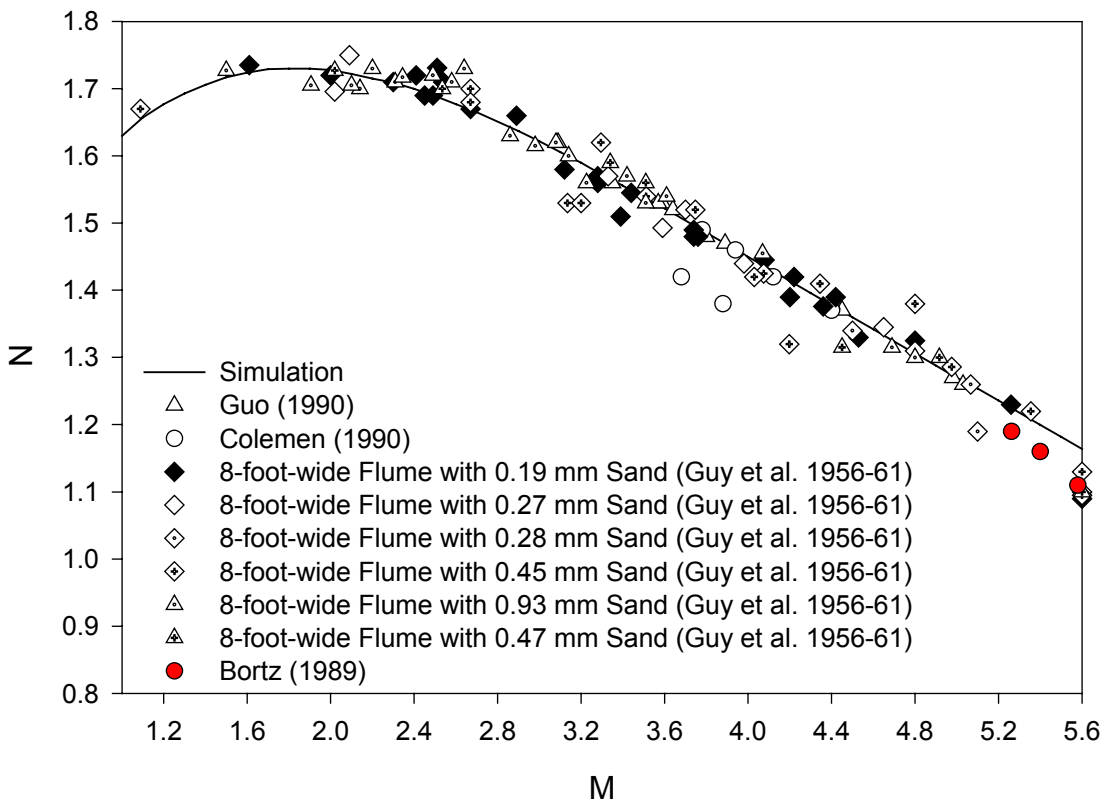


Figure 3.4 Relation between  $N$  and  $M$

### 3.3 MODEL VERIFICATION

Figure 3.5 shows velocity samples on y axis and a two-dimensional velocity distribution computed at section no. 9 in a rectangular channel 10 cm wide and 2.31 cm deep<sup>(23)</sup>. As shown in the figure, the velocities computed by Eq. (2.1) agree with those observed on y axis. Figure 3.6 shows a one-dimensional velocity distribution on y axis with the same velocity samples, and the agreement is as good as those in Figure 3.5. The two figures show the simulated one-dimensional velocity distribution on y axis may indicate a two-dimensional velocity distribution.

Figures 3.7-10 show velocity samples on several verticals and simulated two-dimensional velocity distributions in various rectangular flumes<sup>(26, 27)</sup>. The measured two-dimensional velocities also indicate the accuracy of the simulated velocities as shown in these figures. The performance of this 2-D velocity distribution model can be evaluated from the correlation coefficient ( $\rho$ ) and root-mean-square error (RMSE). The correlation coefficient indicates the strength of association of observed and estimated velocities and is given by

$$\rho = \frac{\sum (u_{obs} - \bar{u}_{obs})(u_{est} - \bar{u}_{est})}{\sqrt{\sum (u_{obs} - \bar{u}_{obs})^2 \sum (u_{est} - \bar{u}_{est})^2}} \quad (3-1)$$

in which  $u_{obs}$  = observed velocity;  $\bar{u}_{obs}$  = mean of observed velocities;  $u_{est}$  = estimated velocity; and  $\bar{u}_{est}$  = mean of estimated velocities.

The root-mean-square error measures the closeness of the observed and estimated velocities and is given by

$$RMSE = \sqrt{\frac{\sum (u_{obs} - u_{est})^2}{n}} \quad (3-2)$$

in which n is the number of observation.

The correlation coefficients of Figures 3.7, 3.8, 3.9 and 3.10 are approx 0.916, 0.942, 0.98 and 0.958, respectively, and RMSEs are approx 0.163 ft/s, 0.226 ft/s, 0.11 ft/s and 0.25 ft/s, respectively. The correlation coefficients are at least above 0.9, and RMSEs are smaller. The results show that the 2-D velocity distribution model can predict velocities quite well in rectangular open channel flow.

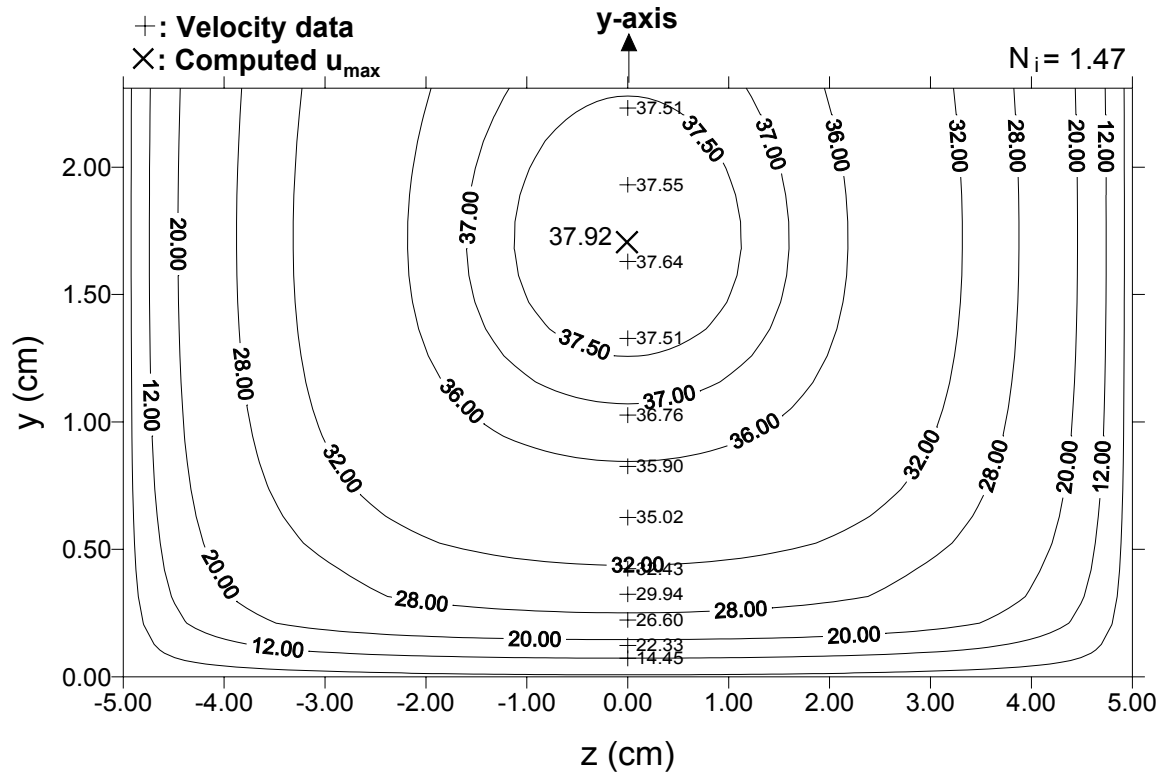


Figure 3.5 Simulated Two-dimensional Velocity Distribution Based in the Rectangular Channel Section on Velocity Samples on Y Axis (Guo 1990)

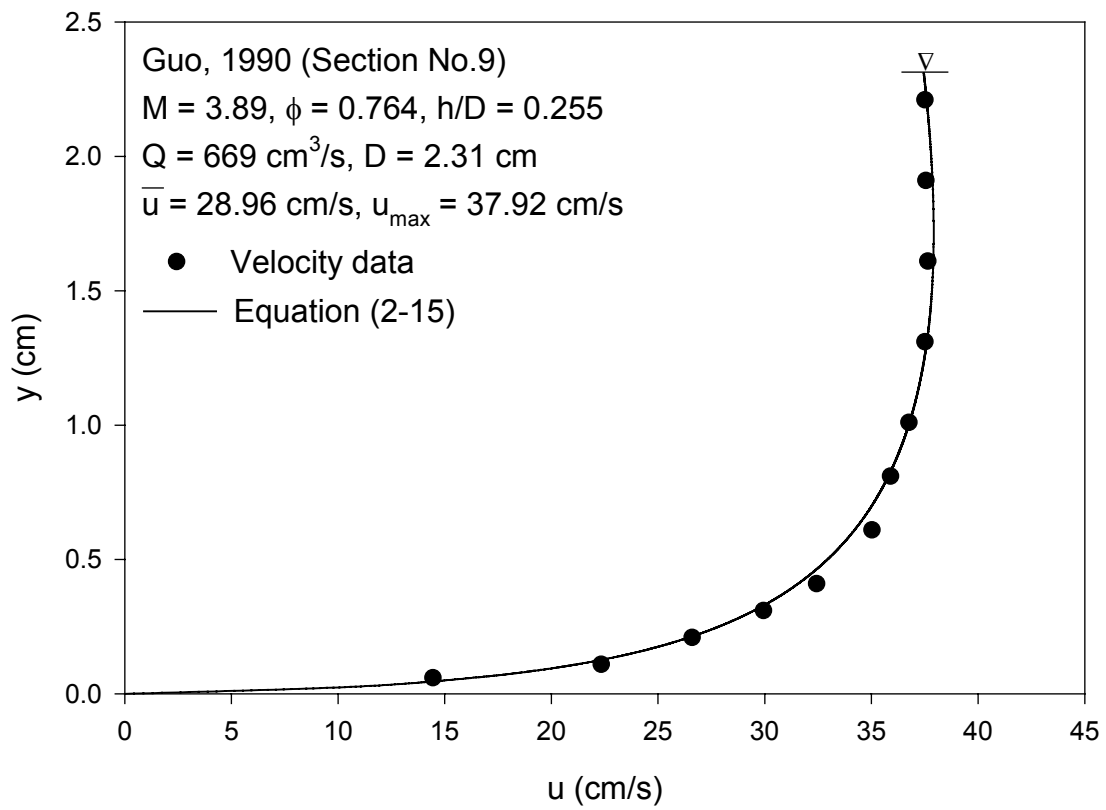


Figure 3.6 Velocity Distribution on y axis (Guo 1990)

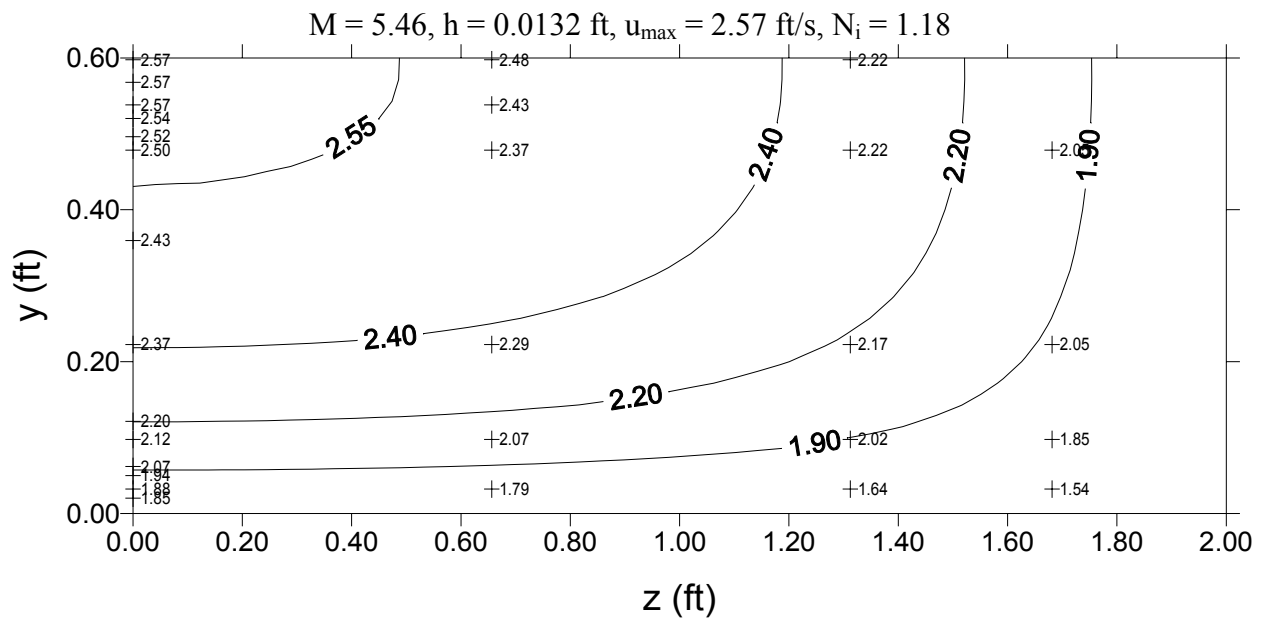


Figure 3.7 Measured and simulated 2D velocities (4-foot wide Flume, Run 41, Bortz 1989)

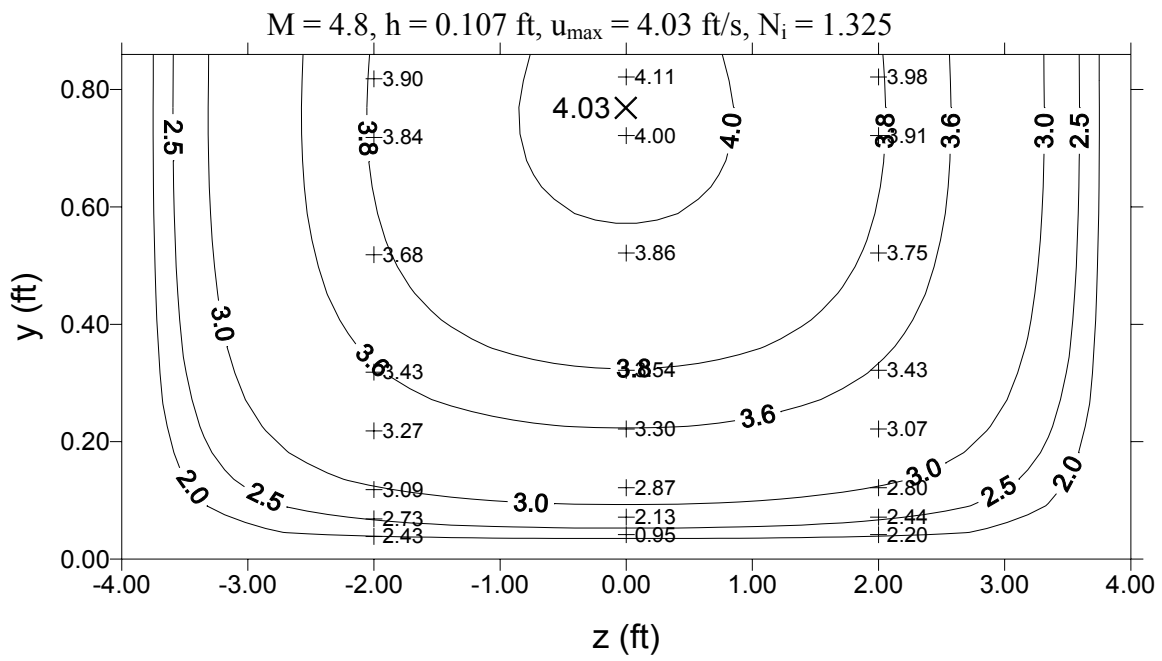


Figure 3.8 Measured and Simulated 2-D Velocities (8-foot Wide Flume with 0.19mm Sand, Run 14, Guy, et al. 1956-61)

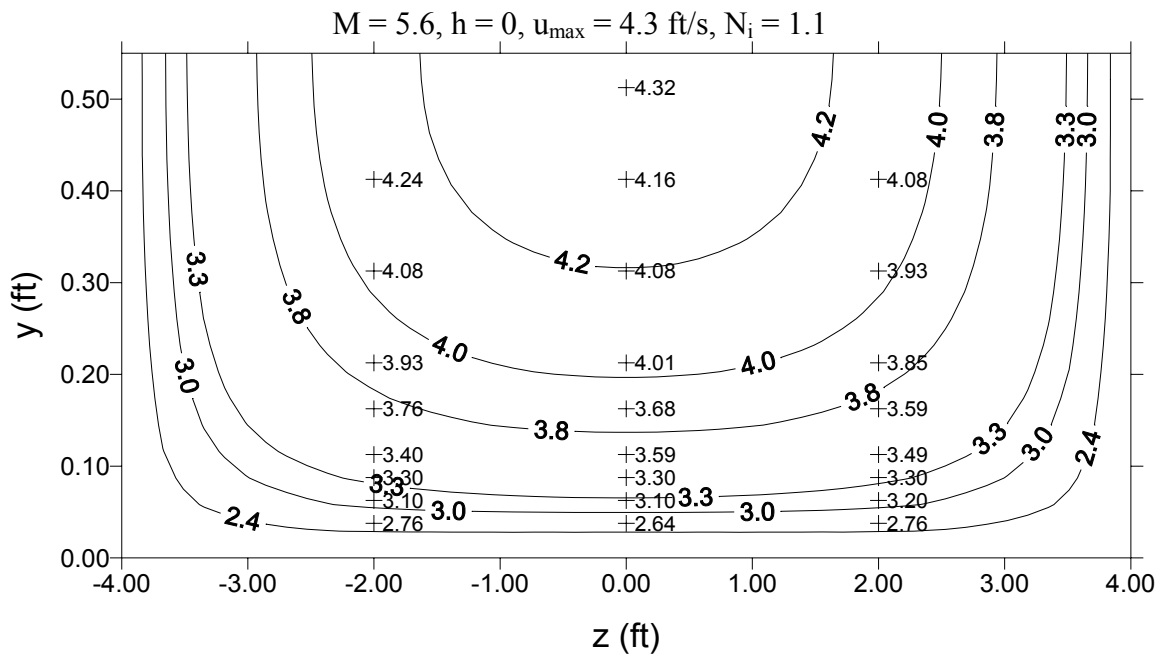


Figure 3.9 Measured and Simulated 2-D Velocities (8-foot Wide Flume with 0.28mm Sand, Run 28, Guy, et al. 1956-61)

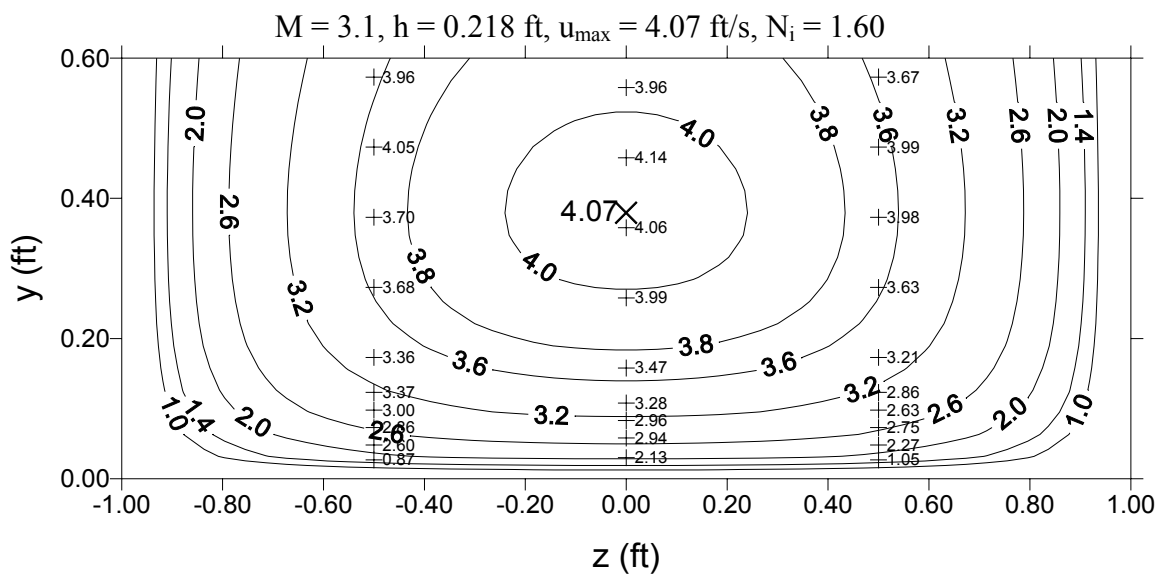


Figure 3.10 Measured and Simulated 2-D Velocities (2-foot Wide Flume with 0.32 mm Sand, Run 7, Guy, et al. 1956-61)

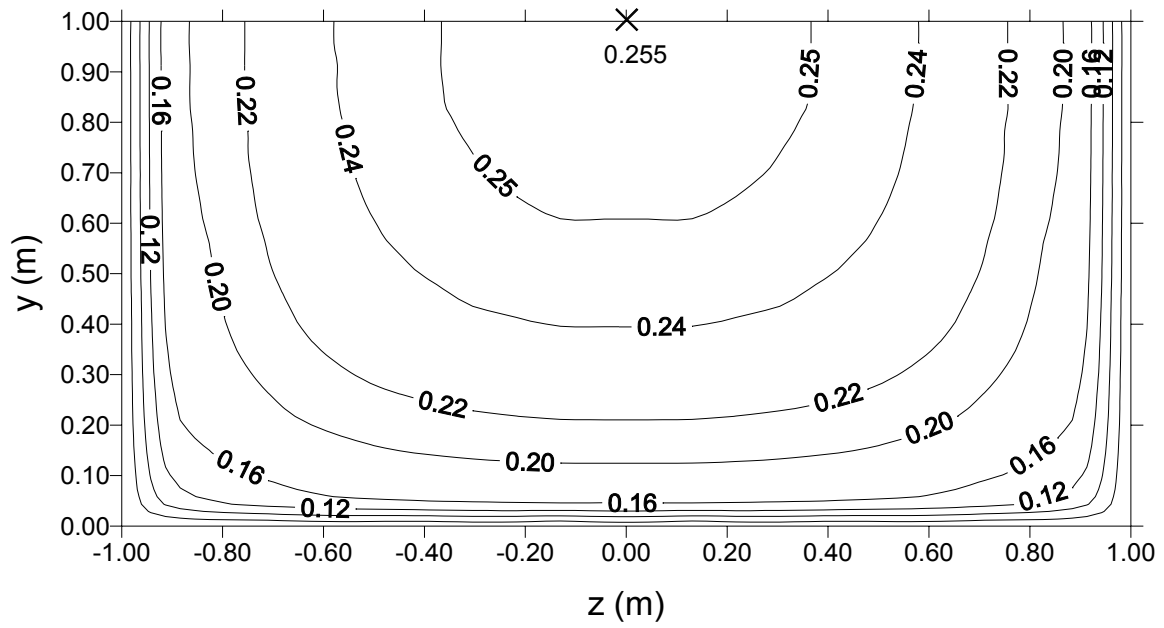
## 3.4 APPLICATION

### 3.4.1 Simulation of 2-D Velocity

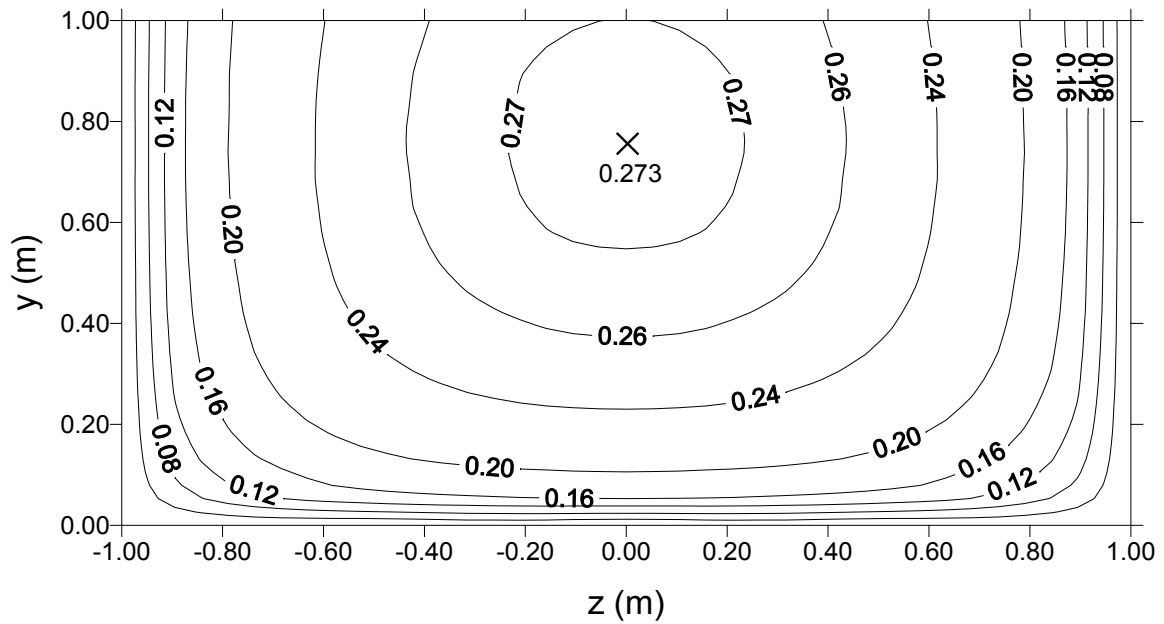
Since  $N$  can be obtained from the relation between  $N$  and  $M$ , if the channel data such as Manning's  $n$ , the channel slope  $S$ , the channel width  $B$  and the water depth  $D$  are known, the two-dimensional velocity distribution can be simulated with any given  $M$  value without using any velocity data. Figures 3.11(a-d) show isovel patterns simulated by using Eq. (2.1) in rectangular channels for various parameters  $M$ , with the Manning's  $n$  of 0.03, the channel slope of 0.0001, the channel width of 2 m and the water depth of 1m, respectively. Various  $M$  may represent different sections along a channel. However, flow patterns along a channel can also be visualized in the four sections as shown in Figure 3.11. For each of the velocity distributions in the figure, the values of  $u_{\max}$ ,  $h$ ,  $M$ , and  $N$  are also indicated. In addition, the mean velocity  $\bar{u}$  for each channel section is 0.21 m/s based on Manning's equation. As shown in Figures 3.11(a-d), the value of  $\bar{u}$  does not change but  $u_{\max}$  and  $h$  vary with  $M$ . It implies that if  $M$  (or  $\phi$ ) decreases,  $u_{\max}$  must increase and its location tends to dip deeper below the water surface in order to retain the constant  $\bar{u}$ . This is similar to the following a bend. When the flow enters a bend from a straight reach, the value of  $\bar{u}$  does not change appreciably but  $u_{\max}$  increases appreciably to reduce  $M$  value, and the location of the maximum velocity dips below the water surface<sup>(5)</sup>.

Figures 3.12(a-c) show other simulation results, which show the relation between the velocity distribution and width-to-depth ratio at a given section; when  $M = 3$ ;  $N = 1.62$ ;

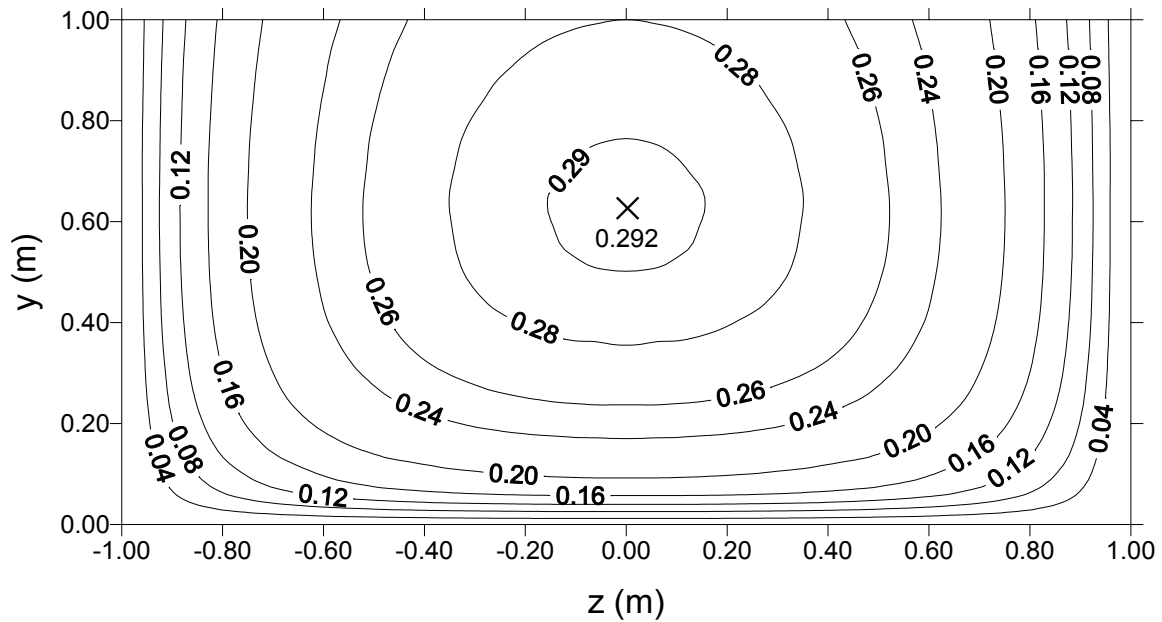
Manning's  $n = 0.03$ ; channel width = 2 m, and channel slope = 0.0001. The values of  $u_{\max}$ ,  $\bar{u}$ ,  
Q and D are indicated in the figure for each of the velocity distributions.



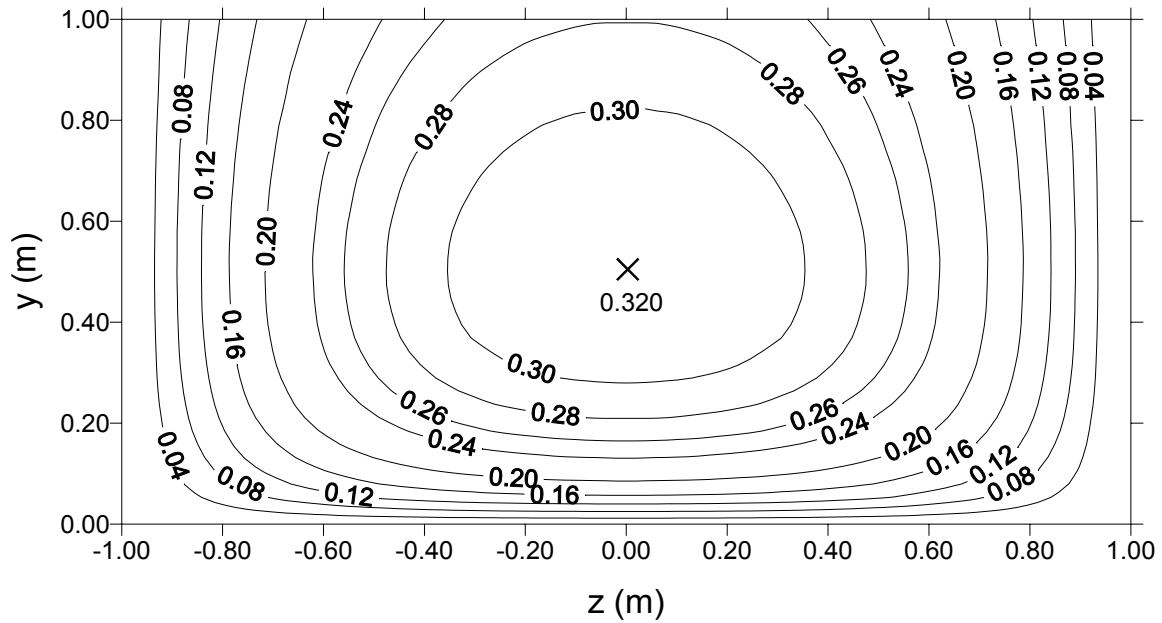
(a)  $M = 5.6$ ,  $h = 0$ ,  $u_{\max} = 0.255$  m/s,  $N_i = 1.16$



(b)  $M = 4$ ,  $h = 0.242$  m,  $u_{\max} = 0.273$  m/s,  $N_i = 1.45$

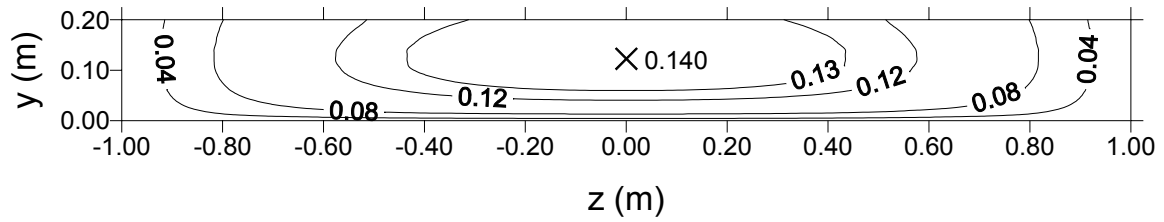


(c)  $M = 3$ ,  $h = 0.377$  m,  $u_{\max} = 0.292$  m/s,  $N_i = 1.62$

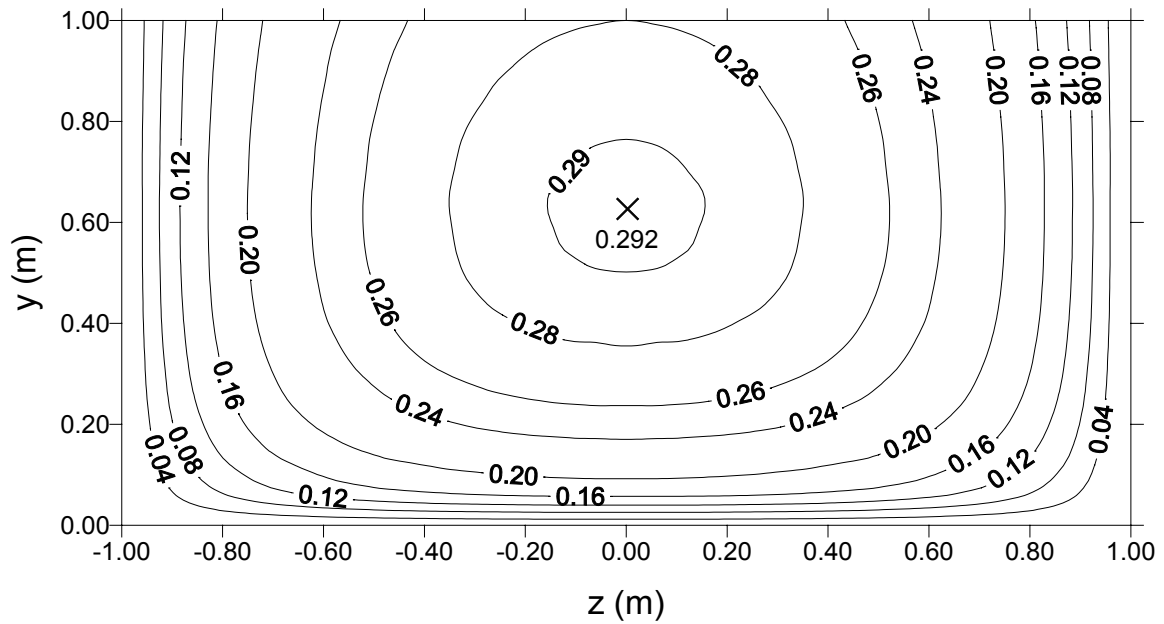


(d)  $M = 2$ ,  $h = 0.479$  m,  $u_{\max} = 0.320$  m/s,  $N_i = 1.73$

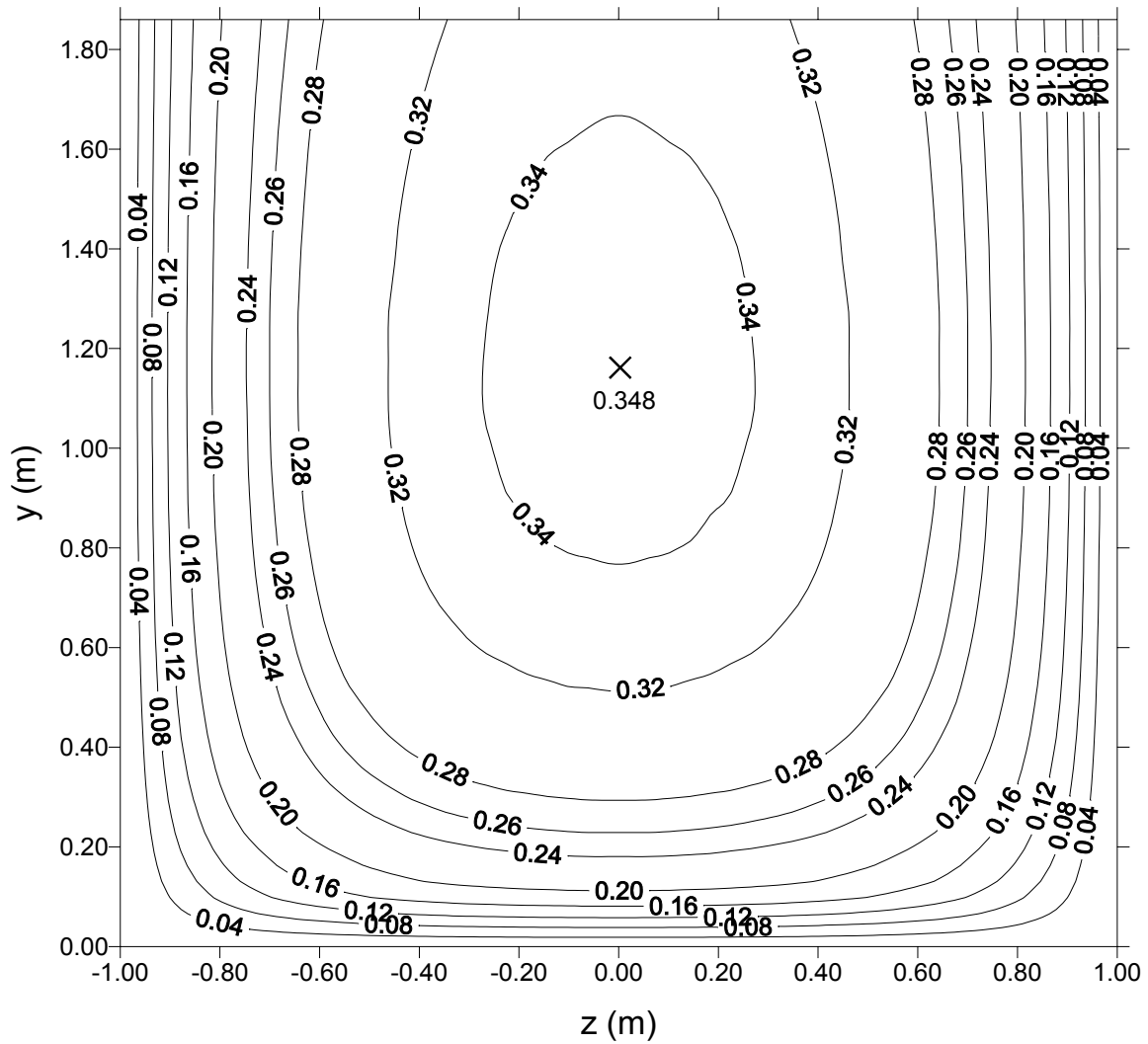
Figure 3.11 Simulations of Two-dimensional Velocity Distribution at Channel Sections where  $n = 0.03$ ,  $S = 0.0001$ ,  $B = 2$  m,  $D = 1$  m  $Q = 0.42$  m<sup>3</sup>/s,  $\bar{u} = 0.21$  m/s. (a)  $M = 5.6$ ,  $h = 0$ ,  $u_{\max} = 0.255$  m/s,  $N_i = 1.16$ ; (b)  $M = 4$ ,  $h = 0.242$  m,  $u_{\max} = 0.273$  m/s,  $N_i = 1.45$ ; (c)  $M = 3$ ,  $h = 0.377$  m,  $u_{\max} = 0.292$  m/s,  $N_i = 1.62$ ; (d)  $M = 2$ ,  $h = 0.479$  m,  $u_{\max} = 0.320$  m/s,  $N_i = 1.73$



(a)  $D = 0.2 \text{ m}$ ,  $h = 0.075 \text{ m}$ ,  $u_{\max} = 0.140 \text{ m/s}$ ,  $\bar{u} = 0.10 \text{ m/s}$ ,  $Q = 0.04 \text{ m}^3/\text{s}$



(b)  $D = 1 \text{ m}$ ,  $h = 0.377 \text{ m}$ ,  $u_{\max} = 0.292 \text{ m/s}$ ,  $\bar{u} = 0.21 \text{ m/s}$ ,  $Q = 0.42 \text{ m}^3/\text{s}$



(c)  $D = 1.86$  m,  $h = 0.700$  m,  $u_{\max} = 0.348$  m/s,  $\bar{u} = 0.25$  m/s,  $Q = 0.93$  m<sup>3</sup>/s

Figure 3.12 Simulations of Two-dimensional Velocity Distribution at Channel Sections where  $M = 3$ ,  $h/D = 0.376$  and  $N = 1.62$ . (a)  $D = 0.2$  m,  $h = 0.075$  m,  $u_{\max} = 0.140$  m/s,  $\bar{u} = 0.10$  m/s,  $Q = 0.04$  m<sup>3</sup>/s; (b)  $D = 1$  m,  $h = 0.377$  m,  $u_{\max} = 0.292$  m/s,  $\bar{u} = 0.21$  m/s,  $Q = 0.42$  m<sup>3</sup>/s; (c)  $D = 1.86$  m,  $h = 0.700$  m,  $u_{\max} = 0.348$  m/s,  $\bar{u} = 0.25$  m/s,  $Q = 0.93$  m<sup>3</sup>/s

### 3.4.2 Estimation of $M$ by simulation of 2-D velocity distribution

A possible application of simulation of two-dimensional velocity distribution is to estimate  $M$ . With velocity distribution parameters other than  $M$  determined, two-dimensional velocity distributions may be simulated with each assumed value of  $M$ . The  $M$  value to be chosen is the one that gives the minimum variance.

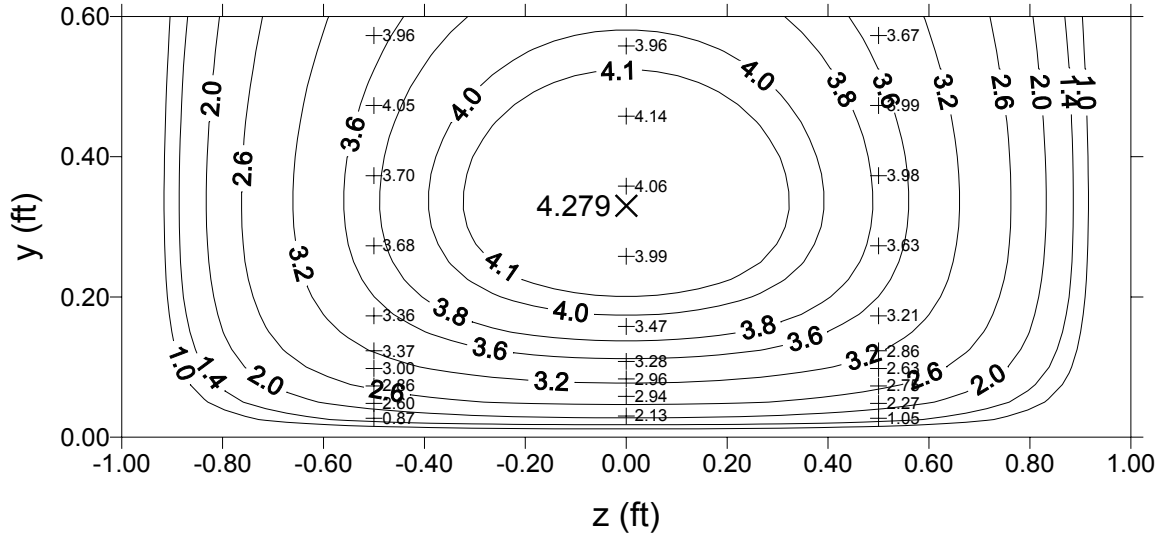
A concise procedure for the estimation approach is described below.

1. Assume a value of  $M$
2. Obtain the corresponding  $N$  from the  $N - M$  relation as shown in Figure 3.3.
3. Obtain the parameters  $u_{\max}$  and  $h$  in Eq (2.1), in which  $u_{\max}$  can be obtained from  $\bar{u}/\phi$  and  $h$  can be determined by Eq. (2-24).
4. Compute the variance for this  $M$ .
5. Return to step 1 until all possible values of  $M$  have been tried. Select  $M$  that gives the smallest variance.

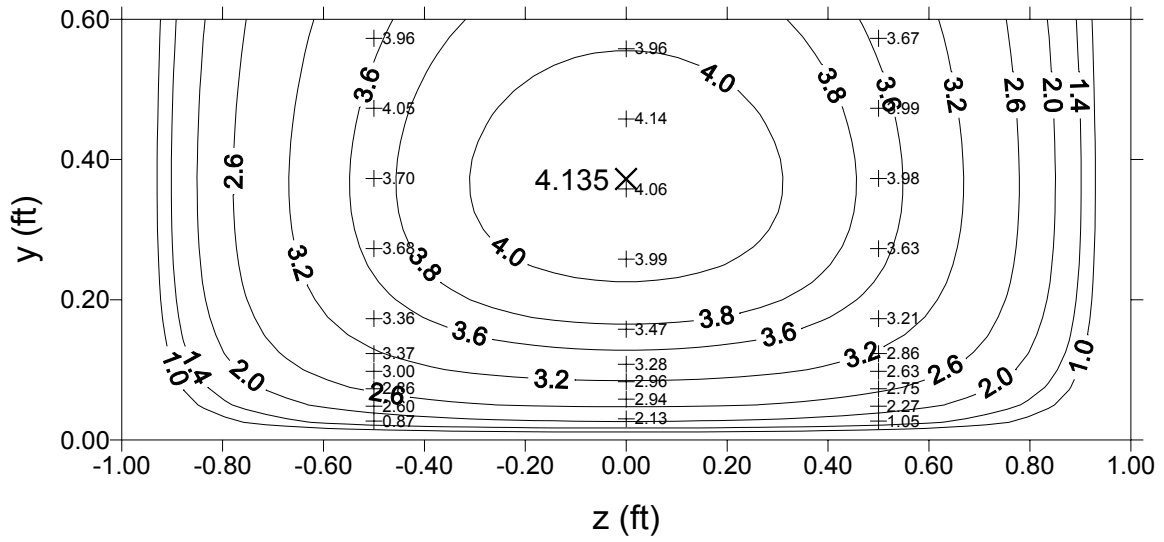
For example, in the velocity data (Run 7) collected by Guy, et al.<sup>(26)</sup> in a 2-foot wide flume with 0.32mm sand,  $M = 3$  gives the minimum variance as shown in Table 3.5. Thus, the optimal value of  $M$  in the cross section is approximately 3 and  $u_{\max} = 4.103$  ft/s, which is close to the measured maximum velocity. The corresponding values of  $N$ ,  $u_{\max}$  and  $h$  for each selected  $M$  are also listed in Table 3-5. Figures 3.13 (a-f) show velocity data in a cross section (Guy, et al. 1956-61) and the computed two-dimensional velocity distribution for each of the selected values of  $M$  ( $M = 2.5, 2.9, 3.0, 3.1, 3.5,$  and  $5.0$ , respectively). The estimated  $u_{\max}$  for each  $M$  and its location are also shown in the Figures, which help determine the possible value of  $M$ .

Table 3-5 Comparison of Variance for the Selected Values of  $M$   
 (2-foot Wide Flume with 0.32 mm Sand, Run 7, Guy, et al., 1956-61)

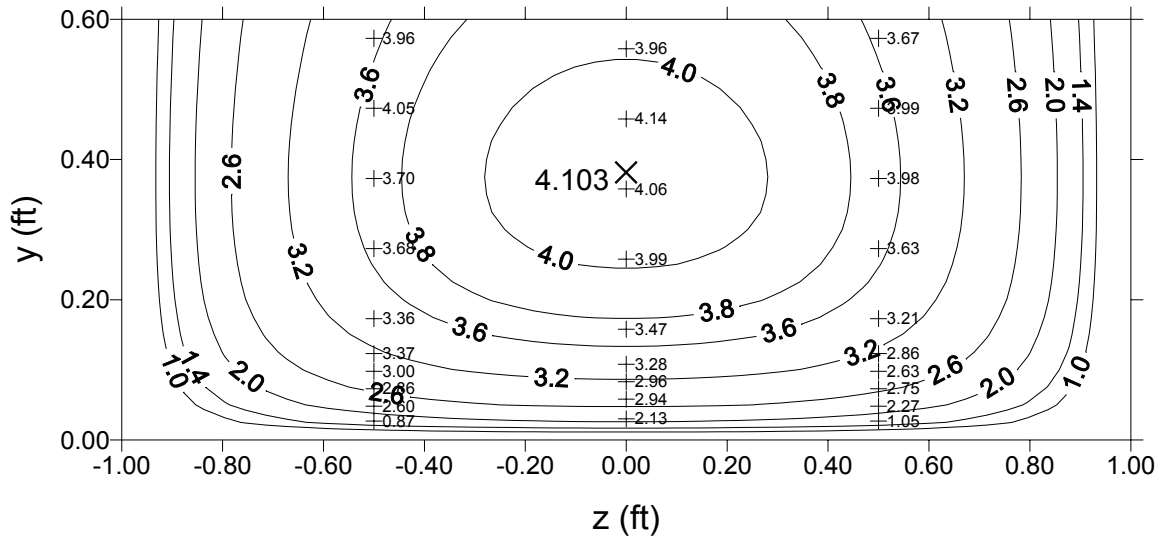
M	N	$u_{\max}$ (ft/s)	h (ft)	Variance (ft/s)
2.0	1.73	4.493	0.298	0.11418
2.5	1.69	4.279	0.263	0.07431
2.7	1.66	4.204	0.249	0.06714
2.8	1.65	4.169	0.241	0.06525
2.9	1.63	4.135	0.234	0.06403
<b>3.0</b>	<b>1.62</b>	<b>4.103</b>	<b>0.226</b>	<b>0.06395</b>
3.1	1.60	4.071	0.219	0.06439
3.2	1.59	4.041	0.211	0.06586
3.5	1.54	3.957	0.187	0.07354
4.0	1.45	3.838	0.145	0.09591
5.0	1.27	3.656	0.056	0.15996



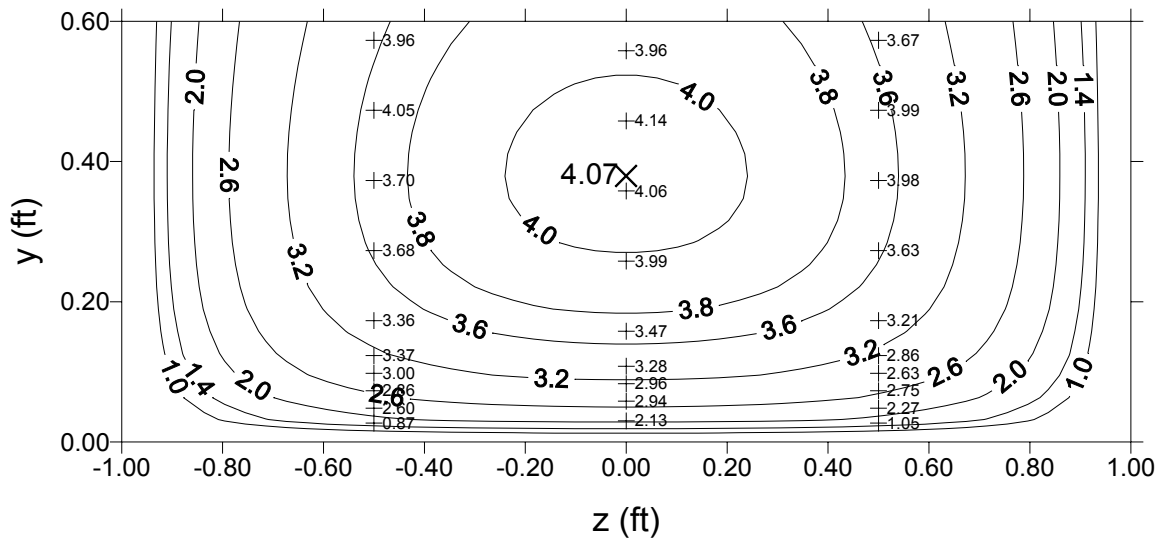
(a)  $M = 2.5$



(b)  $M = 2.9$



(c)  $M = 3$



(d)  $M = 3.1$

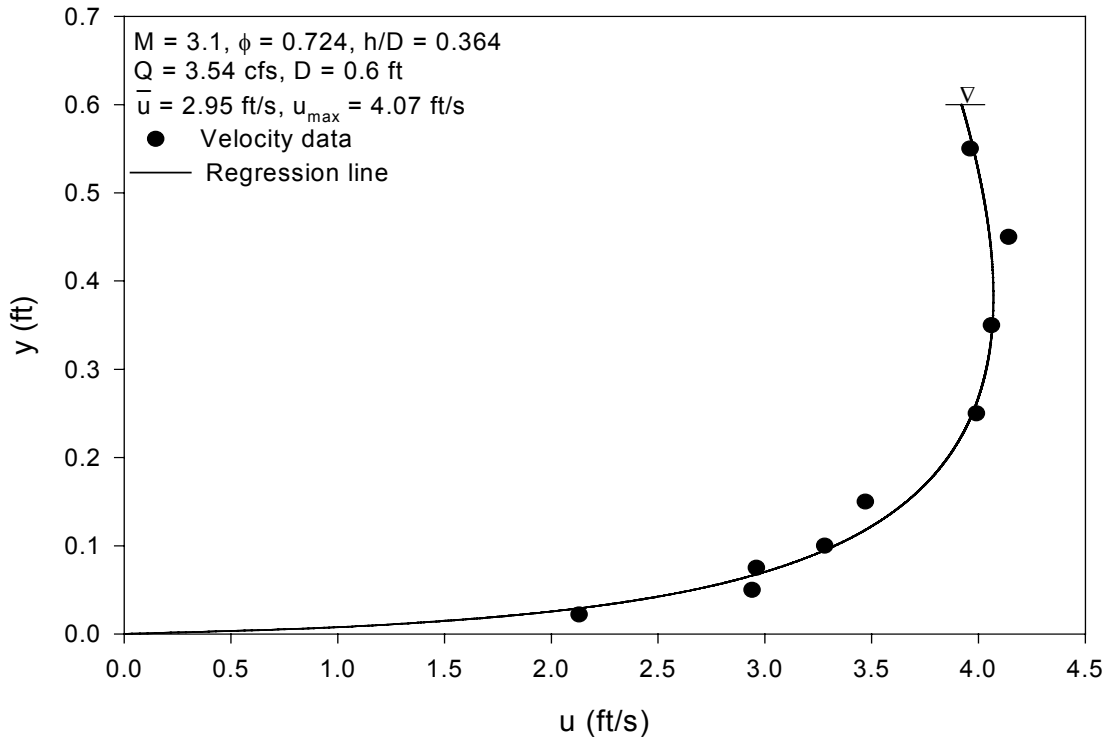


In the preceding analysis of  $M$ , velocity data were taken from several verticals in a cross section. The following study is discussing that the estimation of  $M$  and  $u_{\max}$  only depends on the velocity data of midsection (y-axis). The detailed procedure for estimating  $M$  and  $u_{\max}$  on y-axis is outlined below:

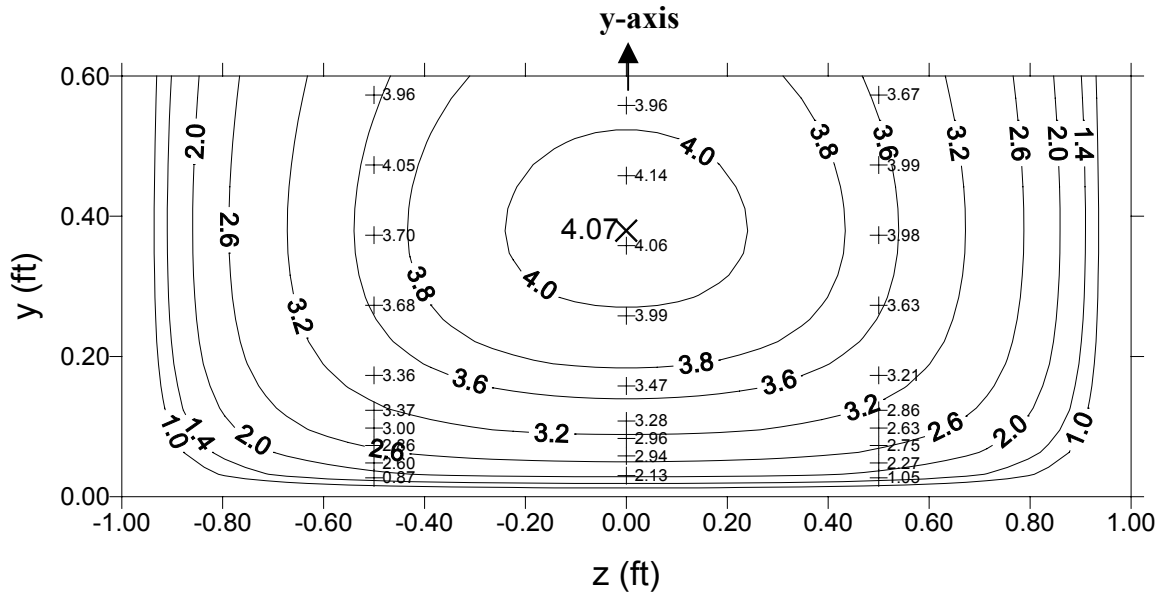
1.  $u_{\max}$  can be determined by the method of least squares.
2.  $M$  can be computed from Eq. (2-19) as  $\bar{u}$  is known.

Based on this procedure,  $u_{\max} = 4.07$  ft/s and  $M = 3.1$  and hence  $h/D = 0.364$  as given by Eq. (2-24). With these three parameters, the velocity distribution on y axis can be shown in Figure 3.14(a). With the N value corresponding to  $M = 3.1$ , the 2-D velocity distribution in the rectangular flume can be computed as shown in Figure 3.14(b), which agrees well with the data.

As compared in Figures 3.13 (c) and 3.14(b),  $M = 3.1$  obtained from velocity samples on y axis is close to that of  $M = 3$  determined by using velocity samples on several verticals, but for  $u_{\max}$ , first approach is better. This implies that if more velocity data on other verticals were available, estimated  $M$  data would be more accurate than that depending on velocity sampler on only one vertical. However, the M value estimated by the second approach can still be acceptable even if velocity data are available only on y axis.



(a) Velocity Distribution on Y Axis



(b) Simulated Two-dimensional Velocity Distribution

Figure 3.14 Estimation of  $M$  from Velocity Samples on Y Axis (a) Velocity distribution on y axis; (b) Simulated two-dimensional velocity distribution

## **4.0 EFFICIENT METHODS OF DISCHARGE ESTIMATION**

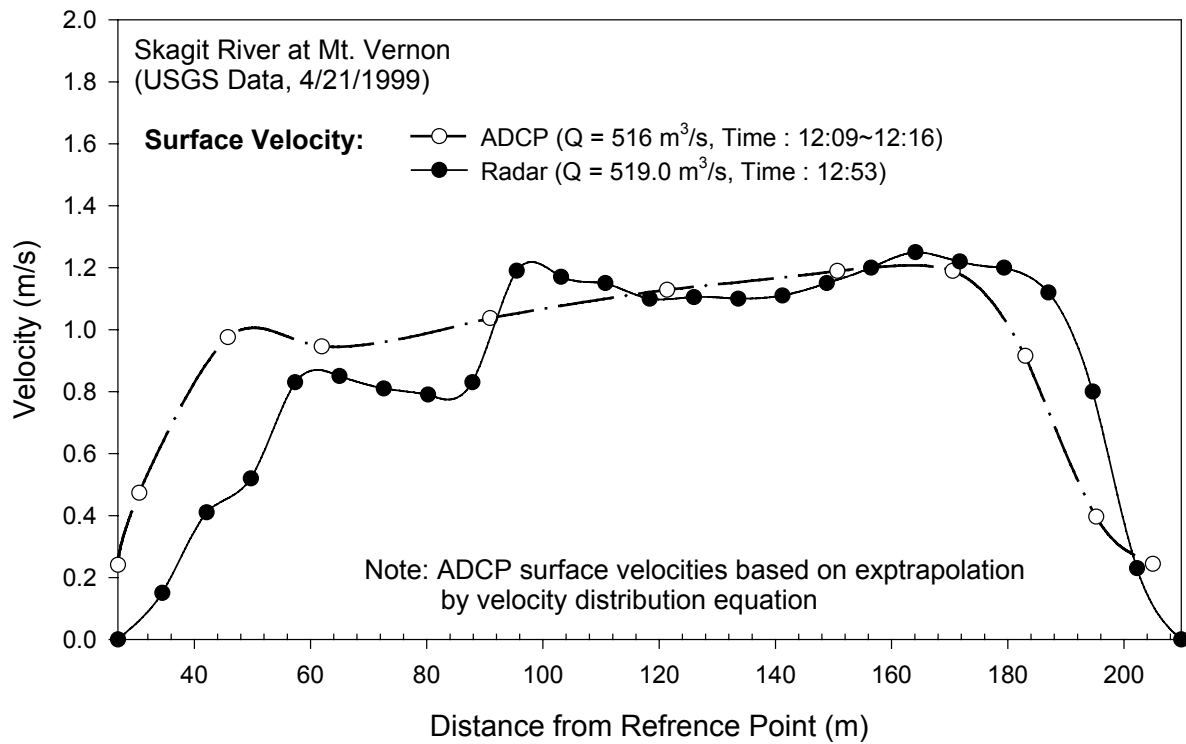
The conventional methods in estimating discharge are time-consuming and cannot be used during high or unsteady flows. By applying the probability concept to derivation of velocity distribution equation, regularities in open channels were determined<sup>(5)</sup>. This generates a new hydraulic parameter called M, which is a constant at a channel section and related to various observed phenomena in open channel flow. One of its applications is to simplify the discharge measurement and overcome the weakness of the conventional method so that the discharge during high flows may become measurable.

### **4.1 SPECIAL FEATURES OF Y-AXIS**

As defined in Section 2.2, y axis is the vertical axis in a channel section on which  $u_{\max}$  occurs. All information about a channel cross section needed in the efficient method of discharge measurement may be taken on the y axis. Thus, y axis may have some features in the flow system at a cross section, such as the stability on space and time and the high correlation with other selected verticals. The stability and correlation in a cross section can be tested as below.

### 4.1.1 Stability of Y Axis

Before verifying the stability of y axis, the location of y axis must be determined. Y axis can be detected from the pattern of isovels in a channel section as shown in Figure 4.1(b), in which  $u_{\max}$  is approximately 1.30 m/s and y axis is near 160 m from the reference point. If detailed velocity samples below the water surface are unavailable, it can be detected from the velocity distribution on the water surface as shown in Figure 4.1(a) since the location of the maximum surface velocity tends to coincide with that of  $u_{\max}$ .



(a)

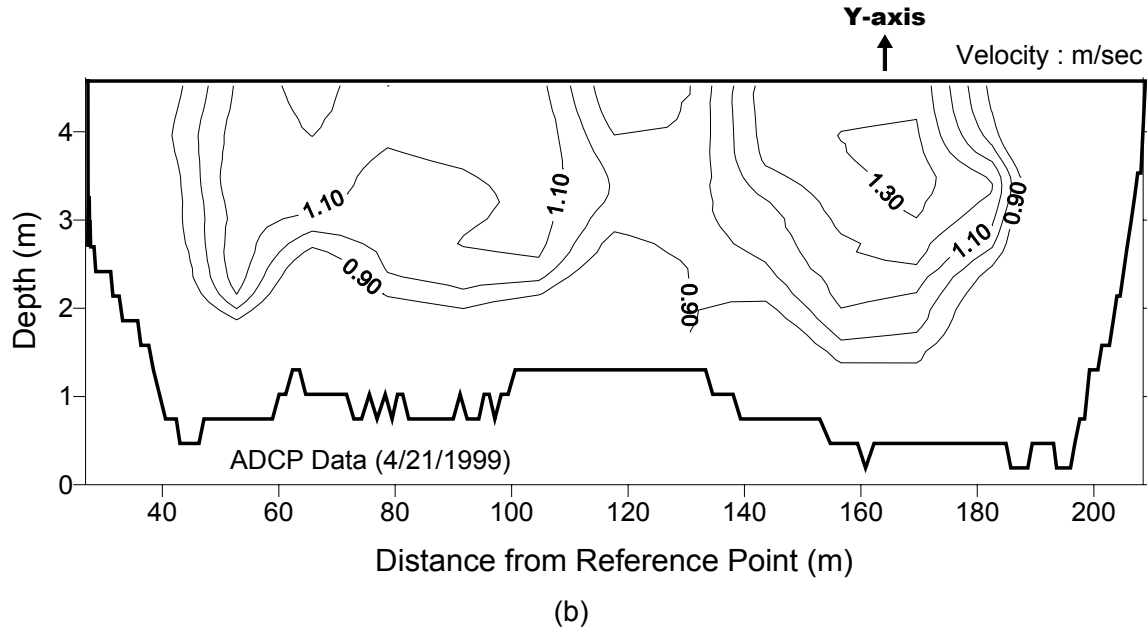


Figure 4.1 Determining the Location of Y Axis: (a) Velocity distribution on water surface; (b) Velocity distribution below water surface

Figure 4.2 shows the locations of y axis in Skagit River at Mt. Vernon during 1986-2000. This at a fifteen-year record indicates that the mean location of y axis from the reference point is 165.8 m. The standard deviation of the y axis is 6.7 m while the channel width is 214 m. As shown in the figure, most of the locations of y axis are within a small range so that the location of the y axis is fairly stable and invariant with time and discharge. Similar other results were obtained from channels<sup>(7, 27)</sup>.

In addition, the velocity data at Mt. Vernon were collected by current meter during the fifteen years. At the same station, velocity data in Figure 4.1(b) were collected by ADCP. A comparison of the mean location of y axis between Figure 4.1(b) and 4.2 shows that two values are almost the same.

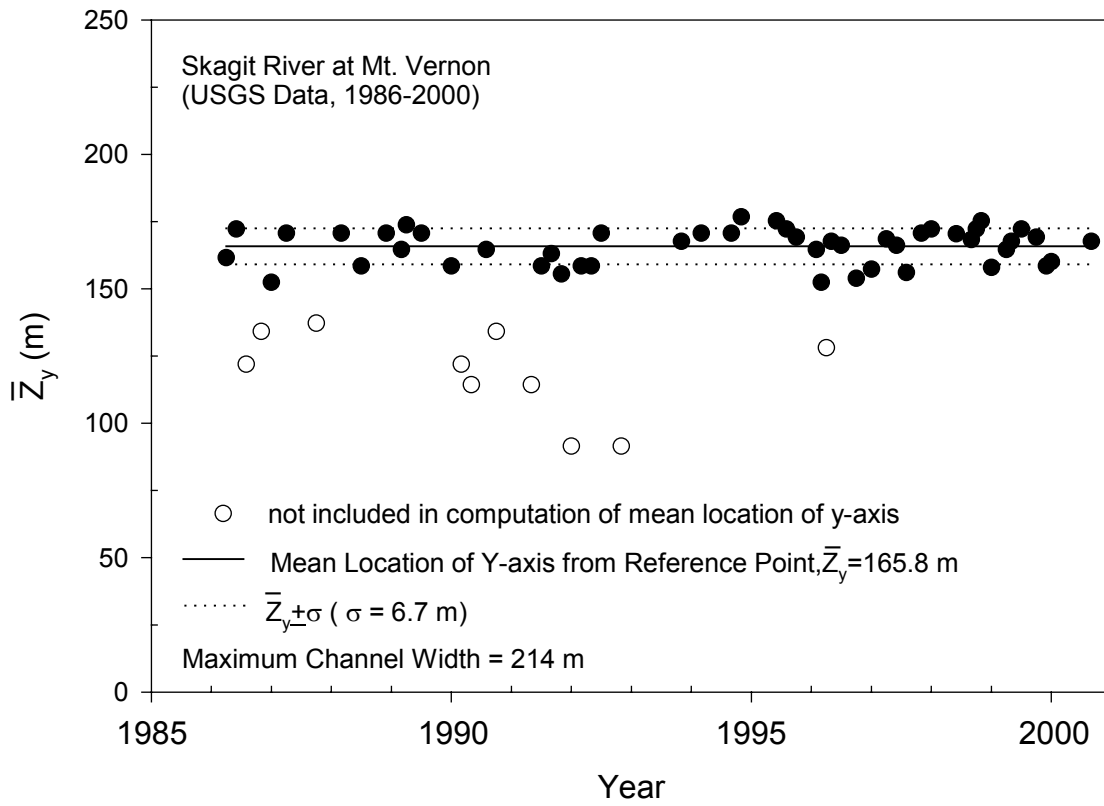


Figure 4.2 Analysis of Location of Y Axis, Skagit River at Mt. Vernon

#### 4.1.2 Concept of Maximum Correlation in Selection of Y Axis as Sampling Site

Figure 4.3 shows a flume section with the unvegetated plain (Tu et al. 1995)<sup>(28)</sup>. Three sampling stations including y axis are also indicated. Figure 4-4 shows the correlation between  $\overline{u_v}$  and  $\overline{u}$  at each of the three sample stations. The correlation coefficient and relation equation for each vertical are listed in Table 4-1. The results indicate the maximum correlation coefficient occurs at y axis.

In the second example, data were collected from South Esk River at Bridge 2 over the five-month period from December 14, 1978 through April 14, 1979 (Bridge and Jarvis 1985)<sup>(29)</sup>. Figure 4.5 shows a sketch of the channel section, in which the locations of sampling stations are numbered from 1 to 8. The velocity samples were taken at the stations 2-6 on March 3, 1979. The correlation between  $\overline{u_v}$  and  $\overline{u}$  at each of the sample stations from the stations 2-5 is shown in Figure 4.6 and listed in Table 4-2. The sampling station No. 3 (y axis) has the maximum value of the correlation coefficient, which is as high as 0.96. It should also be noted that the correlation is higher near y axis but decreases toward the banks. Based on these results, the cross-sectional mean velocity  $\overline{u}$  can be estimated accurately from  $\overline{u_v}$  on y axis without using velocity samples on other verticals. Further,  $\overline{u}$  can also be estimated accurately from  $u_{\max}$  because  $u_{\max}$  is taken from y axis as well. These are the bases of velocity sampling on y axis in the efficient methods of estimating the mean velocity.

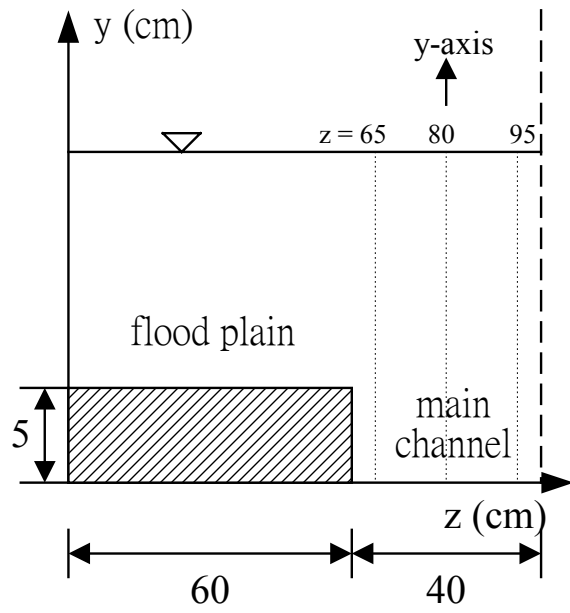


Figure 4.3 A sketch of Flume Section (Tu et al. 1995)

Table 4-1 Comparison of the Correlation Between Vertical and Cross-sectional Mean Velocities, Unsteady Flow in Flume with Unvegetated Plain (Tu et al. 1995)

The position of z	$\bar{u} - \bar{u}_v$ Relation	Correlation Coefficient $\hat{\rho}^2$
65	$\bar{u} = 0.91(\bar{u}_v)_{65} + 0.61$	0.935
80 (y-axis)	$\bar{u} = 0.82(\bar{u}_v)_{80} - 2.38$	0.946
95	$\bar{u} = 0.80(\bar{u}_v)_{95} + 1.65$	0.938

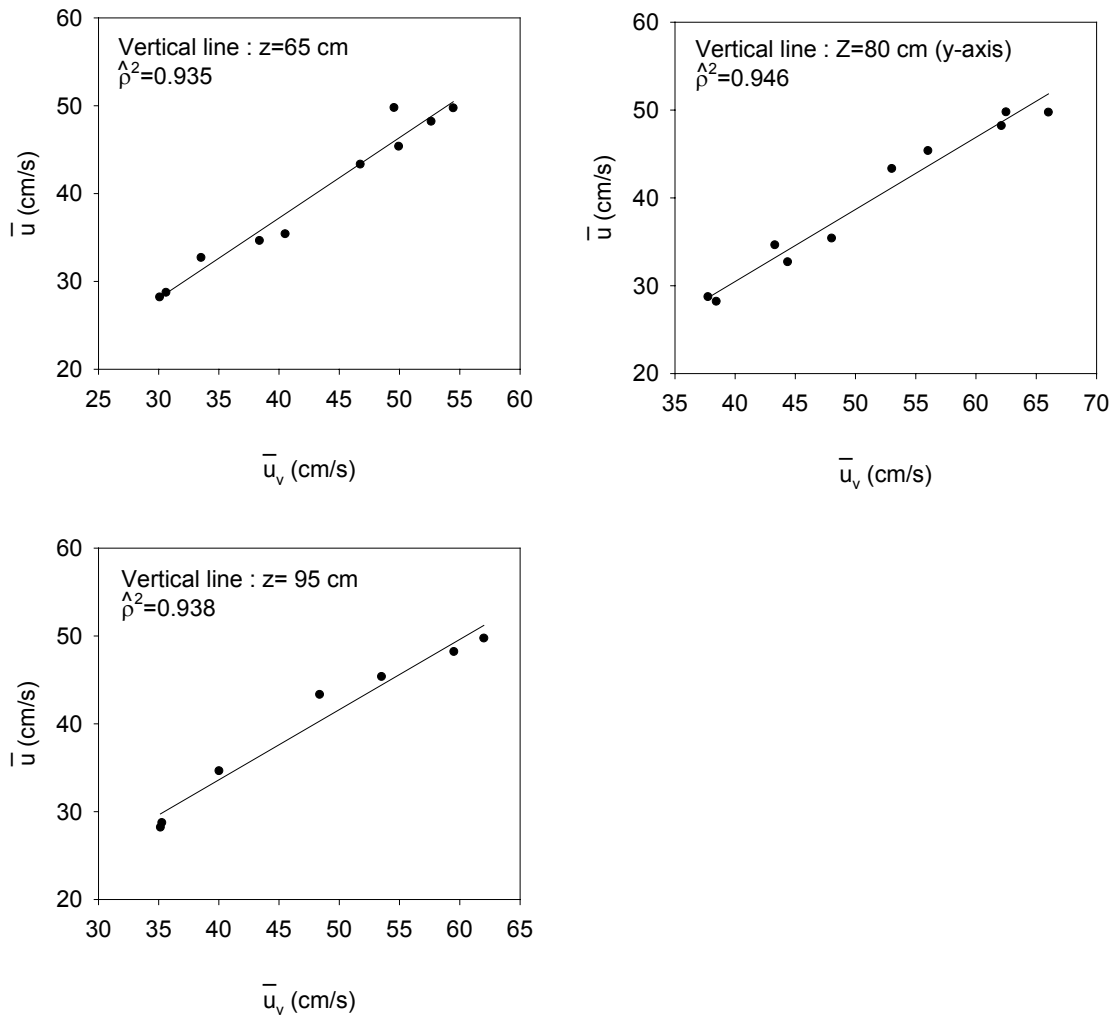


Figure 4.4 Correlations Between Vertical and Cross-sectional Mean Velocity, Unsteady Flow in Flume with Unvegetated Plain (Tu et al. 1995)

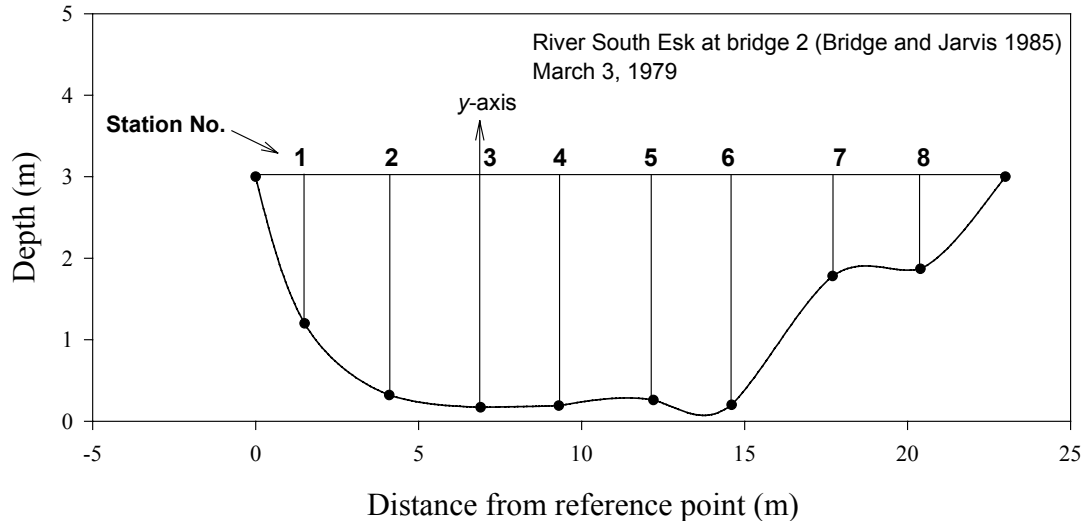


Figure 4.5 Sketch of Channel Cross Section in River South Esk at Bridge 2

Table 4-2 Comparison of the Correlation Between Vertical and Cross-sectional Mean Velocity, River South Esk at bridge 2 (Bridge and Jarvis 1985)

Station No.	$\bar{u} - \bar{u}_v$ Relation	Correlation Coefficient $\hat{\rho}^2$
2	$\bar{u} = 0.61(\bar{u}_v)_2 + 0.16$	0.676
3 (y-axis)	$\bar{u} = 0.84(\bar{u}_v)_3 - 0.07$	0.959
4	$\bar{u} = 0.83(\bar{u}_v)_4 - 0.04$	0.939
5	$\bar{u} = 0.85(\bar{u}_v)_5 + 0.02$	0.901

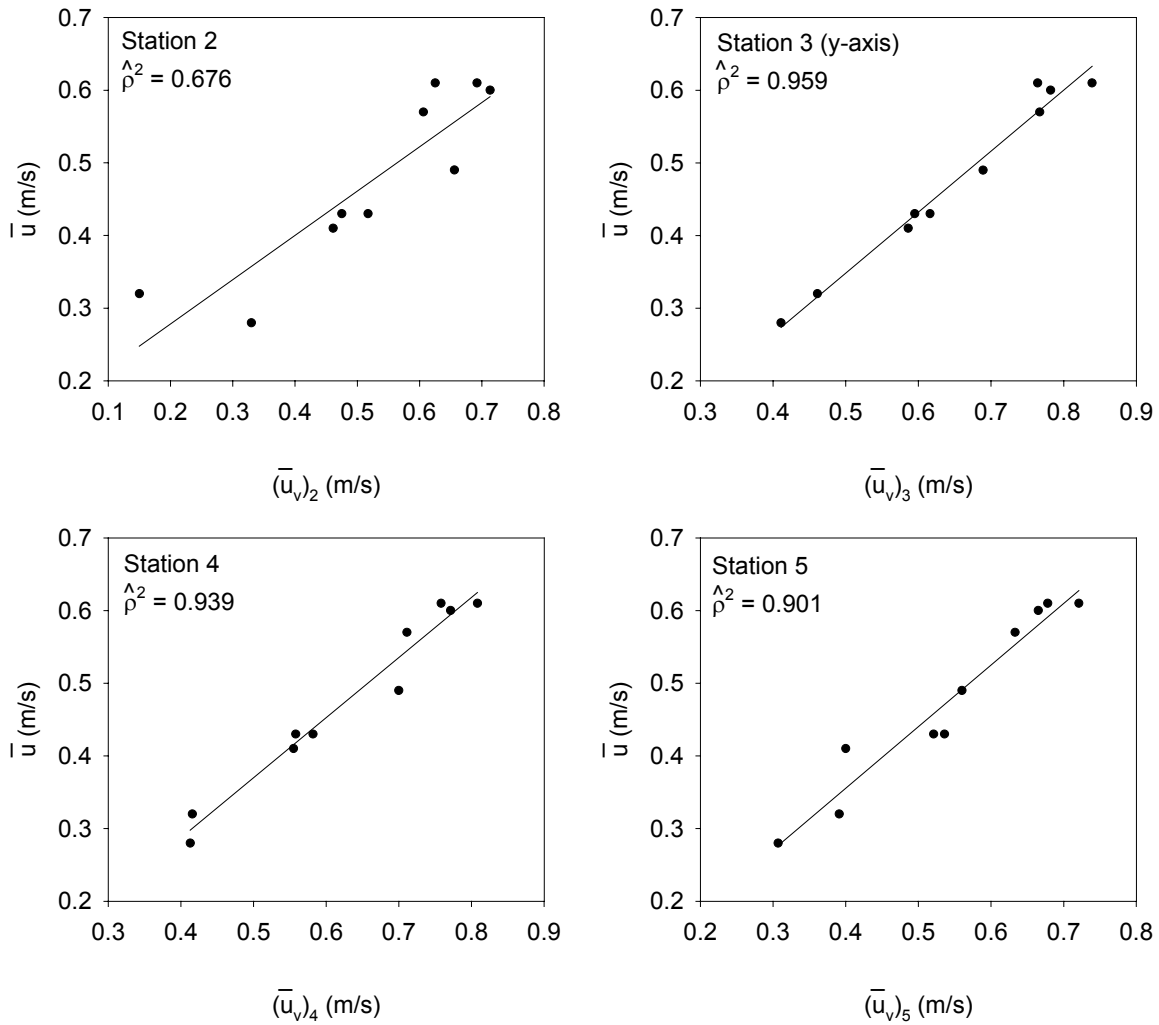


Figure 4.6 Correlation Between Vertical and Cross-sectional Mean Velocity, River South Esk at Bridge 2 (Bridge and Jarvis 1985)

## 4.2 DEVELOPMENT OF EFFICIENT METHODS OF DISCHARGE MEASUREMENT

### 4.2.1 Regularities in Open Channel Flows and Their Applications in Discharge Measurements

There are regularities in open-channel flow<sup>(8)</sup>. The regularities are natural laws deduced through a perpetual process of observation, perception and conception. As derived in the foregoing sections, some variables and quantities such as  $\bar{u}/u_{\max}$ ,  $h/D$ ,  $N$ ,  $\alpha$ ,  $\beta$ ,  $\bar{u}/u_D$ ,  $\bar{u}/\bar{u}_v$ ,  $\bar{y}/D$ , and  $\bar{y}_v/D$  in open-channel flow can be expressed as functions of  $M$ .  $M$  is the parameter of the probability distribution as shown in Eq. (2-9) and remains constant at a given channel section. Since these quantities are functions of  $M$ , they are also constants and can characterize regularities that exist in various flow at a channel section. These regularities form a network in which they are capable of supporting each other as shown in Figure 4.7. If one is known, the others can be determined from it.

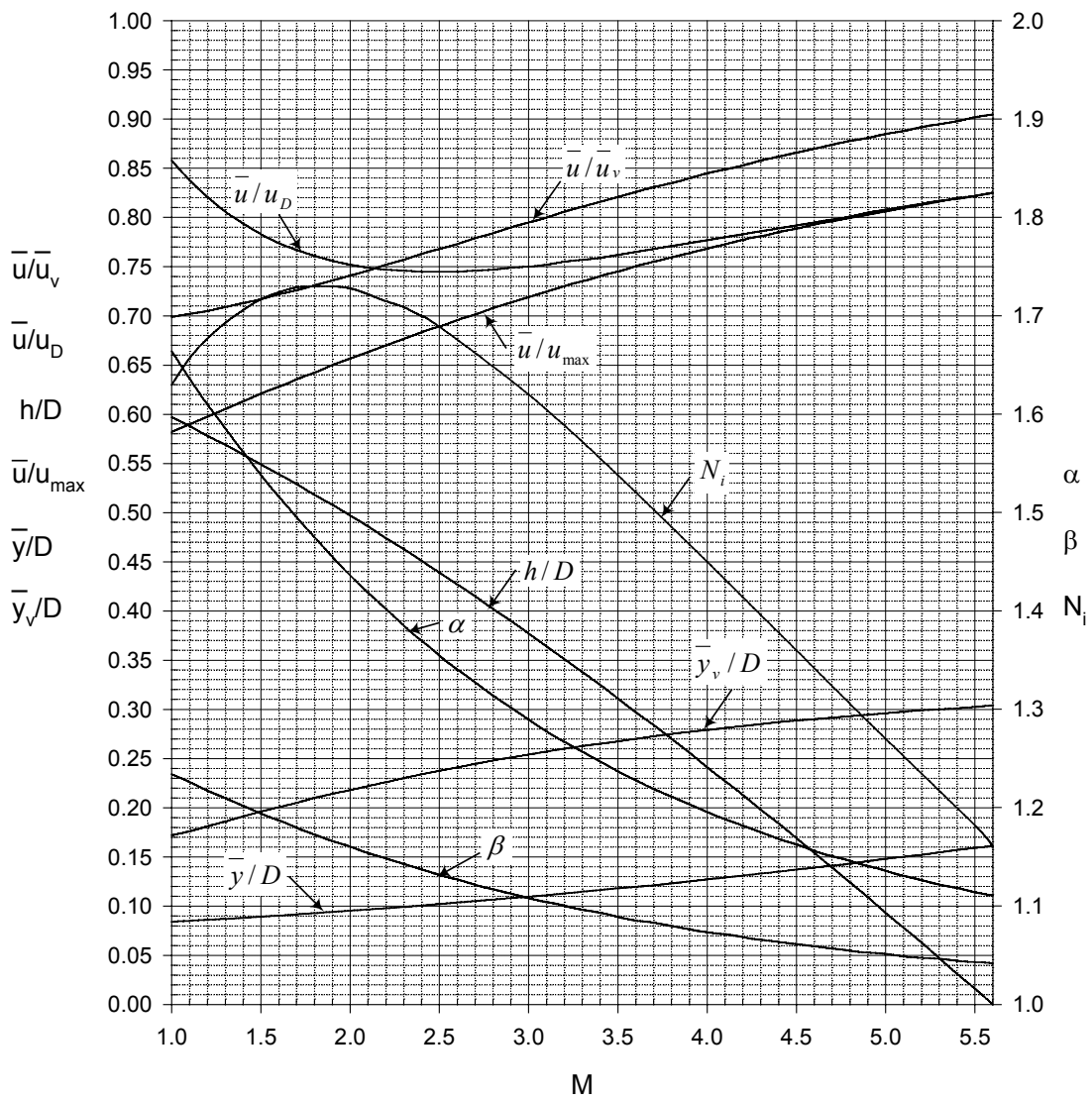


Figure 4.7 Network of Regularities in Open Channel Flows

These regularities in flows can be used in the development of efficient methods of the discharge measurements. For example, if  $M$  is available, the cross-sectional mean velocity can be estimated from  $u_{\max} \phi$ ,  $\bar{u} b(M)$  and  $u_D a(M)$  or directly measured at the point of the location of  $\bar{y}/D$ . Therefore,  $\bar{u}$  can be determined by only taking one or a few velocity samples on  $y$  axis.

Energy coefficient  $\alpha$  and momentum coefficient  $\beta$  can be also estimated from the figure. If the value of  $M$  varies from section to section along a channel,  $\alpha$  and  $\beta$  also will vary.

#### 4.2.2 Estimations of $M$

If the  $M$  value of a channel section is unknown, there are three methods for obtaining it:

##### Method 1: Estimation using historical records of discharge

Figure 2.3 illustrates the  $\bar{u} - u_{\max}$  relation, in which  $\bar{u}$  is determined as  $Q/A$  and  $u_{\max}$  can be obtained by regression when velocity samples are taken on  $y$  axis. The slope of the straight line in the figure is  $\phi$  and hence  $M$  is calculated from Eq. (2-9). Since those points in the figure are based on a long term period (15 years), the historical records of  $\bar{u}$  and  $u_{\max}$  give the average value of  $\bar{u}/u_{\max}$ . Therefore,  $M$  represents an average value and is constant at a given channel section.

##### Method 2: Estimation from velocity samples on $y$ axis

If long records of discharge such as the U. S. Geological Survey's data are unavailable,  $M$  can be estimated from velocity samples taken on  $y$  axis and the network of regularities in

Figure (4.7). When  $u_{\max}$ ,  $h/D$ ,  $u_D$  and  $\bar{u}_v$  are obtained on y axis, the relationships in Figure (4.7) can be used to estimate  $M$ . The estimations of  $u_{\max}$  and  $\bar{u}_v$  will be discussed in the next section. The location of the maximum velocity  $h/D$  can be determined from taking a set of detailed velocity samples on y axis.  $u_D$  can be obtained by taking a velocity sample on y axis at the water surface.

### Method 3: Estimation from velocity samples on more than one vertical

If velocity samples on more than one vertical are taken,  $M$  can be estimated from the  $N - M$  relation with a parameter estimation technique as described in section 3.4.2.

#### **4.2.3 Estimations of $u_{\max}$ and $\bar{u}_v$**

Eq. (2-15) has three parameters  $M$ ,  $h$  and  $u_{\max}$ . If  $M$  is known and  $h$  is given by Eq. (2.24), the three parameters in Eq. (2-15) can be reduced to only one ( $u_{\max}$ ). Once  $u_{\max}$  is obtained, the velocity distribution on y axis can be described. Moreover, in using Eq. (2-19) to estimate  $\bar{u}$ ,  $u_{\max}$  is also needed. There are three methods to estimate  $u_{\max}$ :

#### Method 1: Velocity sampling on y axis

$u_{\max}$  can be determined by taking a number of velocity samples on y axis. If the time and budget allow, detailed sampling may be taken and used to estimate  $u_{\max}$ . The techniques of determining  $u_{\max}$  using Eq. (2-15) with one, two or more velocity samples on the y axis are:

#### **With one velocity sample:**

If only one velocity sample is taken,  $u_{\max}$  can be determined by substituting  $u_1$  and  $y_1$  into Eq. (2-15).  $u_1$  is the velocity at the single sampling point which is situated at distance  $y_1$  above the channel bed.

**With two velocity samples:**

The two velocity samples may be taken at  $y = 0.8D$  and  $0.2D$ , respectively. The U. S. Geological Survey usually takes the two points at each vertical in a channel section in order to estimate the discharge. For this type of data,  $u_{\max}$  can be estimated from the following three equations:

$$u_{0.2} = \frac{u_{\max}}{M} \ln \left[ 1 + (e^M - 1) \frac{0.8D}{D-h} \exp \left( 1 - \frac{0.8D}{D-h} \right) \right] \quad (4-1)$$

$$u_{0.8} = \frac{u_{\max}}{M} \ln \left[ 1 + (e^M - 1) \frac{0.2D}{D-h} \exp \left( 1 - \frac{0.2D}{D-h} \right) \right] \quad (4-2)$$

$$\bar{u}_v = \frac{u_{0.2} + u_{0.8}}{2} = \int_0^1 \ln \left[ 1 + (e^M - 1) \frac{\frac{y}{D}}{1 - \frac{h}{D}(M)} \exp \left( 1 - \frac{\frac{y}{D}}{1 - \frac{h}{D}(M)} \right) \right] d \left( \frac{y}{D} \right) \quad (4-3)$$

in which  $u_{0.2}$  and  $u_{0.8}$  are the velocities at  $y = 0.8D$  and  $0.2D$ , respectively.

**With more than two velocity samples:**

If more than two velocity samples on  $y$  axis are available,  $u_{\max}$  can be estimated by regression analysis of velocity data using Eq. (2-15).

Method 2: Velocity sampling at a single point on water surface

In high flow, strong currents make subsurface velocity measurements difficult or impossible. In such a situation, a single sample  $u_D$  may be taken on the water surface by using a modern device such as radar.  $u_{\max}$  can be estimated by the following equation:

$$u_{\max} = (u_D M) \div \ln \left[ 1 + (e^M - 1) \frac{1}{1 - \frac{h}{D}} \exp \left( 1 - \frac{1}{1 - \frac{h}{D}} \right) \right] \quad (4-4)$$

### Method 3: Velocity samples taken within 95% confidence interval of h/D

According to the results obtained by Chiu and Tung (2002)<sup>(8)</sup> from a study of the  $h/D - M$  relation, the 95% upper and lower confidence limits of  $h/D$  at a given value of  $M$  are the values given by the regression line (Eq. (2-24)) plus and minus 0.11, respectively. If velocity samples are only taken within this interval, the estimated  $u_{\max}$  from regression analysis using Eq. (2-15) may be closer to the real  $u_{\max}$  than the one obtained from the entire water depth because  $u_{\max}$  occurs more likely in the specific interval. Therefore,  $u_{\max}$  can be estimated by regression analysis of velocity data using Eq. (2-15) with samples taken within the interval.

The estimation of  $\bar{u}_v$  is also very important in the development of efficient methods of discharge measurements. The cross-sectional mean velocity  $\bar{u}$  can be determined from  $\bar{u}_v$  as  $\bar{u} = \bar{u}_v b(M)$  given by Eq. (2-30), where the value of  $b(M)$  at a given  $M$  can also be obtained from Figure 4.7.

$\bar{u}_v$  can be obtained by taking one, two or more velocity samples on  $y$  axis. If only one velocity sample on  $y$  axis is taken, it should be taken at the location of  $\bar{y}_v$  which can be obtained

from the  $\bar{y}_v/D - M$  relation shown in Figure 4.7 for a given  $M$ . If two velocity samples are to be taken, they should be  $u_{0.2}$  and  $u_{0.8}$ . Thus,  $\bar{u}_v$  can be estimated by averaging these two points. If several velocity samples on  $y$  axis can be taken,  $\bar{u}_v$  can be estimated by averaging all the velocity samples.

### 4.3 MODEL VERIFICATION

#### 4.3.1 $\bar{y}/D - M$ and $\bar{y}_v/D - M$ Relations

If  $M$  is known, the location of the cross-sectional mean velocity  $\bar{y}/D$  can be obtained from the  $\bar{y}/D - M$  relation in Figure 4.7. Once the location is determined,  $\bar{u}$  can be obtained by taking a velocity sample at the position. Similarly, If  $M$  is available, the location of the mean velocity along  $y$  axis can be obtained from the  $\bar{y}_v/D - M$  relation in Figure 4.7. Once the location is determined,  $\bar{u}_v$  can be obtained by taking a velocity sample at the position, and then  $\bar{u}$  can be calculated as  $\bar{u}_v b(M)$ .

In order to determine the locations of  $\bar{u}$  and  $\bar{u}_v$  using laboratory and field data<sup>(28, 29, 30, 31)</sup>, a velocity distribution along  $y$  axis must be provided first. The velocity distribution can be described by using Eq. (2-15) with three parameters  $M$ ,  $h$  and  $u_{\max}$ . Since  $M$  is known, Eq. (2-24) gives  $h$ .  $u_{\max}$  can be estimated by regression with several velocity samples along  $y$  axis. With the velocity distribution,  $\bar{y}/D$  and  $\bar{y}_v/D$  can be computed by using Eq. (2-15) with  $\bar{u}_{obs}$  and  $\bar{u}_v$ , respectively, in which  $\bar{u}_{obs} = Q/A$  is the observed mean velocity in a cross section;  $\bar{u}_v$

can be estimated by averaging all the velocity samples or by using Eq. (2-29). At last, the computed  $\bar{y}/D$  and  $\bar{y}_v/D$  were compared in Figure 4.7.

Each of Figures 4.8-10 show both velocity samples and velocity distribution along y axis. The locations of  $\bar{u}$ ,  $\bar{u}_v$  and  $u_{\max}$  are also indicated in each of these figures. Each velocity distribution has a good agreement with the velocity samples. This can confirm the reliability of the computed locations of  $\bar{u}$  and  $\bar{u}_v$ . Figure (4.11) shows the accuracy of the  $\bar{y}/D - M$  and  $\bar{y}_v/D - M$  relations for M from 1.0 to 5.6.

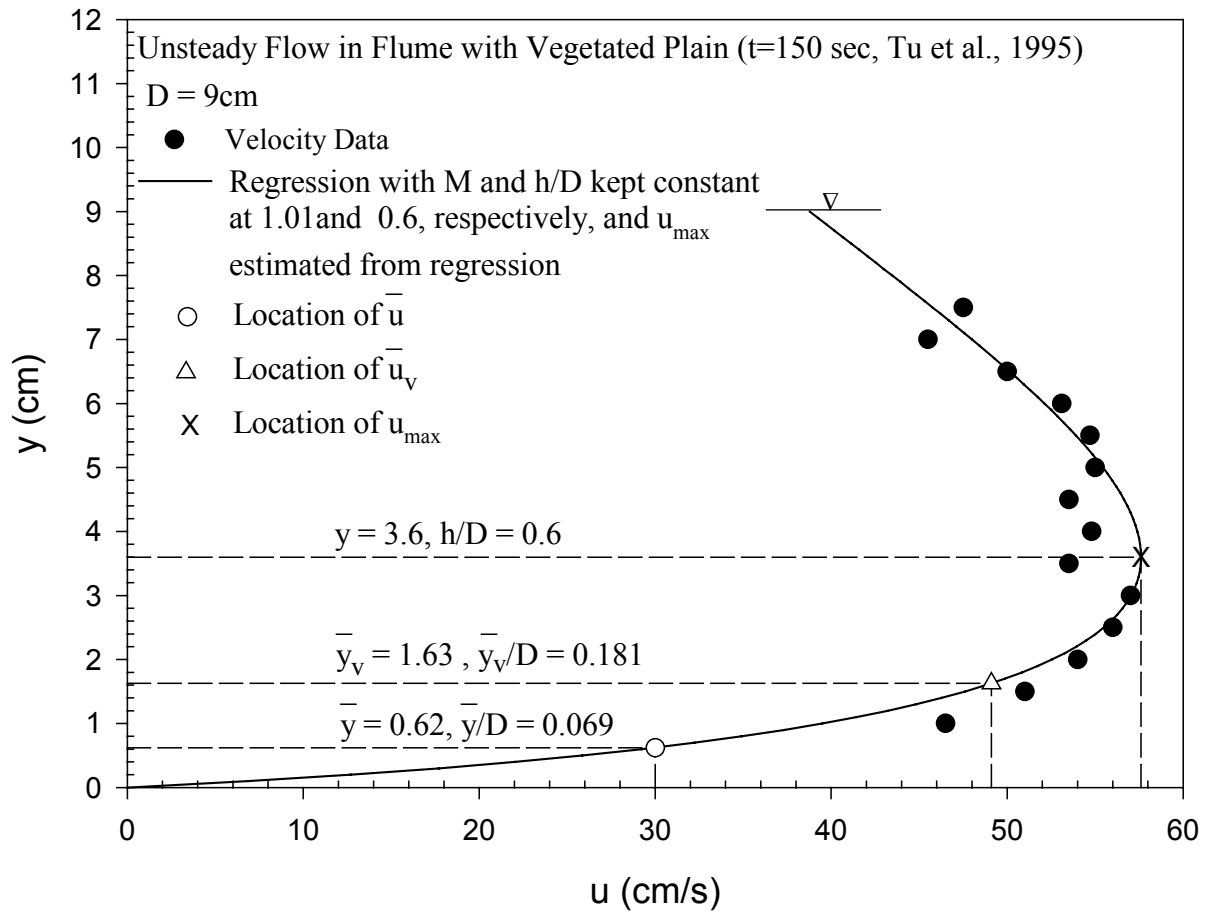


Figure 4.8 Determining the Locations of  $\bar{u}$  and  $\bar{u}_v$ , and Velocity Distribution on Y Axis in Laboratory Flume

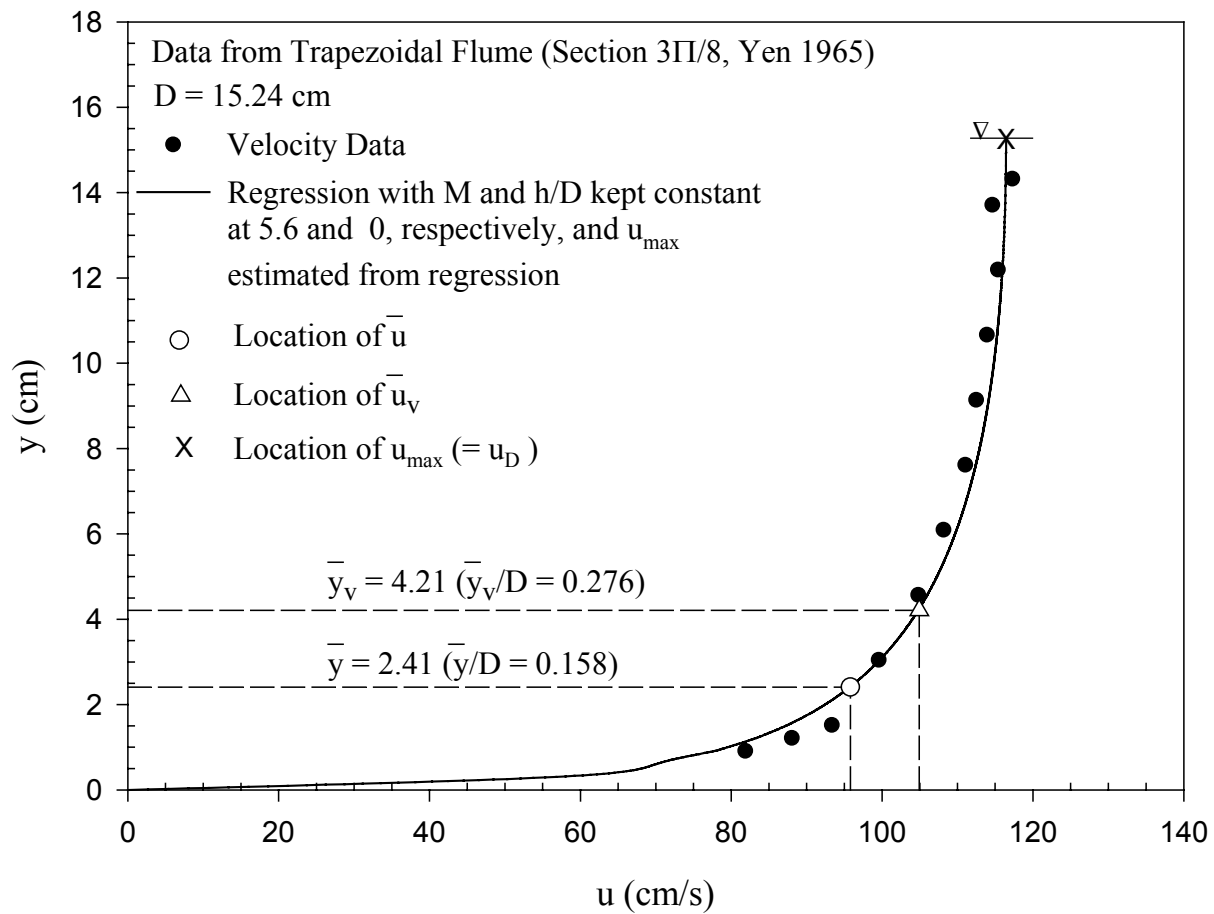


Figure 4.9 Determining the Locations of  $\bar{u}$  and  $\bar{u}_v$ , and Velocity Distribution on Y Axis in Trapezoidal Flume at Section 3Π/8

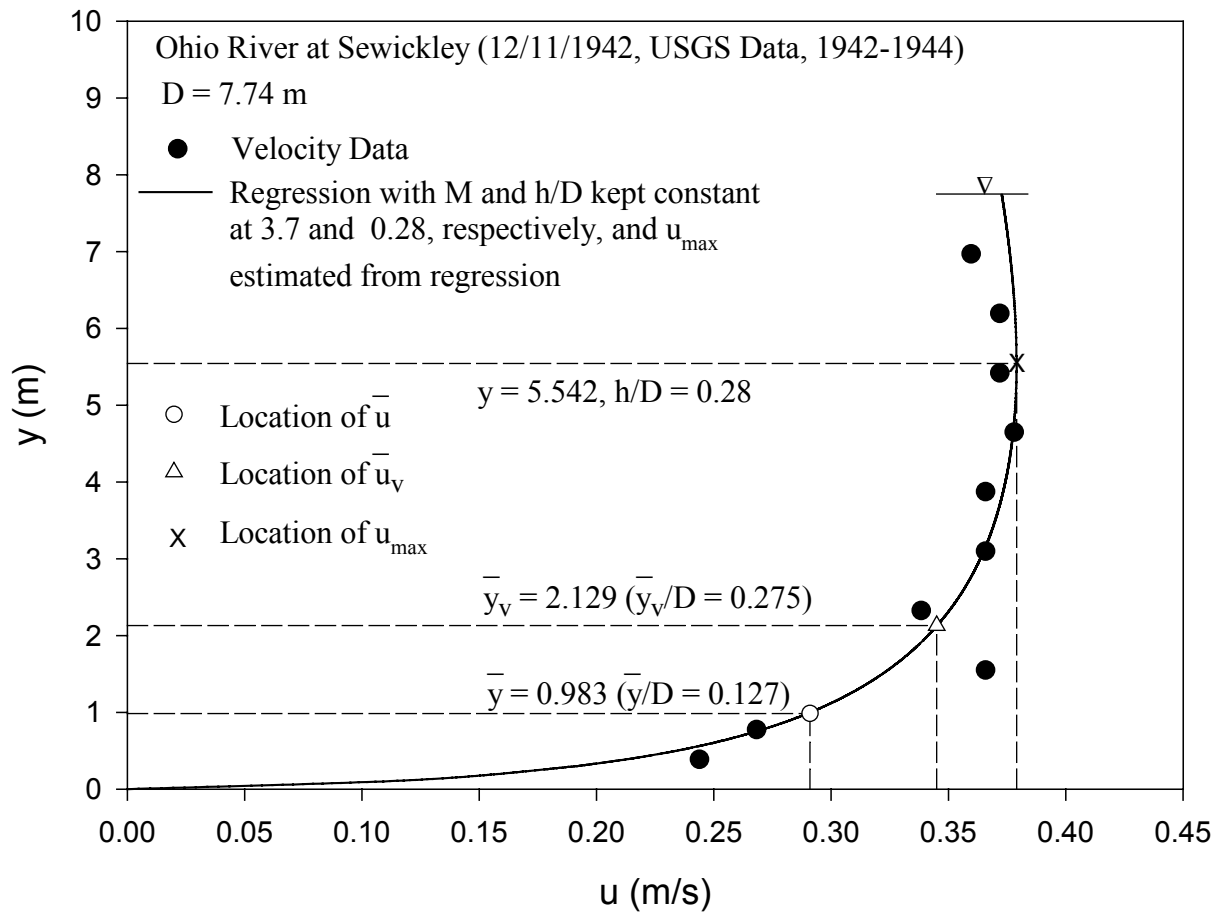


Figure 4.10 Determining the Locations of  $\bar{u}$  and  $\bar{u}_v$ , and Velocity Distribution on Y Axis in Ohio River at Sewickely

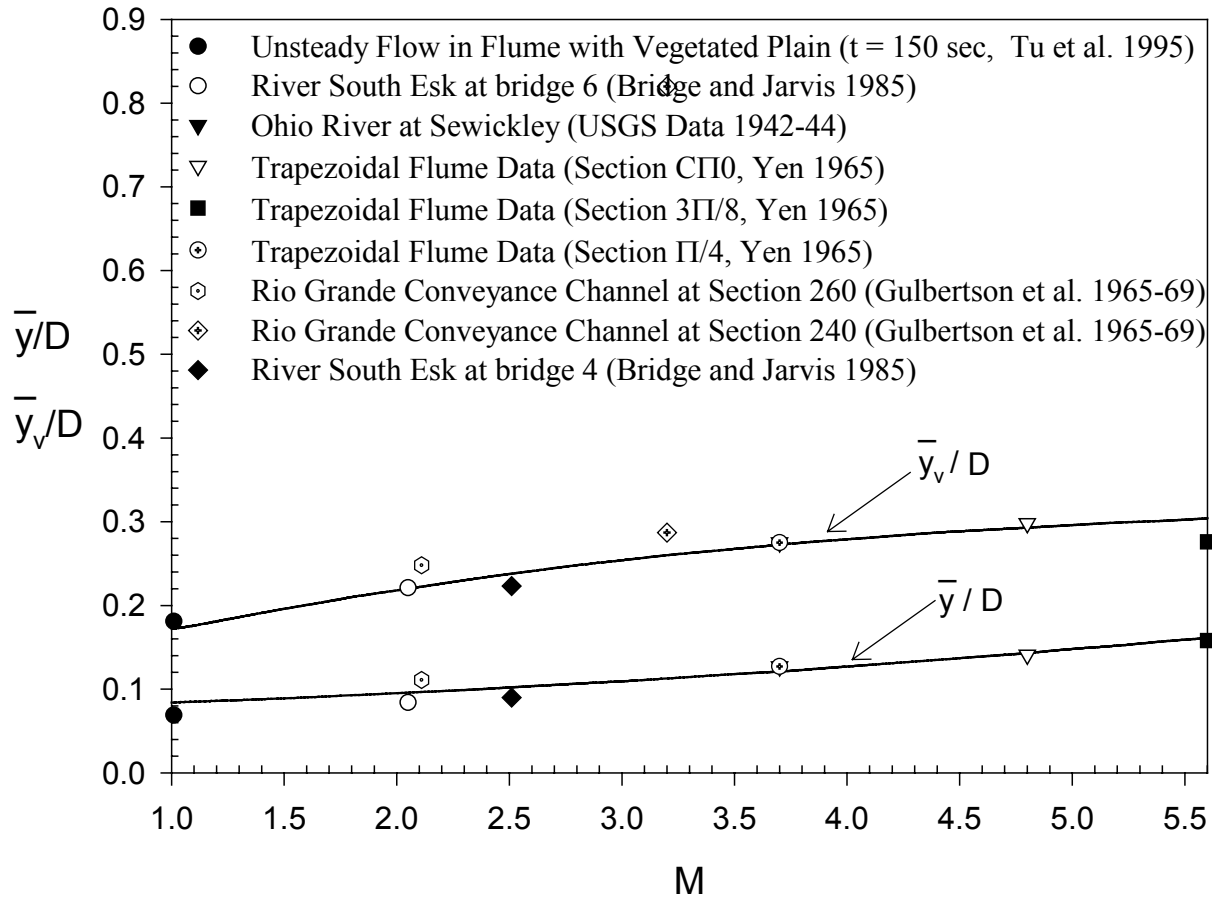


Figure 4.11 Accuracy of  $\bar{y}/D-M$  and  $\bar{y}_v/D-M$  Relations

### 4.3.2 Comparison of $u_{\max}$ Obtained from Velocity Sampling

$u_{\max}$  can be estimated by velocity sampling as mentioned in the preceding section. In this section compared is the difference in results obtained by different methods of sampling.

Figures 4.12 (a-d) show velocity samples and velocity distribution profiles at different discharges in the Ohio River at Sewickly. These data were collected by USGS during 1942-44. The  $M$  value is determined by the average ratio of  $\bar{u}$  to  $u_{\max}$  over two years and the corresponding  $h$  value is given by Eq. (2-24).  $u_{\max}$  is obtained from all velocity samples by regression using Eq. (2-15) with the constant values of  $M$  and  $h$ . The measured value of  $Q$  and the estimated value of  $u_{\max}$  and  $\bar{u}$  are also indicated in each figure. Figures 4.13(a-d) are similar to Figures 4.12 (a-d), except that  $u_{\max}$  was obtained from velocity sampling within 95% confidence interval of  $h/D$ . Each of Figures 4.13(a-d) indicates the confidence interval so that it is clear to see the number of velocity samples.

Between Figures 4.12 and 4.13,  $u_{\max}$  in Figure 4.13 tends to be higher than that of Figure 4.12 and approximates the  $u_{\max}$  value determined from velocity samples. On the other hand, each estimated  $u_{\max}$  in Figure 4.12 is underestimated in comparison with the measured. This result is expected because  $u_{\max}$  is from velocity samples within the confidence interval. Table 4-3 shows a comparison of discharges obtained by two different methods of velocity sampling. The discharge obtained by velocity samples from the confidence interval is more accurate than that obtained from all velocity samples. The average errors of discharge obtained by the two methods are 7.09% and 5.69%, respectively. Table 4.4 shows a similar comparison at different channel sections, which is in South Esk River at Bridge 4 (Bridge and Jarvis 1985)<sup>(29)</sup>.

The average errors in discharge estimated by the two methods are 8.29% and 3.65%, respectively. Therefore, these two results show that the velocity samples obtained within the 95% confidence interval of  $h/D$  are more accurate and efficient in discharge estimation. The former also can reduce the costs because less velocity data are taken.

Ohio River at Sewickley (USGS Data, 1942-1944)

Section constants:  $\Phi = 0.76$ ,  $M = 3.7$ ,  $h/D = 0.28$

- Velocity Data
- Computed with  $M = 3.7$ ,  $h = 0.28$ , and  $u_{\max}$  from all velocity samples
- × Location of  $u_{\max}$

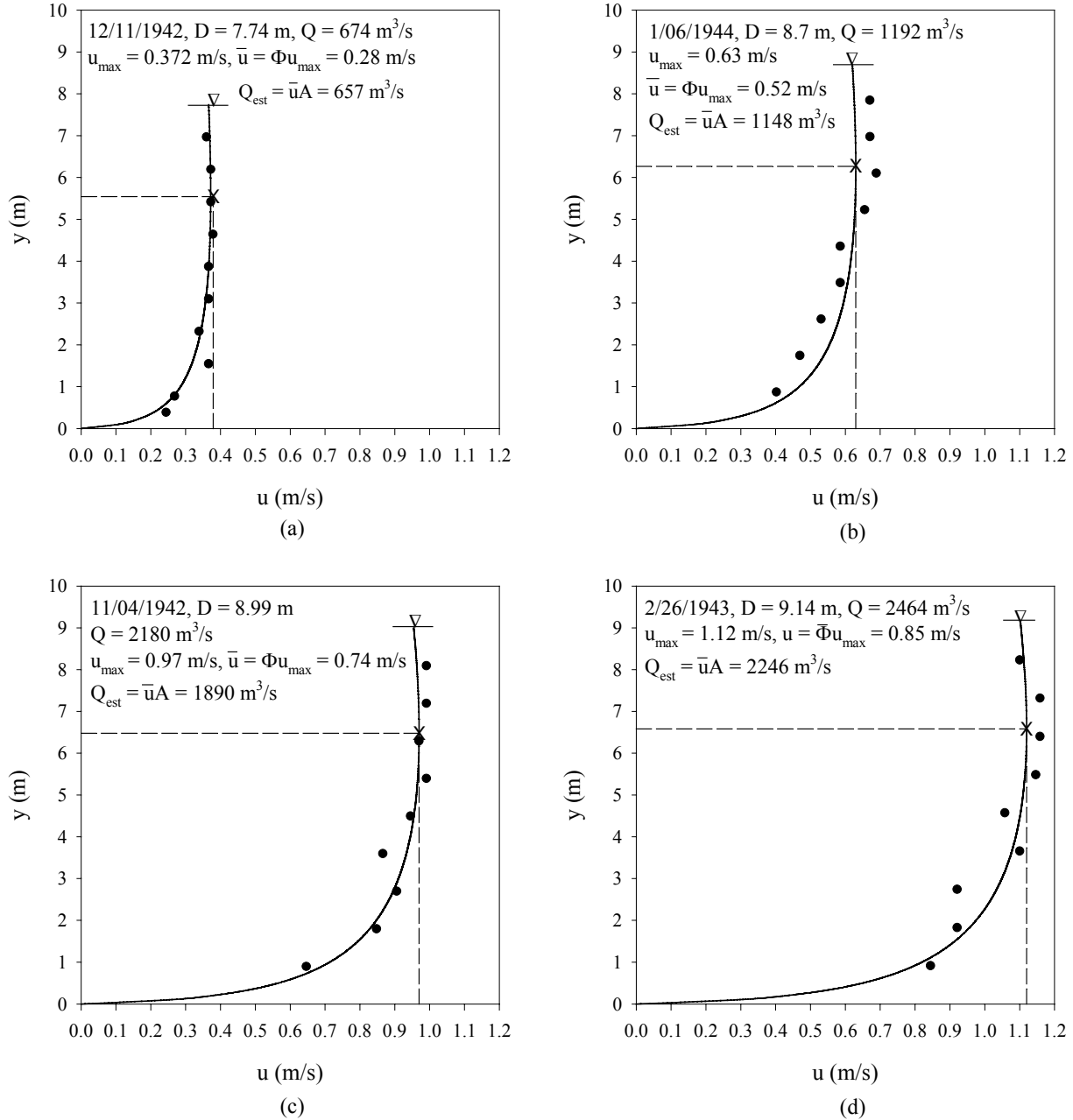


Figure 4.12 Velocity Distribution Profile ( $u_{\max}$  from all velocity samples)

Ohio River at Sewickley (USGS Data, 1942-1944)

Section constants:  $\Phi = 0.76$ ,  $M = 3.7$ ,  $h/D = 0.28$

- Velocity Data

— Computed with  $M = 3.7$ ,  $h/D = 0.28$ , and  $u_{\max}$  from velocity samples within 95% confidence interval of  $h/D$

× Location of  $u_{\max}$

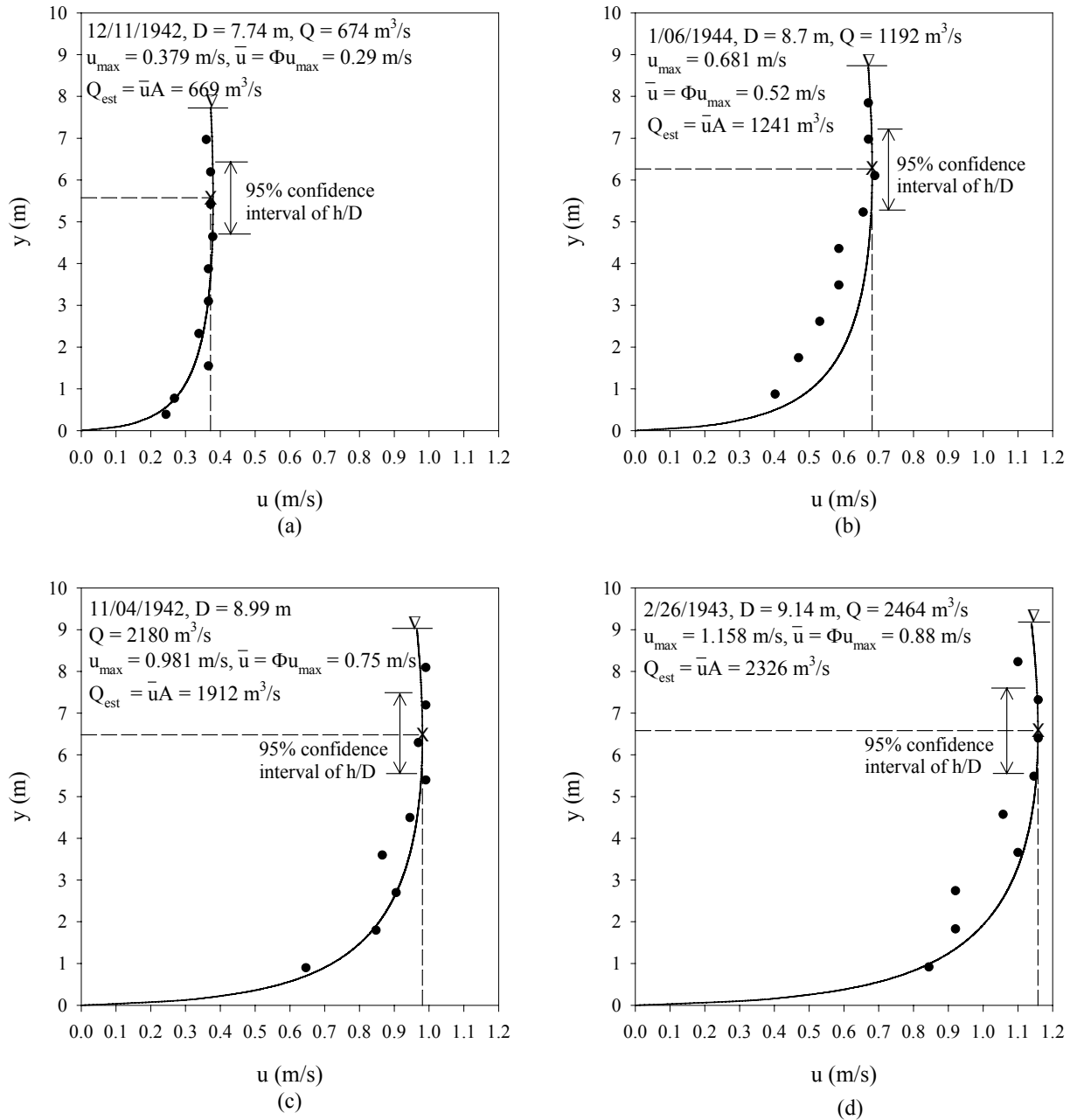


Figure 4.13 Velocity Distribution Profile ( $u_{\max}$  from velocity samples within 95% confidence Interval of  $h/D$ )

Table 4-3 Comparison of Discharge Obtained by Different Methods, Ohio River at Sewickley (USGS data, 1942-1944)

Date	Q <sub>obs</sub> (m <sup>3</sup> /s)	(Q <sub>est</sub> ) <sub>1</sub> (m <sup>3</sup> /s)	(Q <sub>est</sub> ) <sub>2</sub> (m <sup>3</sup> /s)	(Error) <sub>1</sub> (%)	(Error) <sub>2</sub> (%)
12/11/1942	674	657	669	2.52	0.74
1/06/1944	1192	1148	1241	3.69	4.11
11/04/1942	2180	1890	1912	13.30	12.29
2/26/1943	2464	2246	2326	8.85	5.60
$Error(\%) = \left  \frac{Q_{est} - Q_{obs}}{Q_{obs}} \right  \times 100$			(Error) <sub>ave</sub> =	<b>7.09%</b>	<b>5.69%</b>
Notes: 1. Computed with u <sub>max</sub> from all velocity samples 2. Computed with u <sub>max</sub> from velocity samples within 95% confidence interval of h/D					

Table 4-4 Comparison of Discharge Obtained by Different Methods, South Esk River at Bridge 4 (Bridge and Jarvis 1985)

Date	Q <sub>obs</sub> (m <sup>3</sup> /s)	(Q <sub>est</sub> ) <sub>1</sub> (m <sup>3</sup> /s)	(Q <sub>est</sub> ) <sub>2</sub> (m <sup>3</sup> /s)	(Error) <sub>1</sub> (%)	(Error) <sub>2</sub> (%)
12/14/78	13.5	14.92	13.48	10.55	0.15
12/16/78	7.3	7.85	7.86	7.54	7.67
12/18/78	4.31	4.79	4.64	11.21	7.66
3/1/79	2.81	2.98	2.88	5.95	2.49
3/3/79	27.99	27.77	27.04	0.78	3.39
3/4/79	7.98	8.77	8.13	9.91	1.88
3/7/79	6.83	7.66	6.67	12.08	2.34
$Error(\%) = \left  \frac{Q_{est} - Q_{obs}}{Q_{obs}} \right  \times 100$ Notes: 1. Computed with u <sub>max</sub> from all velocity samples 2. Computed with u <sub>max</sub> from velocity samples within 95% confidence interval of h/D			(Error) <sub>ave</sub> =	<b>8.29%</b>	<b>3.65%</b>

### 4.3.3 Verification of Efficient Methods of Discharge Estimation

By taking advantage of the regularities in open channel system, discharge measurements only require velocity samples at one, two or several points on  $y$  axis. Since the measurements can be quick and economical, these methods can be said to be efficient.

Two efficient methods of discharge measurements are presented in the present study.

**Efficient Method 1:** The method uses several velocity samples along  $y$  axis to determine  $u_{\max}$  by regression in which  $M$  and  $h/D$  are kept constant.

**Efficient Method 2:** The method uses the velocity  $u_D$  sampled on the water surface to estimate  $u_{\max}$  in which  $M$  and  $h/D$  kept constant.

To illustrate the efficient methods, velocity data collected at four different cross sections in a curved flume were used as shown in Figure 4.18(b) (Yen 1965)<sup>(30)</sup>. Figures 4.14-17 show velocity samples obtained at section  $S0$ ,  $\Pi/0$ ,  $\Pi/4$ , and  $\Pi/2$ , respectively. The velocity distributions determined by efficient methods 1 and 2 at each section are shown by the curves in solid line and dashed line, respectively. Each figure also indicates a single velocity sample  $u_D$  on the water surface. The discharges estimated by the two different methods are shown in each figure, and the results by both agree with the observed discharge,  $Q = 0.29 \text{ m}^3/\text{s}$ . The error is only about 3.4 percent.

The values of  $M$  from  $S0$  to  $\Pi/2$  are 5.97, 4.8, 3.7, and 6.0, respectively. When flow enters the bend, the cross-sectional mean velocity does not change but the bend reduces the  $M$  value and hence increases the information entropy by adjusting the magnitude and location of  $u_{\max}$ . For instance, as flow moves from  $S0$  to  $\Pi/4$ ,  $M$  decreases from 5.97 to 3.7. Conversely, when the flow leaves the bend, the  $M$  value increases along the channel in order to keep the

same  $\bar{u}$  at different sections. For instance, as flow leaves from  $\Pi/4$  to  $\Pi/2$ ,  $M$  increases from 3.7 to 6.6.

In order to compare the efficient methods of discharge measurements with other existing methods, three conventional methods of discharge measurements are selected. Figure 4.18(a) compares five different methods. The results show these methods except the floats method are quiet good. As shown in Figure 4.18(a), floats method underestimated the discharge. Therefore, without considering the cost and time, all methods except the floats method can be used in discharge estimation. If the time and budget are considered, the two efficient methods are superior to the conventional methods. However, in high or unsteady flow efficient method 2 would be the best.

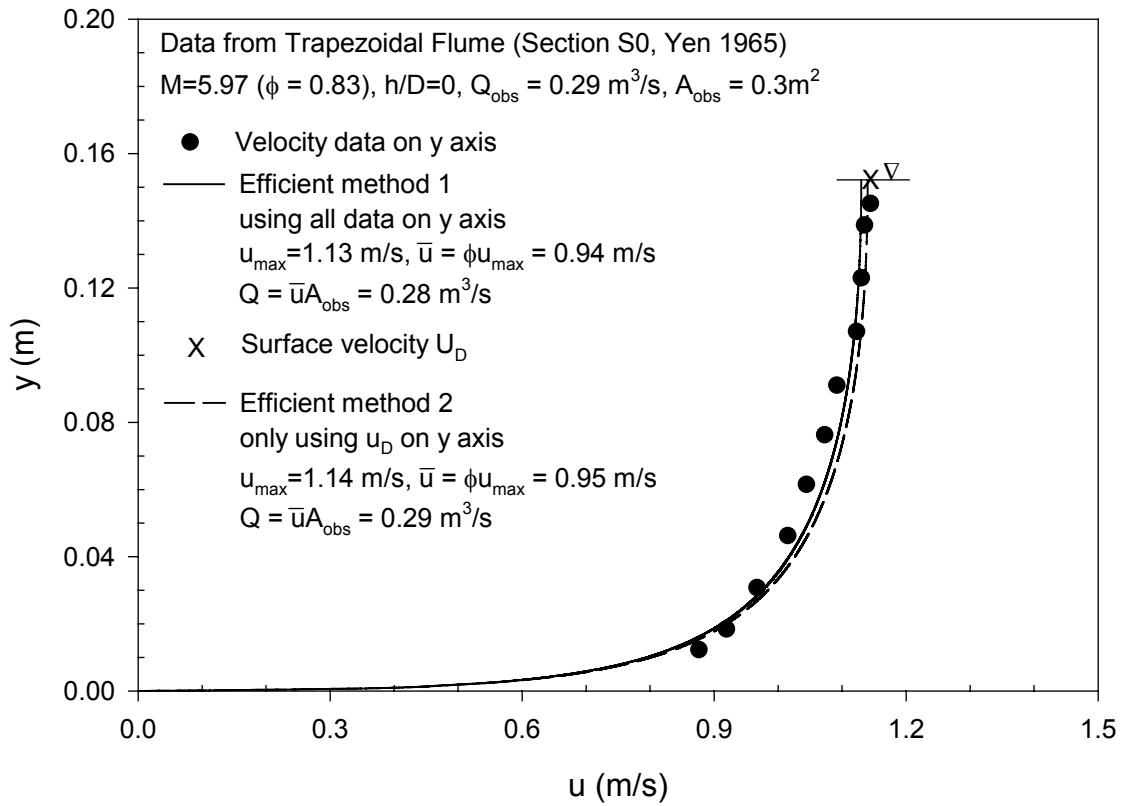


Figure 4.14 Comparison of Efficient Methods 1 and 2 of Discharge Estimation at Section S0

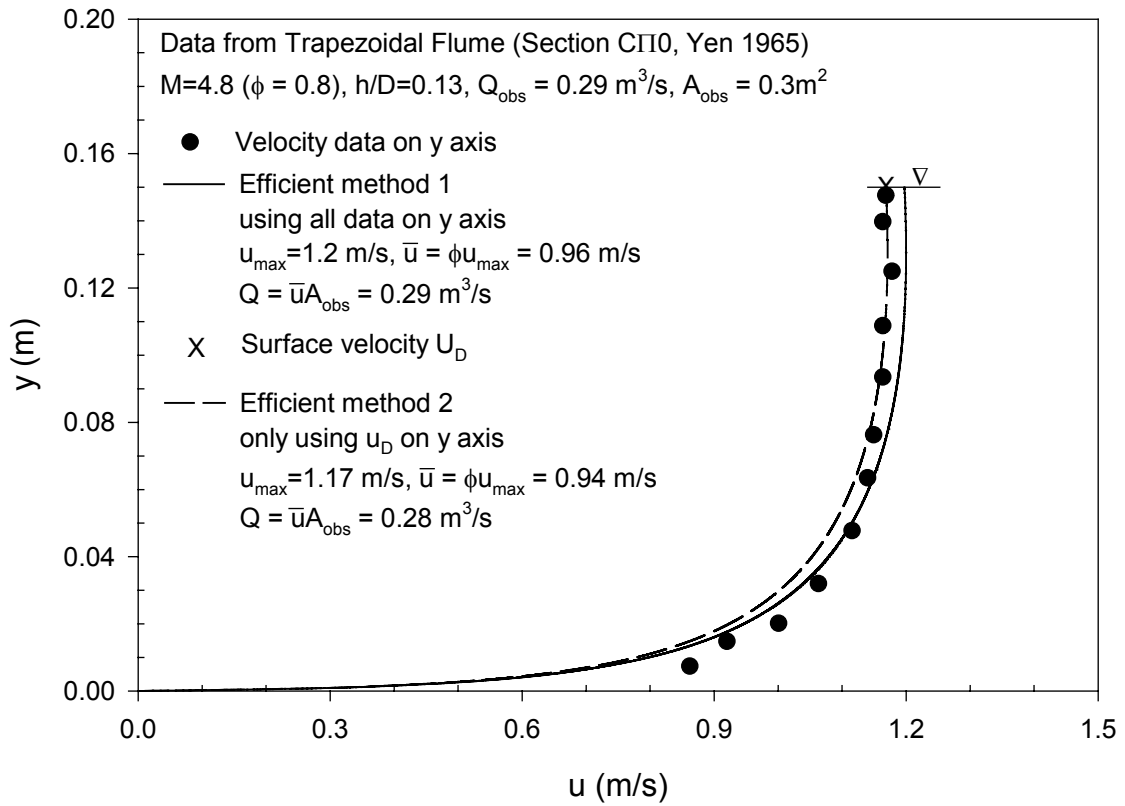


Figure 4.15 Comparison of Efficient Methods 1 and 2 of Discharge Estimation at Section CII0

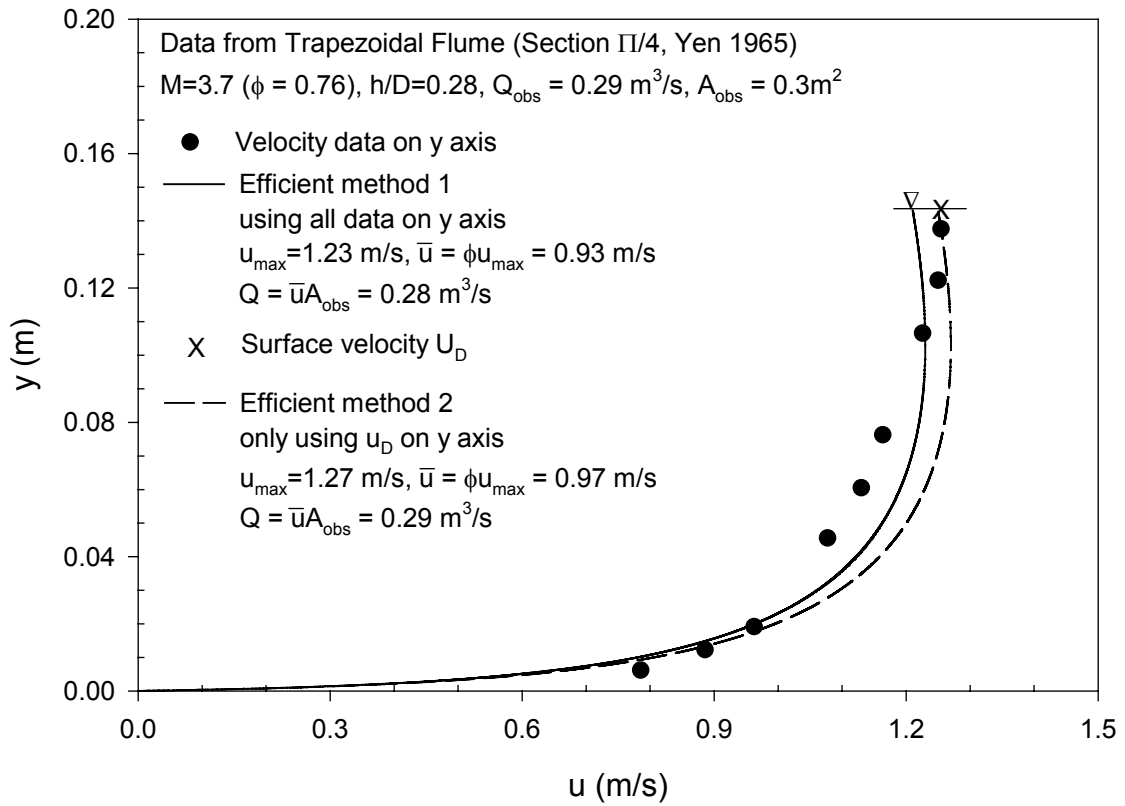


Figure 4.16 Comparison of Efficient Methods 1 and 2 of Discharge Estimation at Section  $\Pi/4$

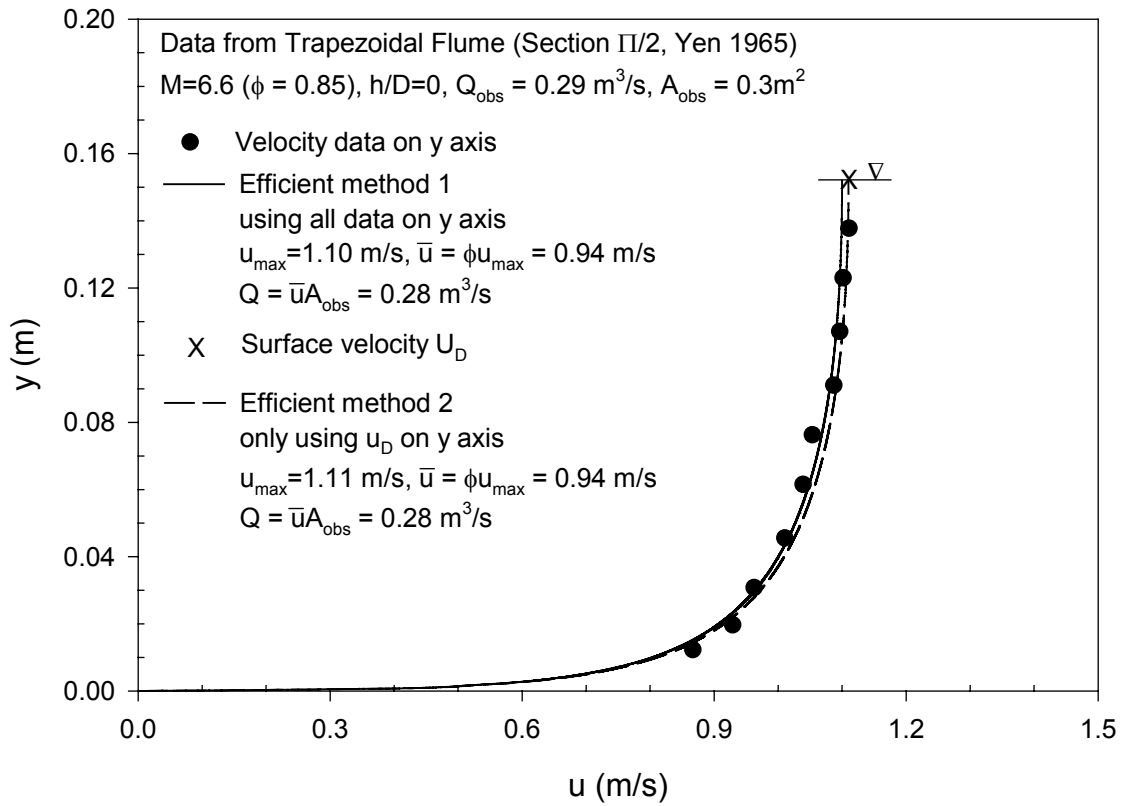
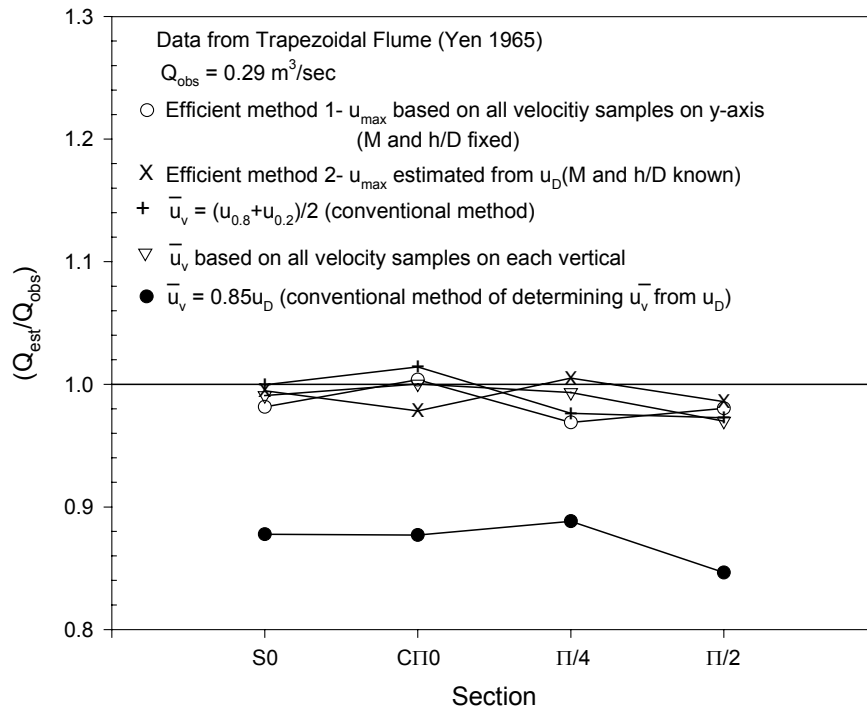
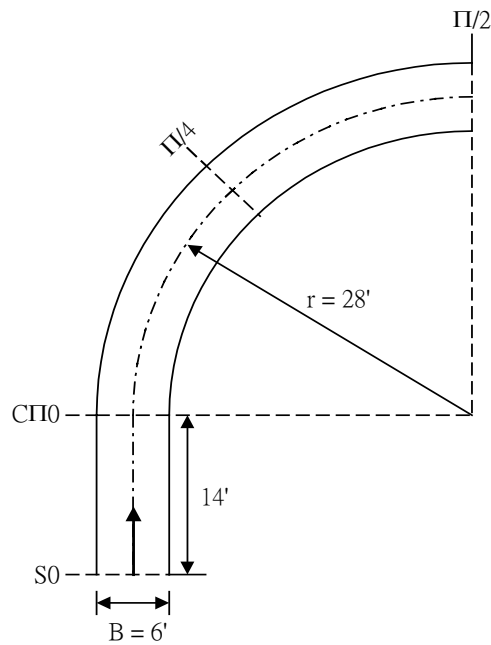


Figure 4.17 Comparison of Efficient Methods 1 and 2 of Discharge Estimation at Section  $\Pi/2$



(a)



(b)

Figure 4.18 Comparison of Different Methods of Estimating Discharge: (a) Ratios of estimated discharges to the known; (b) Locations of the four sections

## 5.0 RELATION BETWEEN SURFACE AND VERTICAL MEAN VELOCITIES

### 5.1 BACKGROUND

Recently, the non-contact method by using a radar device became popular in discharge measurement. This method is to collect the surface velocity, then convert the surface velocity into the vertical mean velocity by multiplying a coefficient, and then calculate the flow discharge. The coefficient is a ratio of the vertical mean velocity to the surface velocity. If the velocity distribution follows the Prandtl-von Karman Logarithmic law, the theoretical ratio of the vertical mean velocity to the surface velocity is 0.85<sup>(1)</sup>.

According to the latest USGS research, the ratio is not a constant of 0.85 for all channel sections and rivers<sup>(21)</sup>. For instance, the measured ratio varies between 0.8 and 0.93 in San Joaquin River at Vernalis, California<sup>(21)</sup>. These findings indicate that the estimation of flow discharge may not be accurate if the coefficient of 0.85 is universally adapted. The ratio is very important factor to the non-contact method. This gives a motivation to verify the relation by using Chiu's velocity equation. As discussed in the preceding sections, Chiu's velocity equation works well in predicting the velocity distribution.

## 5.2 COMPUTATION AND STABILITY OF $\overline{u_v}/u_D$ IN A CHANNEL SECTION

Based on Chiu's velocity equation, the procedure for computing  $\overline{u_v}/u_D$  at a vertical is as follows:

1. With a set of velocity data at any vertical, estimating three parameters  $M$ ,  $h$ , and  $u_{\max}$  of Chiu's velocity equation by the method of least squares for using Eq. (2-15) if  $u_{\max}$  occurs below the water surface, or Eq. (2-17) if  $u_{\max}$  occurs on the water surface.
2. Compute the surface velocity using the velocity equation from the step 1.
3. Compute the vertical mean velocity using Eq. (2-29).
4. Compute  $\overline{u_v}/u_D$ .

$\overline{u_v}/u_D$  of each vertical tends to be different in a channel section. It is difficult to estimate the discharge if  $\overline{u_v}/u_D$  in the section is not constant. For simplicity, the ratio is generally treated as a constant for estimating the discharge in practice. Therefore, the present study examined whether the ratio may be treated as a constant.

Figures 5.1 shows the values of  $\overline{u_v}/u_D$  across the width of the channel section and estimation of the overall section average of  $\overline{u_v}/u_D$  in the Ohio River at Sewickley. A similar analysis was made for data from different natural rivers as shown in Figures 5.2-4. Figures 5.1-4 show that  $\overline{u_v}/u_D$  varies along a channel, but the variation at each section is small. Moreover, there is no tendency of variation from the right bank to the left bank in any section. It may conclude that one can utilize a constant ratio of  $\overline{u_v}/u_D$  for converting the surface velocity into

the vertical mean velocity for each vertical in a channel section. In addition, the overall section mean of  $\bar{u}_v/u_D$  determined in each figure is more reliable.

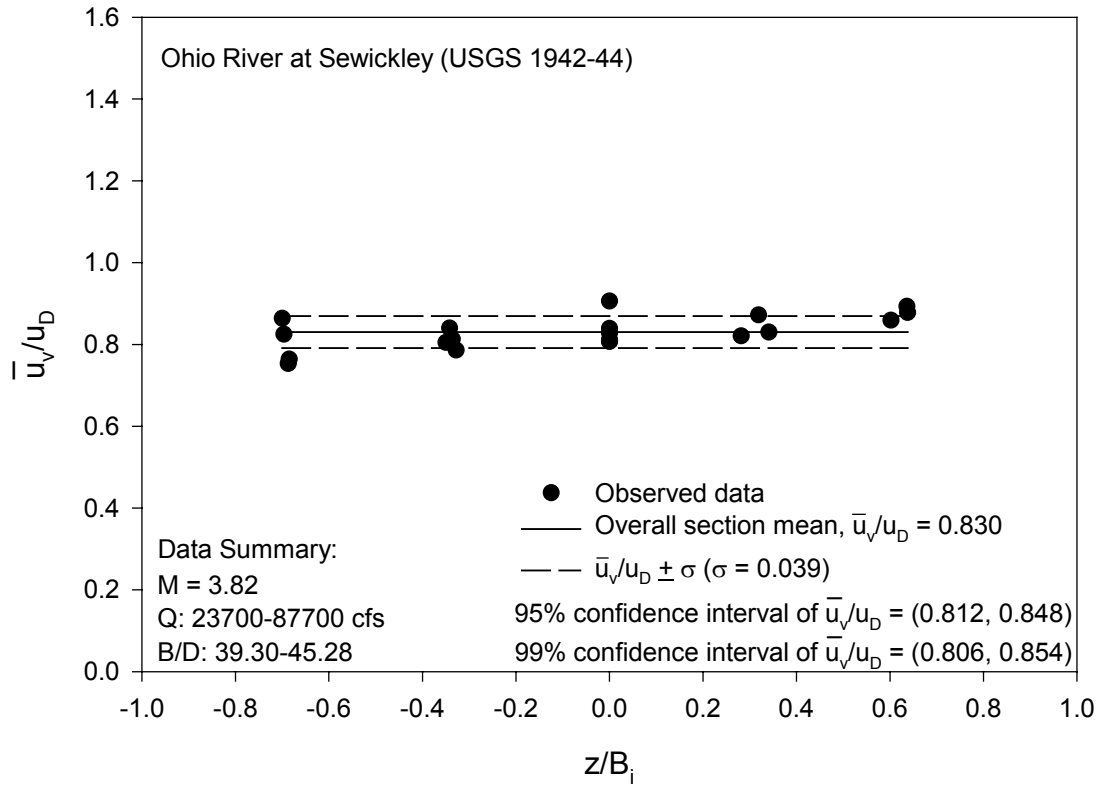


Figure 5.1 Values of  $\bar{u}_v/u_D$  in Channel Section and Estimation of Overall Average in Ohio River at Sewickley

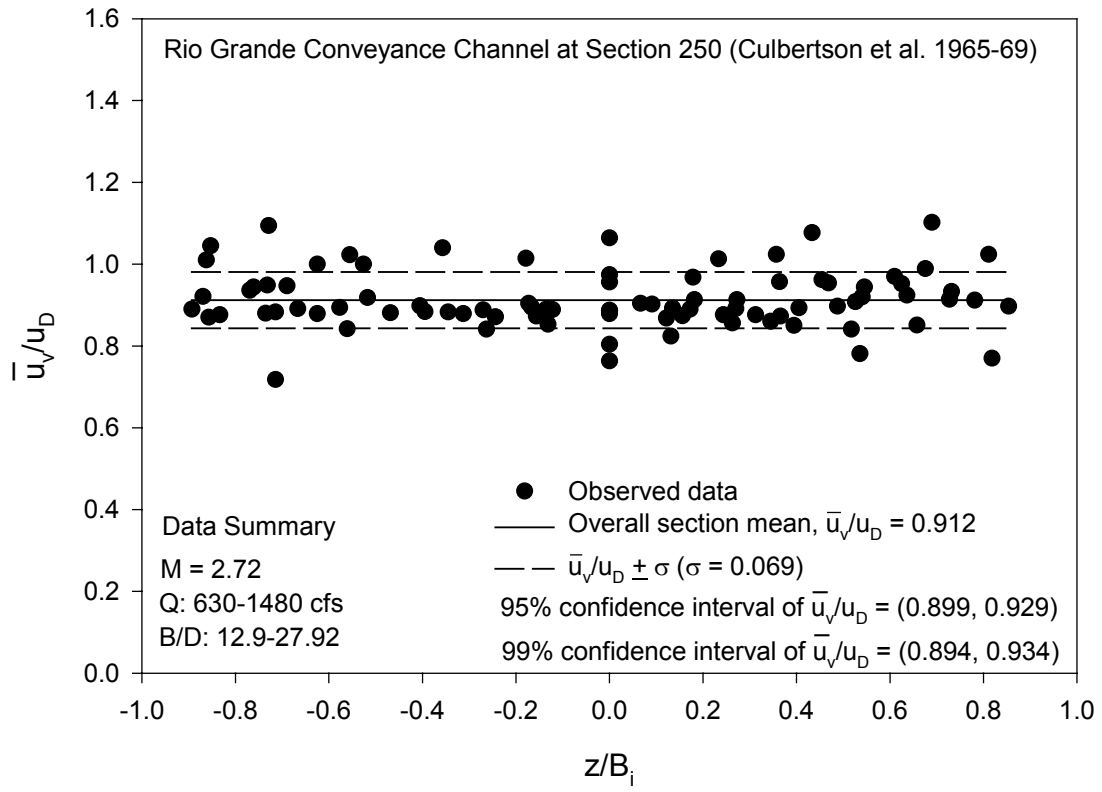


Figure 5.2 Values of  $\bar{u}_v/u_D$  in Channel Section and Estimation of Overall Average in Rio Grande Conveyance Channel at Section 250

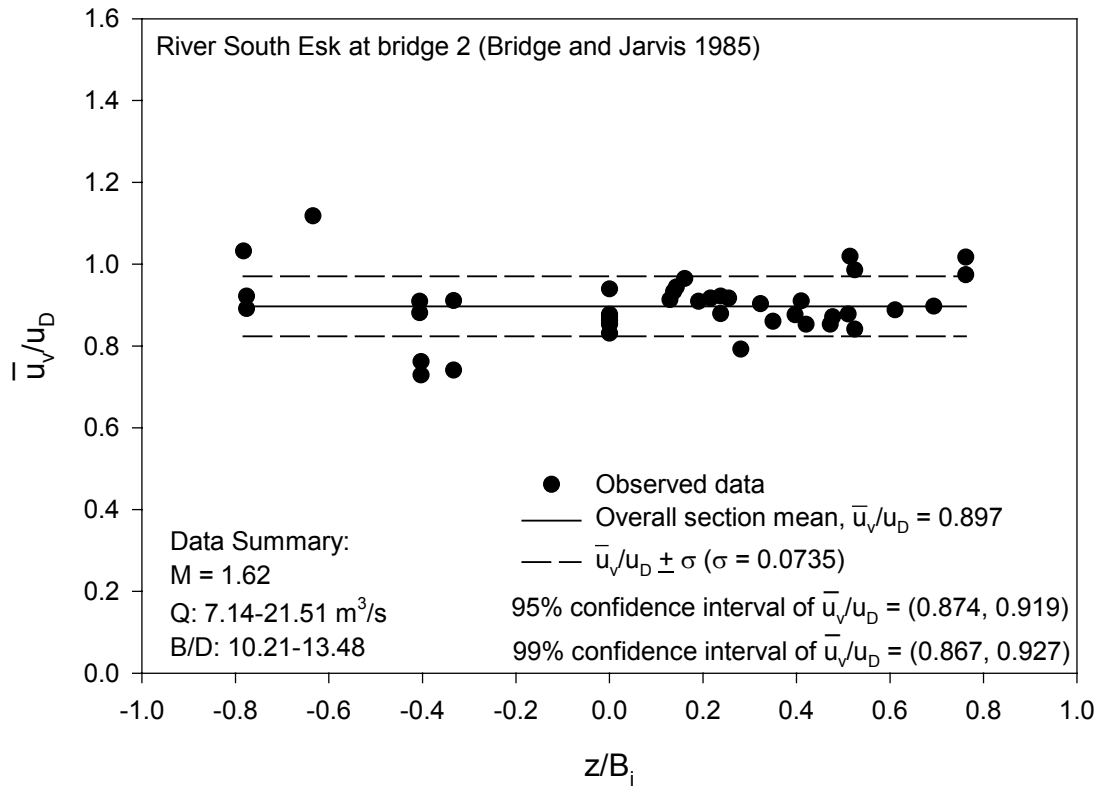


Figure 5.3 Values of  $\bar{u}_v/u_D$  in Channel Section and Estimation of Overall average in River South Esk at Bridge 2

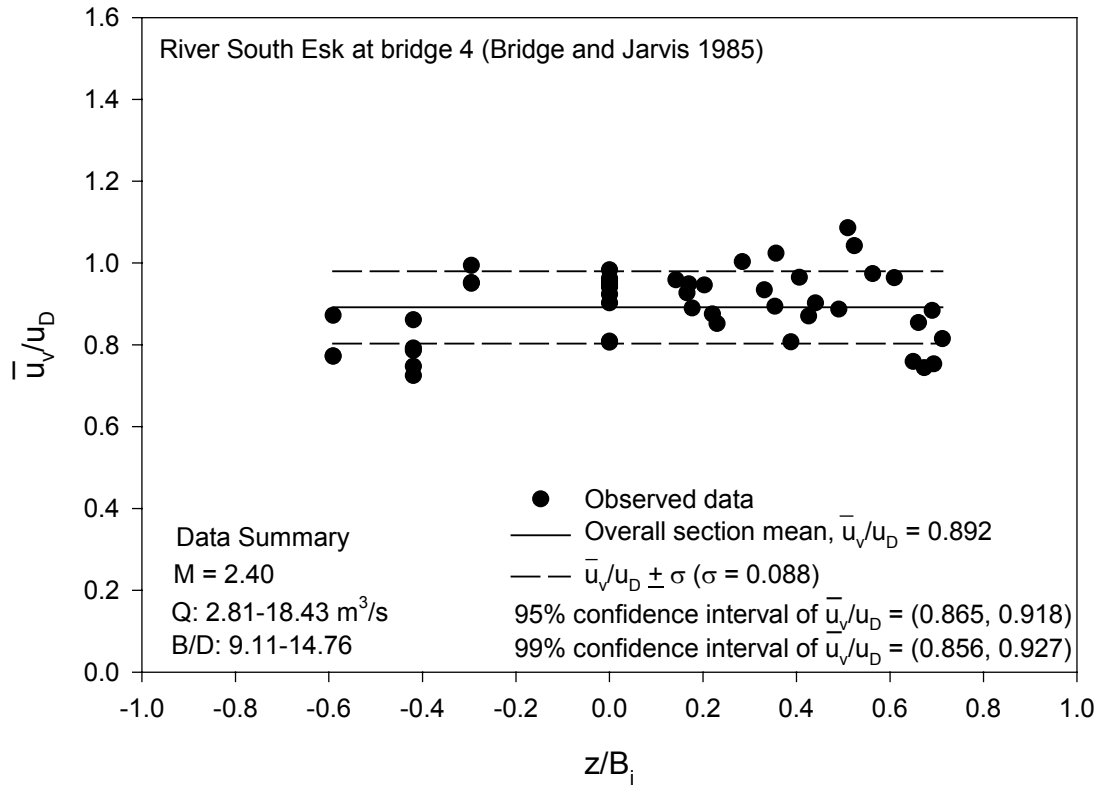


Figure 5.4 Values of  $\bar{u}_v/u_D$  in Channel Section and Estimation of Overall Average in River South Esk at Bridge 4

### 5.3 RELATION BETWEEN $\bar{u}_v/u_D$ AND DISCHARGE AND B/D

In light of the results in section 5.2, the ratio of  $\bar{u}_v/u_D$  can be assumed to be constant in a channel section. Hydraulic variables tend to interact. The ratio  $\bar{u}_v/u_D$  is related to other variables. This can help predict  $\bar{u}_v/u_D$  from other variables. The present study tried to find its

relations with discharge and B/D. Analyses of data from different rivers show that  $\overline{u_v}/u_D$  does not vary neither discharge nor B/D as shown in Figures 5.5-8.

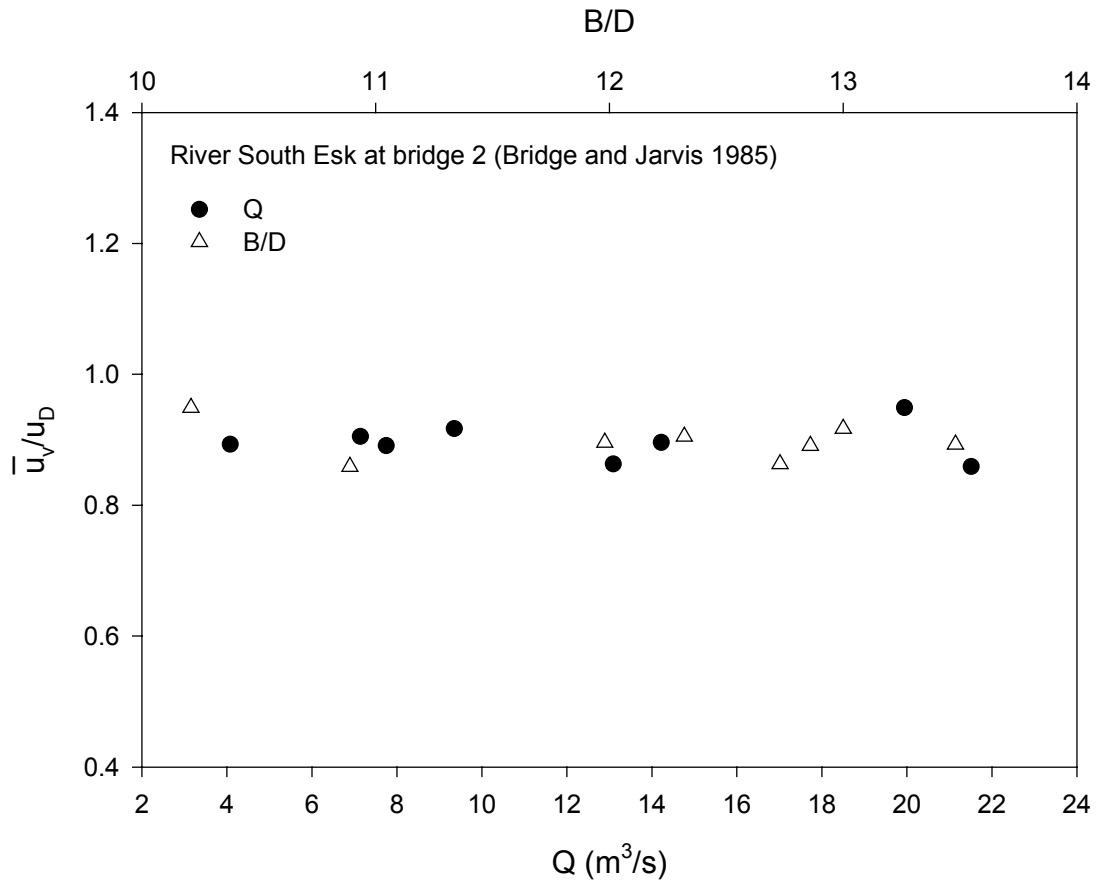


Figure 5.5 Relations between  $\overline{u_v}/u_D$  and Q and B/D in River South Esk at Bridge 2

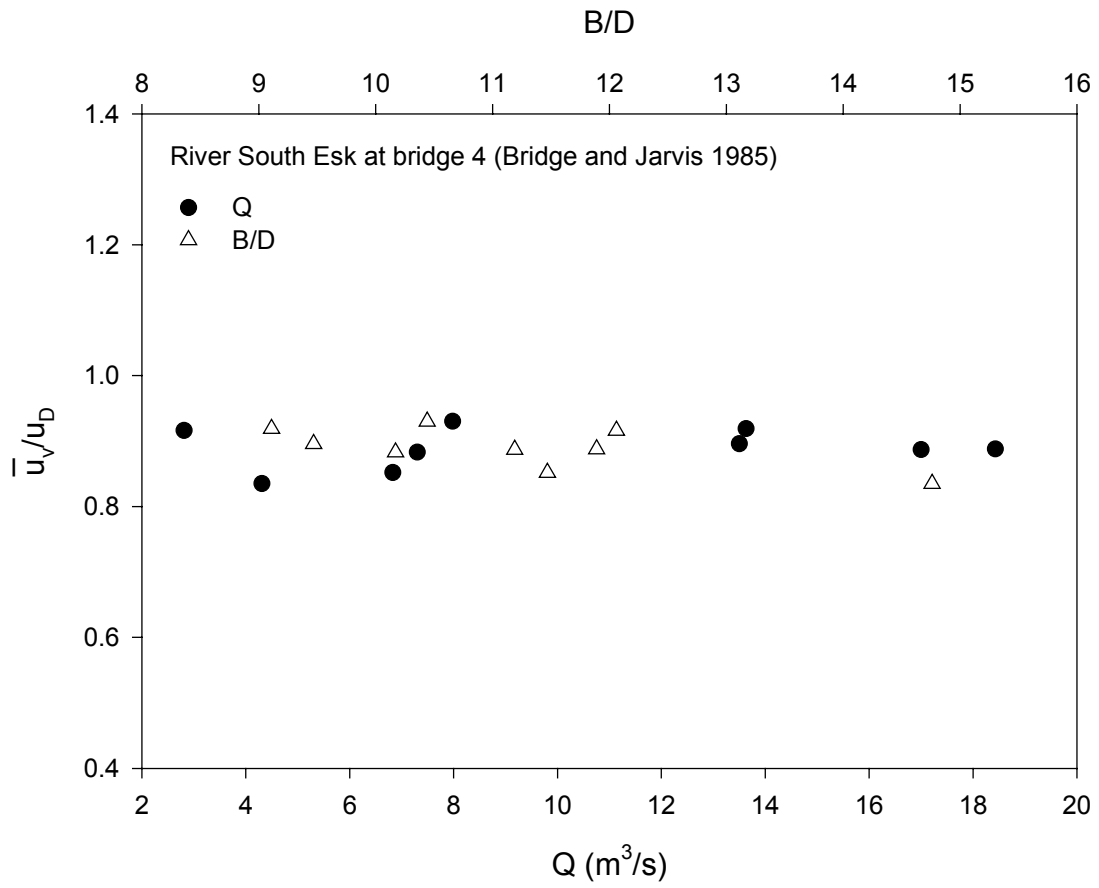


Figure 5.6 Relations between  $\overline{u}_v/u_D$  and  $Q$  and  $B/D$  in River South Esk at Bridge 4

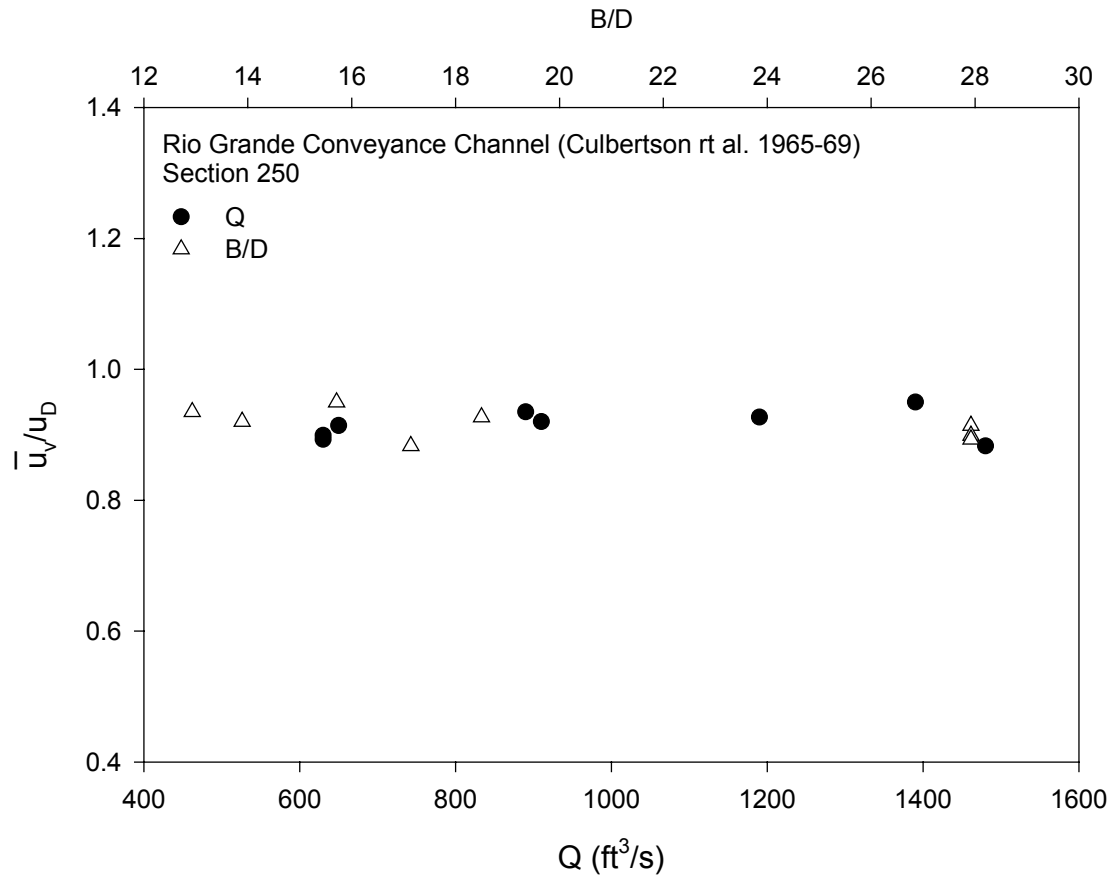


Figure 5.7 Relations between  $\bar{u}_v/u_D$  and Q and B/D in Rio Grande Conveyance Channel at Section 250

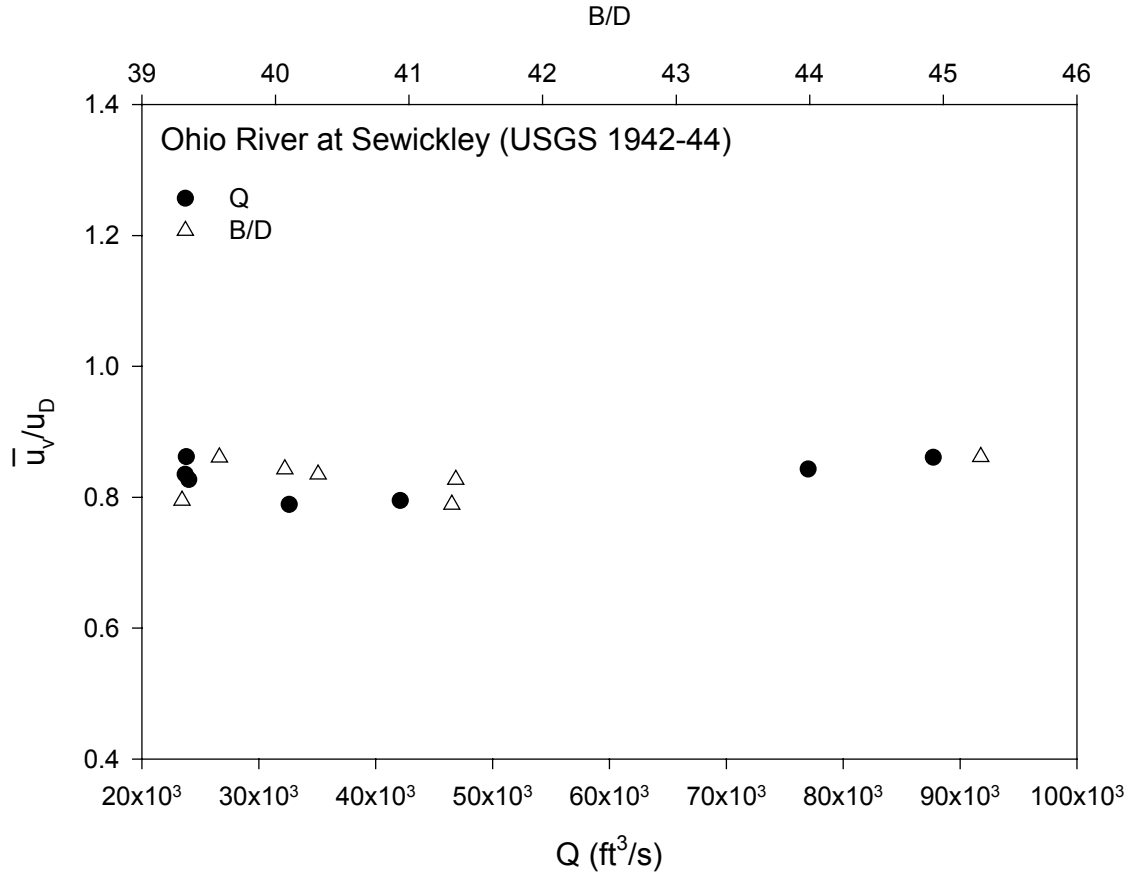


Figure 5.8 Relations between  $\bar{u}_v/u_D$  and  $Q$  and  $B/D$  in Ohio River at Sewickley

#### 5.4 RELATION BETWEEN $\bar{u}_v/u_D$ AND $M$

The parameter  $M$  characterizes a channel section. Many hydraulic variables or parameters can be expressed in terms of  $M$ . Since  $M$  is constant at a given section, these variables or parameters also become constant at the section. Once  $M$  is determined at a given channel section,  $\bar{u}_v/u_D$  can be obtained from its relation to  $M$ .

The mean value of  $\bar{u}_v/u_D$  in a channel section can be determined by using the procedure in section 5.2; estimation of  $M$  is given in section 4.2.2.

There is a tendency for  $\bar{u}_v/u_D$  to increase with M. When M is between 2 and 5, their relationship is shown in Figure 5.9. The regression line (solid line) in the figure can be expressed as the following formula:

$$\bar{u}_v/u_D = 0.0361M + 0.7842 \quad 2 \leq M \leq 5 \quad (5-1)$$

for which  $r^2 = 0.774$ . The 95% confidence interval of  $\bar{u}_v/u_D$  is plotted as two dash lines in the figure. Eq. (5-1) may be used for rivers in the United States. The reason is that the maximum velocity is generally between about  $1.25\bar{u}$  and  $1.50\bar{u}$  in natural rivers of the United States<sup>(5)</sup>.

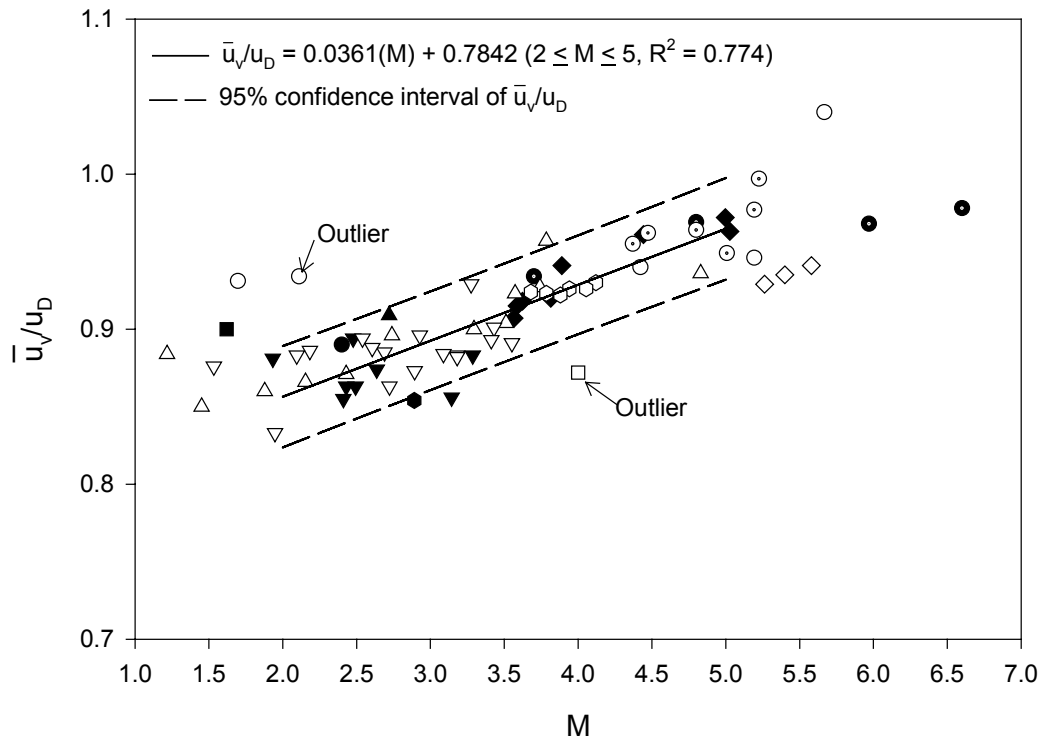


Figure 5.9 Relation between  $\bar{u}_v/u_D$  and M

## 6.0 A MODIFIED SLOPE-AREA METHOD FOR DISCHARGE ESTIMATION

### 6.1 BACKGROUND and OVERVIEW

The direct measurement is not feasible during high or rapid flows because the conventional device used to measure the velocity cannot be put in water, and because the personnel are often subjected to dangerous conditions. In order to estimate the discharge during such periods, an indirect method of measurement is often used after the high flows have passed. This indirect method is the so-called “slope-area method”, which the discharge is estimated by using the well-known Manning’s equation. Although Manning’s equation was originally derived for uniform flows, it is widely used in river flows.

Generally, errors within 25% of peak discharge in applying the slope-area method are assumed to be acceptable<sup>(33)</sup>. However, the errors may reach as much as 100% or more due to the complexity of natural rivers. A large error may lead to overestimating or underestimating the peak discharge. Manning’s  $n$  and energy losses are main sources of errors in applying the slope-area method.

Manning’s  $n$  in the slope-area method is customarily treated as a constant and is selected by the user under uncertainties. Generally, Manning’s  $n$  is not a constant and changes during unsteady flows. The energy coefficient  $\alpha$  reflects the effect of non-uniformity of velocity distribution. When the velocity distribution is uniform, the coefficient is equal to unity.

However, velocity distribution in rivers is non-uniform. If the coefficient is assumed to be unity, it cannot reflect reality.

The reason why Manning's  $n$  and the energy coefficient  $\alpha$  are assumed to be constants is that there is no reliable method to estimate them. In 1991, Chiu<sup>(37)</sup> introduced a probability-based approach to hydraulics that can be used to estimate  $n$  and  $\alpha$ <sup>(37)</sup>.

One of the objectives of the present study is to make improvements on the conventional slope-area method by using the new techniques of estimating Manning's  $n$  and the energy coefficient  $\alpha$ . The modified slope-area method will be verified by a set of flume data to demonstrate its improved performance in discharge estimation.

## 6.2 NEW SLOPE-AREA METHOD

### 6.2.1 Manning's $n$ Based on Probability Concept

As described in the previous section, Manning's  $n$  tends to vary with discharge and water depth.

Consider that the velocity distribution near a channel bed is in the viscous sublayer; then, the shear stress at the channel bed in the  $\xi - \eta$  curvilinear coordinate system is

$$\tau_0 = \mu \left( \frac{1}{h_\xi} \frac{du}{d\xi} \right)_0 \quad (6-1)$$

in which  $\mu$  = the fluid viscosity; and  $( )_0 = ( )$  evaluated at  $\xi = \xi_0$ . The mean boundary shear can be expressed as

$$\overline{\tau_0} = \mu \left( \frac{1}{\overline{h_0}} \frac{du}{d\xi} \right)_0 \quad (6-2)$$

in which  $\overline{h_0}$  = the mean value of  $h_\xi$  along the channel boundary.

According to Eqs. (2-2) and (2-3),

$$\frac{du}{d\xi} = [(\xi_{\max} - \xi_0)\exp(a_1 + a_2 u)]^{-1} \quad (6-3)$$

which (at  $\xi = \xi_0$ , where  $u = 0$ ) is

$$\left(\frac{du}{d\xi}\right)_0 = [(\xi_{\max} - \xi_0)\exp(a_1)]^{-1} \quad (6-4)$$

Therefore, substitution of Eq. (6-4) into Eq. (6-1) with  $\tau_0 = \rho u_*^2$  and  $\nu = \mu / \rho$  gives

$$a_1 = \ln \left[ \frac{\nu}{(\xi_{\max} - \xi_0) \bar{h}_0 u_*^2} \right] \quad (6-5)$$

in which  $\rho$  = the density of the fluid;  $\nu$  = the kinematic viscosity of the fluid; and  $u_*^2$  = the shear velocity.

By combing Eqs. (2-2)-(2-7), the parameter  $a_1$  can be derived another following form:

$$\bar{u} e^{a_1} = (Me^M - e^M + 1)(e^M - 1)^{-2} \quad (6-6)$$

Eqs. (6-5) and (6-6) give

$$\bar{u} = \frac{(\xi_{\max} - \xi_0) \bar{h}_0 u_*^2}{\nu F(M)} \quad (6-7)$$

in which

$$F(M) = (e^M - 1) \left[ Me^M (e^M - 1)^{-1} - 1 \right]^{-1} \quad (6-8)$$

Comparison of Eq. (6-7) with the Manning equation yields<sup>(37)</sup>

$$n = \frac{F(M)\nu}{(\xi_{\max} - \xi_0) \bar{h}_0 g R^{1/3} S^{1/2}} \quad (6-9)$$

in which  $n$  = Manning's  $n$ ;  $g$  = the gravity;  $R$  = the hydraulic radius; and  $S$  = the energy slope.

If  $\xi$  is represented by Eq. (2-14),  $\xi_0 = 0$ , and  $\bar{h}_0 = D$  for the simplification, Eq. (6-9) gives

$$n = \frac{F(M)\nu}{DgR^{1/3}S^{1/2}} \quad (6-10)$$

If the channel is wide,  $\xi = y/D$ ;  $\bar{h}_0 = D$ ;  $\xi_0 = 0$ ;  $\xi_{\max} = 1$ ; and  $R \approx D$ . Eq. (6-9) gives

$$n = \frac{F(M)\nu}{gD^{4/3}S^{1/2}} \quad (6-11)$$

It is worth to note that  $n$  in Eqs. (6-10) and (6-11) varies with the water stage.

## 6.2.2 New Slope-Area Method with Two Selected Channel Sections

The Manning equation for discharge is:

$$Q = \frac{1}{n} AR^{2/3} S_f^{1/2} \quad (6-12)$$

in which  $S_f$  = energy slope.

Substitution of Eq. (6-10) into Eq. (6-12) gives

$$Q = \frac{ARgD}{F(M)\nu} S_f = K' S_f \quad (6-13)$$

in which

$$K' = \frac{ARgD}{F(M)\nu} \quad (6-14)$$

which is similar to the conveyance  $AR^{2/3}/n$  used in the slope-area method.

A comparison of Eq. (6-13) with Manning's equation shows that Manning's  $n$  and the uncertainty resulting from it no longer exist.

Based on the Eq. (6-13), the discharge can be estimated by iteration:

1. With the known values of  $A$ ,  $R$ ,  $D$ ,  $M$ , and  $\nu$ , the value of  $K'$  at the upstream ( $K'_u$ ) and downstream ( $K'_d$ ) sections of the channel reach can be computed.

2. The average value of  $K'$  of the reach can be computed as the geometric mean of  $K'_u$  and  $K'_d$ .
3. The energy slope  $S_f$  at the first iteration can be approximated as the fall  $h_w$  of water surface in the reach divided by the length  $L$  of the reach. Thus, the corresponding discharge is computed by Eq. (6-13), which gives the first approximation of the discharge.
4. Computing the velocity heads at the upstream and downstream sections using the first approximation of discharge. The energy slope is, thus, equal to

$$S_f = \frac{h_f}{L} \quad (6-15)$$

in which

$$h_f = h_w + k(\alpha_u V_u^2 / 2g - \alpha_d V_d^2 / 2g) \quad (6-16)$$

where  $\alpha_u$  and  $\alpha_d$  can be computed by Eq. (2-22), and  $k$  is a coefficient. When the reach is contracting,  $k = 1$ . When the reach is expanding,  $k = 0.5$ . The corresponding discharge is then computed by Eq. (6-13) using the revised energy slope by Eq. (6-15). This gives the second approximation of the discharge.

5. Repeating step 4 until the computed discharges converge to a value.

The slope-area method by iteration has some restrictions. Bad selections for the length of a reach and the fall of the water surface between two sections result in obtaining a negative  $h_f$  in the step 4. Mathematically,  $h_w$  (the first term in Eq. (6-16)) should dominate the total head loss  $h_f$ . If  $h_f$  is incorrect, the computed discharges during iterations cannot converge to a discharge. To

avoid obtaining a negative value of  $h_f$  in computation, one can choose either a long reach or a small fall of water surface between two sections.

### 6.2.3 New Slope-Area Method with Multiple Channel Sections

Beson and Dalrymple (1967)<sup>(32)</sup> suggested that the discharge estimation by the slope-area method should be made with at least three cross sections. More cross sections and greater spacing generally reduce some of the errors associated with the method, particularly the definition of energy slope. To minimize the errors associated with the number of cross sections, a new slope-area method with multiple channel sections also needs to be developed. Thus, the new method can be developed by using the energy equation and Eq. (6-13) as follows:

According to Section 6.2.2, the value of  $K'$  of a channel section with the probability and entropy concept can be expressed as

$$K'_i = \frac{ARgD}{F(M)v} \quad (6-17)$$

in which  $K'_i$  is  $K'$  at the  $i$ th channel section.

The geometric mean of  $K'$  between section 0 and section 1 of a reach (see Figure 6.1) is

$$K' = \sqrt{K'_0 K'_1} \quad (6-18)$$

Therefore, the discharge with the new method is

$$Q = \sqrt{K'_0 K'_1} S_f = \sqrt{K'_0 K'_1} \frac{h_f}{L} \quad (6-19)$$

which gives the friction loss as:

$$h_f = \frac{LQ}{\sqrt{K'_0 K'_1}} \quad (6-20)$$

In addition, the energy equation may be written for sections 0 and 1 as:

$$h_0 + h_{v_0} = h_1 + h_{v_1} + h_e + h_f \quad (6-21)$$

in which  $h_0$  and  $h_1$  = elevations of the water surface at sections 0 and 1, respectively, as shown in Figure 6.1;  $h_{v_0}$  and  $h_{v_1}$  = velocity heads at sections 0 and 1, respectively;  $h_f$  = head loss due to friction; and  $h_e$  = head loss due to expansion or contraction of the channel.

Independently, the difference of the velocity heads between sections 0 and 1 is

$$h_{v_1} - h_{v_0} = \frac{Q^2}{2g} \left( \frac{\alpha_1}{A_1^2} - \frac{\alpha_0}{A_0^2} \right) \quad (6-22)$$

The head loss due to an expansion or a contraction of the channel can be expressed as

$$h_e = k(h_{v_1} - h_{v_0}) \quad (6-23)$$

in which

$$k = \begin{cases} -0.5 & \text{if } h_{v_1} < h_{v_0} \text{ (expanding)} \\ 0 & \text{if } h_{v_1} > h_{v_0} \text{ (contracting)} \end{cases}$$

Substitution of Eqs. (6-20), (6-22) and (6-23) into (6-21) gives

$$h_w = h_0 - h_1 = \frac{LQ}{\sqrt{K'_0 K'_1}} + (1+k) \frac{Q^2}{2g} \left( \frac{\alpha_1}{A_1^2} - \frac{\alpha_0}{A_0^2} \right) \quad (6-24)$$

The above equation can be applied to each of the M subreaches,  $i = 1, 2, \dots, M$

$$h_w = \left( \sum_{i=1}^M \frac{L_i}{\sqrt{K'_i K'_{i-1}}} \right) Q + \left( \sum_{i=1}^M (1+k_i) \frac{1}{2g} \left( \frac{\alpha_i}{A_i^2} - \frac{\alpha_{i-1}}{A_{i-1}^2} \right) \right) Q^2 \quad (6-25)$$

in which  $h_w$  is the sum of the falls in water surface elevation.

Since Eq. (6-25) is a quadratic equation, it can be solved to give

$$Q = \frac{-B + \sqrt{B^2 + 4Ah_w}}{2A} \quad (6-26)$$

in which

$$A = \sum_{i=1}^M (1 + k_i) \frac{1}{2g} \left( \frac{\alpha_i}{A_i^2} - \frac{\alpha_{i-1}}{A_{i-1}^2} \right) \quad (6-27)$$

$$B = \sum_{i=1}^M \frac{L_i}{\sqrt{K'_i K'_{i-1}}} \quad (6-28)$$

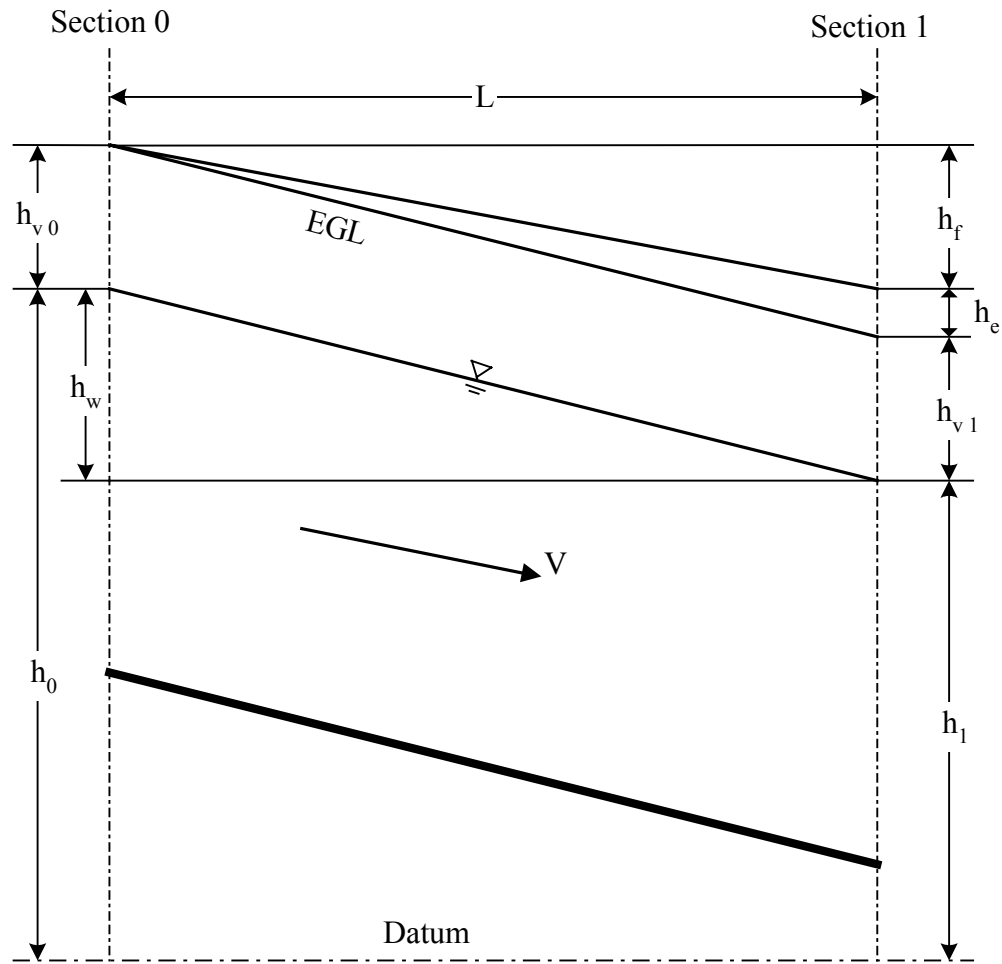


Figure 6.1 Definition sketch for new slope-area formula

### 6.3 MODEL VERIFICATION

The new slope-area method assumes the  $M$  value of each channel section is given, and only measurement required is the water level of each section. Since  $M$  is constant at a given channel section, discharge can be estimated by using Eq. (6-26) with the water level data. A set of non-uniform flow data<sup>(23)</sup> was used to verify the accuracy of the "New Slope-Area Method". There are eleven sections in the rectangular flume. Only seven of these sections (No. 2-8) in the middle reach were used during verification because flow was fully developed among these sections.

To estimate the discharge using the new slope-area method,  $M$  was obtained in advance. Only the water levels at these seven sections were measured. Comparisons were made on the influence of energy coefficient  $\alpha$  in the slope-area method; accuracy of the new slope-area method with two sections; and accuracy of the new slope-area method with more than two sections.

Table 6-1 shows a comparison of the influence of  $\alpha$  on the slope-area method at two sections. In the slope-area method, Manning's  $n$  is a constant and must be given prior to using the method. A reasonable value of  $n$  in the channel can be obtained from a uniform reach of the channel with Manning's equation. The estimated  $n$  value in this study is 0.0089. The water depth and  $M$  value at each section and the length of each subreach are also shown in Table 6-1, in which the difference between  $Q_1$  and  $Q_2$  is the energy coefficient  $\alpha$ .  $Q_1$  was estimated with  $\alpha = 1$ , and  $Q_2$  was computed with  $\alpha$  obtained from Eq. (2-22). Therefore,  $\alpha$  in method 1 is always equal to unity at any section, and  $\alpha$  in method 2 may vary with cross sections. The average errors for method 1 and method 2 are 17.10% and 13.28%, respectively (see table 6-1). Thus, the result indicates that the discharge estimated by the slope-area method with  $\alpha$  obtained from Eq.

(2-22) is more accurate than that estimated by the slope-area method with  $\alpha = 1$  and that the errors in Table 6-1 are within 25%.

When using the new slope-area method, the kinematic viscosity of the fluid  $\nu$  must be given.  $\nu$  varies with temperature. However, the flume data used did not provide this information. Discharge estimation with different values of  $\nu$  may lead to different results. Table 6-2 shows the accuracy of the new slope-area method with two sections and a comparison of discharges obtained at different temperatures. The average errors for  $T = 20^\circ\text{C}$ ,  $T = 15^\circ\text{C}$ , and  $T = 10^\circ\text{C}$  are 14.63%, 12.38%, and 10.50%, respectively. The results show that the new slope-area method is reliable and errors are within the 25%. The temperature may affect the results of the estimated discharge.

Table 6-3 compares discharges obtained by the slope-area method and the new slope-area method with multiple cross sections. The new slope-area method with seven cross sections is more accurate than the traditional method with the same number of sections. The errors in Table 6-3 are smaller than those in Tables 6-1 and 6-2. This implies that the number of cross sections for discharge estimation is an important factor. With more information from more channel sections, errors associated with these two methods can be reduced.

Table 6-1 Comparison of Discharges Obtained by Different Methods by Slope-Area Method with Two Sections (Guo 1990)

Section No.	Du	Dd	L (cm)	Mu	Md	$Q_1 \times 10e^{-4}$ (cms)	$Q_2 \times 10^{-4}$ (cms)	Error <sub>1</sub> (%)	Error <sub>2</sub> (%)
8 and 7	2.37	2.33	20	4.45	4.48	8.3278	8.1897	24.48	22.42
7 and 6	2.33	2.3	20	4.48	4.37	7.8598	8.2715	17.49	23.64
6 and 5	2.3	2.16	20	4.73	3.74	8.985	7.5021	34.30	12.14
5 and 4	2.16	1.96	20	3.74	4.61	8.253	8.632	23.36	29.03
4 and 3	1.96	1.75	20	4.61	4.66	7.0809	6.7524	5.84	0.93
3 and 2	1.75	1.57	20	4.66	5.03	5.9161	5.8076	11.57	13.19
8 and 6	2.37	2.3	40	4.45	4.73	8.1107	8.2369	21.24	23.12
8 and 5	2.37	2.16	60	4.45	3.74	8.4645	7.7176	26.52	15.36
8 and 4	2.37	1.96	80	4.45	4.61	8.2456	7.9629	23.25	19.03
8 and 3	2.37	1.75	100	4.45	4.66	7.7257	7.432	15.48	11.09
8 and 2	2.37	1.57	120	4.45	5.03	7.1564	6.9307	6.97	3.60
7 and 5	2.33	2.16	40	4.48	3.74	8.5659	7.6297	28.04	14.05
7 and 4	2.33	1.96	60	4.48	4.61	8.3164	8.0043	24.31	19.65
7 and 3	2.33	1.75	80	4.48	4.66	7.7582	7.443	15.97	11.26
7 and 2	2.33	1.57	100	4.48	5.03	7.1649	6.9281	7.10	3.56
6 and 4	2.3	1.96	40	4.73	4.61	8.5144	8.0691	27.27	20.61
6 and 3	2.3	1.75	60	4.73	4.66	7.8618	7.4739	17.52	11.72
6 and 2	2.3	1.57	80	4.73	5.03	7.2227	6.9449	7.96	3.81
5 and 3	2.16	1.75	40	3.74	4.66	7.5871	7.5017	13.41	12.13
5 and 2	2.16	1.57	60	3.74	5.03	6.9516	6.8517	3.91	2.42
4 and 2	1.96	1.57	40	4.61	5.03	6.4755	6.2732	3.21	6.23
$Error(\%) = \left  \frac{Q_i - Q_{obs}}{Q_{obs}} \right  \times 100$ $Q_{obs} = 6.69 \times 10^{-4} \text{ cms}$ <p>Notes:                      1: Computed with <math>\alpha = 1</math> (method 1).                      2: Computed with <math>\alpha</math> obtained by Eq. (2-22) (method 2).</p>							<b>Average Error</b>	<b>17.10%</b>	<b>13.28%</b>

Table 6-2 Accuracy of New Slope-Area Method with Two Channel Sections at Different Temperatures (Guo 1990)

Section No.	$Q \times 10^{-4}$ (cms) (T = 20°C)	$Q \times 10^{-4}$ (cms) (T = 15°C)	$Q \times 10^{-4}$ (cms) (T = 10°C)	Error (%) (T = 20°C)	Error (%) (T = 15°C)	Error (%) (T = 10°C)
8 and 7	8.3275	7.7819	7.2002	24.48	16.32	7.63
7 and 6	7.9348	7.1886	6.4482	18.61	7.45	3.61
6 and 5	7.6371	7.4882	7.315	14.16	11.93	9.34
5 and 4	9.135	8.9466	8.7278	36.55	33.73	30.46
4 and 3	6.4849	6.3098	6.1084	3.07	5.68	8.69
3 and 2	5.1239	4.9096	4.6695	23.41	26.61	30.20
8 and 6	7.98	7.3406	6.6825	19.28	9.72	0.11
8 and 5	8.2602	7.9852	7.6722	23.47	19.36	14.68
8 and 4	7.9122	7.6054	7.2596	18.27	13.68	8.51
8 and 3	7.2539	6.9935	6.6986	8.43	4.54	0.13
8 and 2	6.4144	6.151	5.8555	4.12	8.06	12.47
7 and 5	8.0424	7.8135	7.5508	20.22	16.79	12.87
7 and 4	7.952	7.6813	7.3736	18.86	14.82	10.22
7 and 3	7.2717	7.0379	6.7713	8.70	5.20	1.22
7 and 2	6.4424	6.1998	5.9259	3.70	7.33	11.42
6 and 4	7.8982	7.6761	7.4213	18.06	14.74	10.93
6 and 3	7.2054	6.9987	6.7616	7.70	4.61	1.07
6 and 2	6.3824	6.1571	5.9016	4.60	7.97	11.78
5 and 3	7.7181	7.5619	7.3804	15.37	13.03	10.32
5 and 2	6.8032	6.6301	6.4307	1.69	0.90	3.88
4 and 2	5.7234	5.52	5.2896	14.45	17.49	20.93
$Error(\%) = \left  \frac{Q_i - Q_{obs}}{Q_{obs}} \right  \times 100$ $Q_{obs} = 6.69 \times 10^{-4} \text{ cms}$			<b>Average Error</b>	<b>14.63%</b>	<b>12.38%</b>	<b>10.50%</b>

Table 6-3 Comparison of Discharges Obtained by Different Methods with Seven Channel Sections (Guo 1990)

Methods	SAM ( $\alpha = 1$ )	SAM ( $\alpha$ obtained by Eq. (2-22))	NSAM ( $T = 20^\circ\text{C}$ )	NSAM ( $T = 15^\circ\text{C}$ )	NSAM ( $T = 10^\circ\text{C}$ )
Estimated Discharge ( $Q \times 10^{-4}$ (cms))	7.329	7.088	6.852	6.626	6.369
Error (%)	9.56	5.94	2.42	0.96	4.8
$Error(\%) = \left  \frac{Q - Q_{obs}}{Q_{obs}} \right  \times 100$ $Q_{obs} = 6.69 \times 10^{-4} \text{ cms}$ <p>Note:            SAM: Slope-area method            NSAM: New slope-area method</p>					

## **7.0 CONCLUSION AND FUTURE WORK**

### **7.1 CONCLUSION**

Regularities in open channel flow have been found. The regularities can be represented by a set of constants in terms of entropy parameter  $M$ , which is a probability distribution that remains stable and resilient under various flow conditions, and forms a network that they are able to connect each other. The results can be used to ease not only discharge measurements in hydraulic engineering but also determination of two-dimensional velocity distribution in rectangular channel flow.

A technique for estimating the model parameter  $N$  has been developed. It can be used to simulate or predict a primary or two-dimensional velocity distribution in a rectangular channel section for various types of flow. The two-dimensional velocity distribution can be determined by using one or several velocity data, or even without using any velocity data, which depends on the given conditions. Without using velocity data, the two-dimensional velocity distribution can be determined by using any given set of values of width-to-depth ratio, channel slope, and roughness at a given channel section. If the above hydraulic variables are unknown, the two-dimensional velocity distribution can be determined by taking velocity samples at one or several points. The simulation technique is useful when studying the two-dimensional velocity distribution in a channel section. Besides the various velocity distributions help understand flow properties, existence of maximum velocity, the location of maximum velocity, and presence of

secondary flow. The technique can also be used to generate velocity data in an entire section so that it supplements the available experimental data.

In order to ease the use in engineering practice, the relation between entropy parameter  $M$  and  $N$  has been established and verified by a great amount of laboratory data. The discovery of the  $M$ - $N$  relation also provides an alternative method for determining entropy parameter  $M$ . It can be used in the development of discharge measurements. Since the determined parameter  $M$  is estimated from velocity samples at several verticals, its accuracy could be better than that depending on only one vertical ( $y$  axis).

Two inimitable features of  $y$  axis including stability and maximum information content in a channel section have been demonstrated. The results imply it is reliable for velocity sampling at  $y$  axis and give the basis for development of discharge measurements.

According to equation (2-19), the cross-sectional velocity is determined by parameters  $M$  and  $u_{\max}$ . Three approaches for estimation of  $M$  have been presented. Meanwhile,  $u_{\max}$  also can be determined from three velocity-sampling techniques. These methods for estimation of  $M$  and  $u_{\max}$  can compose various efficient methods of discharge measurements. Depending on a practical situation in a channel section, a suitable efficient method can be selected to estimate river discharges from the above methods of parameter estimation. It is worth to note that these efficient methods can be used to estimate river discharges whether the flow is steady or not, or whether historical velocity data is available or not. Therefore, various methods of discharge estimation in rivers and streams have been developed. It only requires a quick velocity sampling on  $y$  axis.

The present study also compares different velocity sampling techniques that affect the accuracy of  $u_{\max}$  and discharge. It turns out that an efficient and economic method in discharge measurements needs to take velocity samples within the 95% confidence interval of  $h/D$ .

By utilizing the advantages of regularity in open channel flow, discharge measurements require taking velocity samples at one specific axis with one or several points. The proposed study illustrated two efficient methods in discharge measurements in a bend with four different channel sections, in which efficient method 1 can determine discharge by taking several velocity samples on the vertical that the maximum velocity occurs and efficient method 2 can determine discharge by taking only a single velocity sample on water surface. In order to elucidate advantages of the developed efficient methods, three conventional methods, which are the two-point, several-point, and floats methods, respectively, are compared with the two efficient methods. The results show the floats method greatly underestimates discharge, however the others can determine discharge with reasonable accuracy. From the viewpoint of accuracy of discharge, all of them except the floats method can be used to estimate discharge. From the viewpoint of cost and time, the two efficient methods in discharge measurements are superior to the traditional methods because they only require that velocity samples be taken at one specific vertical with one or several points. In contrast, the conventional methods need to take velocity samples from verticals as many as possible in a channel section in order to estimate more accurate discharge.

Based on Chiu's velocity distribution model, the relationship between surface and vertical mean velocities has been studied. Results show that (1) the ratio of  $\overline{u}_v/u_D$  differs from 0.85, which is based on the velocity distribution obeying the Prandtl-von Karman logarithmic law; (2) the ratio of  $\overline{u}_v/u_D$  does not change with discharge or  $B/D$ ; (3) there is a linear relation

between  $\overline{u_v}/u_D$  and the entropy parameter M in which the data range of M is between 2 and 5. These results can provide references to developing a non-contact method in discharge measurement.

A novel method called the modified slope-area method for determining peak discharge is derived in the present study. The method is developed by making a modification to eliminate the weaknesses of the traditional slope-area method that occur when  $\alpha = 1$  and Manning's n is a constant. Alternatively, Chiu's mathematical models for estimating these two coefficients are used in the modified slope-area method. In his models, Manning's n is able to vary with the water depth and discharge, and  $\alpha$  at a given section can easily be determined by Eq. (3). Thus, the behavior of these two coefficients more closely approaches reality in natural rivers. The performance of the modified slope-area method is verified by using a set of non-uniform flow data in a rectangular flume<sup>(23)</sup>. Results demonstrate that the influence of  $\alpha$  and n in the slope-area method is apparent for improving the accuracy of discharge measurement. Thus, the modified slope-area method for determining discharge is more accurate than the traditional one. Meanwhile, one of the results indicates that the more cross sections are used in the slope-area method or the modified slope-area method, the better the performance will be in determining discharge. Therefore, the number of cross sections, Manning's n, and the energy coefficient  $\alpha$  are capable of minimizing estimation errors.

## 7.2 FUTURE WORK

Although the present study has done a lot for discharge measurements and simulation of 2-D velocity distribution in rectangular open channel flow, studies that based on the present models can still be enhanced in the future. Therefore, the present study recommends the following topics for improving the current models.

1. To enhance the reliability of the relation between the parameter M and N as well as the relation between  $\overline{u_v} / u_D$  and the parameter M by analyzing more data.
2. The modified slope-area method must be verified by the field data in order to estimate discharge from measurements of high-water marks in natural rivers.
3. In the modified slope-area method, the result shows that the kinematic viscosity of the fluid  $\nu$  is a factor to affect the accuracy of estimated discharge. In clear water,  $\nu$  is a function of temperature. However, the kinematic viscosity of a sediment-laden flow in natural rivers is not just a function of temperature. It may affect by the concentration of sediment because water and sediment together make up the fluid. Thus, developing a method to estimate the kinematic viscosity of a sediment-laden flow is an important issue when using the modified slope-area method

## BIBLIOGRAPHY

1. Chow, V. T. "Open Channel Hydraulics", McGraw-Hill Book Company, New York, 1959.
2. Chiu, C.-L. "Entropy and Probability Concepts in Hydraulics," Journal of Hydraulic Engineering, ASCE, Vol. 113, No. 5 (1987), pp. 583-600.
3. Chiu, C.-L. "Velocity Distribution in Open-channel Flow," Journal of Hydraulic Engineering, ASCE, Vol. 115, No. 5 (1989), pp. 576-594.
4. Chiu, C.-L. and Said C. A. A. "Maximum and Mean Velocities and Entropy in Open-channel Flow," Journal of Hydraulic Engineering, ASCE, Vol. 121, No. 1 (1995), pp. 26-35.
5. Chiu, C.-L. "A Natural Law of Open-channel Flows," Stochastic Hydraulics '96, Proc. Of 7<sup>th</sup> Int. Symp. On Stochastic Hydraulics, Mackay, Australia, 29-31 July 1996, edited by K. S. Tickle et al, A. A. Balkema, Rotterdam, 15-27.
6. Xia, R. "Relation Between Mean and Maximum Velocities in A Natural River," Journal of Hydraulic Engineering, ASCE, Vol. 123, No. 8 (1997), pp. 720-723.
7. Chen, Y. C. "An Efficient Method of Discharge Measurement," Unpublished Doctoral Dissertation, Dept. of Civil Engineering, University of Pittsburgh, Pittsburgh, PA, 1998.
8. Chiu, C.-L. and Tung, N.-C. "Maximum Velocity and Regularities in Open-channel Flow," Journal of Hydraulic Engineering, ASCE, Vol. 128, No. 4 (2002), pp. 390-398.
9. Chiu, C.-L. and Lin, G.-F. "Computation of 3-D Flow and Shear in Open Channels," Journal of Hydraulic Engineering, ASCE, Vol. 109, No. 11 (1983), pp. 1424-1440.
10. Chiu, C.-L. and Chiou, J.-D. "Structure of 3-D Flow in Rectangular Open Channels," Journal of Hydraulic Engineering, ASCE, Vol. 112, No. 11 (1983), pp. 1050-1068.
11. Chiu, C.-L. and Hsu S.-M. "Probability Law in Fluid Flow," (Being Reviewed for Possible Publication in Journal of Hydraulic Engineering, ASCE, March, 2003)
12. Chiu, C.-L., Lin, H. C., and Mizumura, K., "Simulation of Hydraulic Processes in Open Channels", Journal of Hydraulic Division, ASCE, Vol. 102, No. HY2 (1976), pp. 185-206.

13. Chiu, C.-L., Hsiung, D. E., and Lin, H. C., "Three-Dimensional Open Channel Flow," Journal of Hydraulic Division, ASCE, Vol. 104, No. HY8 (1978), pp. 1119-1136.
14. Chiu, C.-L. and Hsiung, D. E., "Secondary Flow, Shear Stress and Sediment Transport," Journal of Hydraulic Division, ASCE, Vol. 107, No. HY7 (1981), pp. 879-897.
15. Chiu, C.-L. "Entropy and 2-D Velocity Distribution in Open Channels," Journal of Hydraulic Engineering, ASCE, Vol. 114, No. 7 (1988), pp. 738-756.
16. Wahl, K.L., Thomas, W.O., Jr., and Hirsch, R.M., "The Stream-gaging Program of the U.S. Geological Surveys," U.S. Geological Survey Circular 1123, 22 p (1995).
17. Melcher, N.B., Cheng, R.T., and Haeni, F.P., "Investigating Technologies to Monitor Open-channel Discharge by Direct Measurement of Cross-sectional Area and Velocity Flow," in Hydraulic Engineering for Sustainable Water Resources Management at the Turn of the Millennium: Graz, Austria, Technical University Graz, Institute for Hydraulic and Hydrology XXVIII International Association of Hydraulic Research Congress, August, 22-27, 1999, Paper No. 181, 6 p.
18. Costa, J. E., et al., "Measuring Stream Discharge by Non-contact Methods: A Proof-of-concept Experiment," Geophysical Research Letters, Vol. 27, No. 4, February 2000, pp. 553-556.
19. Rantz, S.E. et. al. "Measurement and Computation of Streamflow, Vol. 1, Measurement of Stage and Discharge," U.S. Geol. Surv. Water-Supply Paper 2175, Washington D.C., 1982, 284 p.
20. Mason, R.R. et. al. "A Proposed radar-based Streamflow Measurement System for the San Joaquin River at Vernalis, California," Proceedings, ASCE 2002 Hydraulic Measurements and Experimental Methods Conference, Estes Park, CO, July 2002.
21. Cheng, R.T. and Gartner, J.W. "Complete Velocity Distribution in River Cross-sections Measured by Acoustic Instruments," in Proceedings of 7<sup>th</sup> Working Conf. On Current Measurement Technology, IEEE, San Diego, California, March 13-15, 2003, p. 21-26.
22. Shannon, C. E. "A Mathematical Theory of Communication," The Bell System Tech. Journal, October 1948, pp. 623-656.
23. Guo, Z. R. Personal Communication, (1990), Southeast China environmental Science Institute, Yuancun, Guangzhou, China.
24. Coleman, N. L. Personal Communication, (1990), Mid South Area National Sedimentation Laboratory, ARS, U.S, Dept. of Agriculture.
25. Bortz, K. M. "Parameter Estimation for Velocity Distribution in Open Channel Flow," Unpublished Mater Thesis, Dept. of Civil Engineering, University of Pittsburgh, Pittsburgh, PA, 1989.

26. Guy H. P., Simons, D. B., and Richardson, E. V. "Summary of Alluvial Channel Data from Flume Experiments, 1956-1961", Geological Survey Professional Paper 462-I, U.S. Government Printing Office, Washington, D.C., 1966.
27. Fetsko, M. E. "Application of A Probability and Entropy-based Model to Estimate Discharge in A Small-scale Open Channel," Unpublished Mater Thesis, Dept. of Civil Engineering, University of Pittsburgh, Pittsburgh, PA, 1999.
28. Tu, H., Tamai, N., and Kawahara, Y. "An Experimental Investigation of unsteady Compound Open-Channel Flows," Technical Report, Graduate School and College of Engineering, University of Tokyo, Vol. XLIII, No. 2, 1995.
29. Bridge, J. S., and Jarvis, J., "Flow and Sediment Transport Data, River South Esk, Glen Glova, Scotland", Unpublished Rep., Dept. of Geological Sciences, State Univ. of New York, Binghamton, N.Y., 1985.
30. Yen, B. C., "Characteristics of Subcritical Flow in a Meandering Channel", Tech. Report, Institute of Hydraulic Research, University of Iowa, Iowa City, Iowa, 1965.
31. Culbertson, J. K., Scott, C. H., and Bennett, J. P., "Summary of Alluvial Channel Data from Rio Grande Conveyance Channel, New Mexico, 1965-69", Open File Report, U.S. Geological Survey, Water Resources Division, (Aug.).
32. Benson, M.A. and Dalrymple, T. "General Field and Office Procedures for Indirect Discharge Measurements", U.S. Geol. Surv. Techniques of Water-Resources Investigations. Book 3, Chapter A-1, 30pp., 1967.
33. Jarrett, R.D. "Errors in Slope-Area Computations of Peak Discharges in Mountain Streams", Journal of Hydrology, 96(1987), pp.53-67.
34. King, H. W., and Brater, E.F. "Handbook of Hydraulics", 5<sup>th</sup> ed., McGraw-Hill Book Company, New York, 1963.
35. Fox, R. W., and McDonald, A. T. "Introduction to Fluid Mechanics", John Wiley and Sons, New York, pp. 358-361, 1985.
36. Chen, C.-L. "Momentum and Energy Coefficients Based on Power-Law Velocity Profile," Journal of Hydraulic Engineering, ASCE, Vol. 118, No. 11 (1992), pp. 1571-1584.
37. Chiu, C.-L. "Application of Entropy Concept in Open Channel Flow Study," Journal of Hydraulic Engineering, ASCE, Vol. 117, No. 15 (1991), pp. 615-628.